

JAERI-Review

99-005



JP9950181



ANNUAL REPORT OF JMTR
FY 1997
(April 1, 1997 – March 31, 1998)

March 1999

Department of JMTR

日本原子力研究所
Japan Atomic Energy Research Institute

本レポートは、日本原子力研究所が不定期に公刊している研究報告書です。
入手の間合わせは、日本原子力研究所研究情報部研究情報課（〒319-1195 茨城県那珂郡東海村）あて、
お申し越してください。なお、このほかに財団法人原子力弘済会資料センター（〒319-1195 茨城県那珂郡
東海村日本原子力研究所内）で複写による実費領布をおこなっております。

This report is issued irregularly.
Inquiries about availability of the reports should be addressed to Research Information Division,
Department of Intellectual Resources, Japan Atomic Energy Research Institute, Tokai-mura, Naka-
gun, Ibarakiken 319-1195, Japan.

Annual Report of JMTR
FY1997
(April 1, 1997 - March 31, 1998)

Department of JMTR*

Oarai Research Establishment
Japan Atomic Energy Research Institute
Oarai-machi, Higashiibaraki-gun, Ibaraki-ken

(Received February 3, 1999)

During FY1997, the JMTR was operated for 3 complete cycles (120th, 121st and 122nd cycles) and was utilized for the research and development programs on the technology of LWRs and fusion reactor, as well as for fundamental research of fuels and materials, and for radioisotope productions.

The improvement of evaluation technique in a local neutron spectrum for irradiation utilization and development of capsule having the vertical migration, the reinstrumentation and loading mechanism have been carried out. Development of a new oxygen potential sensor for oxide fuel pellets has been done as an elemental technology of irradiation for high burn-up fuels.

As for post irradiation examination, the techniques for measuring of crack length using an alternating current potential drop method and machining of miniaturized specimen by the remote handling have been developed.

A research on the blanket materials and components for thermonuclear fusion reactor were also progressed.

Keywords: JMTR, Annual Report, Research Reactor, Irradiation, Post Irradiation Examination, Reactor Operation, Maintenance

* Editorial group of the Annual Report of JMTR

Norikazu OOKA(Leader), Taiji HOSHIYA, Toshio TABATA, Kimihiro OHTAKA,
Akira SHIBATA, Akihiro SHIZUKA, Yoshinori MATSUI, Hisashi SAGAWA,
Takashi IWAI, Toshimitsu ISHII, Isamu HISA, Keiichirou NISHIWAKI, Toshishiro FURUTA

材料試験炉 英文年報 (1997年度)
(1997年4月1日～1998年3月31日)

日本原子力研究所大洗研究所
材料試験炉部*

(1999年2月3日受理)

1997年度は、軽水炉及び核融合炉の研究開発、燃料・材料の基礎研究及びRI生産等の照射利用のために、120、121及び123サイクルの合計3サイクルの運転を行った。

照射利用の技術開発では、照射場評価として照射試料位置における中性子スペクトル評価精度を向上させるための技術の開発を進めた。

一方、照射技術に関しては照射試料の垂直移動、再照射、応力負荷が行える照射キャプセルの開発を行うとともに、要素技術としての燃料棒用酸素ポテンシャルセンサ等の開発を行っている。

照射後試験技術に関しては、交流電位差法を用いたき裂長さ測定技術及び遠隔操作による微小試験片加工技術の開発を行った。

核融合開発に関しては、ブランケット照射挙動及び関連材料に関する照射研究を進めた。

大洗研究所：〒311-1394 茨城県東茨城郡大洗町成田町新掘3607

※ 大岡紀一(編集長)、星屋泰二、田端俊夫、大高公宏、柴田晃、静明宏
松井義典、佐川尚司、岩井孝、石井敏満、比佐勇、西脇圭一郎、古田敏城

Contents

1. Introduction	1
2. Overview	3
2.1. JMTR	5
2.2. Irradiation Facilities	14
2.3. Hot Laboratory	23
3. Activities in FY1997	34
3.1. Reactor Operation	34
3.2. Fuel and Reflector Management	37
3.3. Utilization of Irradiation Facilities	39
3.4. Maintenance Engineering	42
3.5. Post Irradiation Examinations	43
4. Topics in FY1997	45
4.1. Evaluation of Neutron Field for Irradiation	45
4.2. Design of Capsules and Irradiation Facilities	48
4.3. Safety Analysis of JMTR with New Core Configuration	52
4.4. Neutron Irradiation Studies for Fusion Blanket Development	54
4.5. Post Irradiation Examination(PIE)	64
4.6. Application of Infrared Thermography to Nondestructive Diagnostic for Structures and Components in the JMTR	69
4.7. Replacement of Vent Valves in Primary Cooling System	70
5. International Cooperation	71
5.1. International Cooperation	71
5.2. STA Scientist Exchange Program	72
5.3. Report of Third International Workshop on Beryllium Technology for Fusion	73
6. Summary	74
7. Publications	75
8. Organization	79

目 次

1. はじめに	1
2. 概 要	3
2.1. 原子炉施設	5
2.2. 照射設備	14
2.3. ホットラボ施設	23
3. 1997年度の活動	34
3.1. 原子炉の運転	34
3.2. 燃料及び反射体の管理	37
3.3. 照射設備の利用	39
3.4. 原子炉の保守点検	42
3.5. 照射後試験	43
4. 1997年度の話題	45
4.1. 中性子照射場の評価	45
4.2. 照射キャプセル及び照射設備の設計	48
4.3. 混合炉心の構成変更に係わる安全解析	52
4.4. 核融合炉ブランケットに関する研究開発	54
4.5. 照射後試験	64
4.6. 赤外線サーモグラフィーを用いた非破壊診断技術の開発	69
4.7. 一次冷却系ベント弁の更新	70
5. 国際協力	71
5.1. 国際協力	71
5.2. 科学技術庁研究交流制度	72
5.3. 第三回核融合炉ベリリウム技術ワークショップに関する報告	73
6. あとがき	74
7. 外部発表	75
8. 材料試験炉部の組織	79

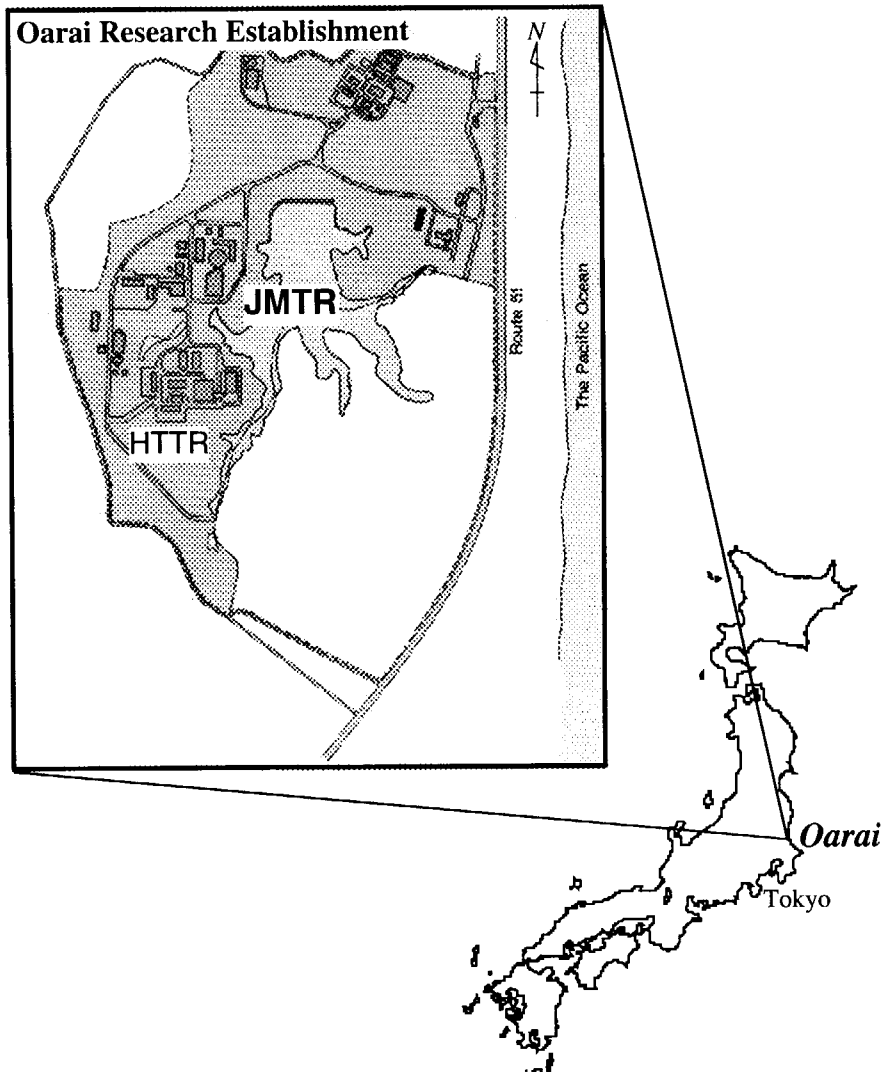
1. Introduction

Location of JMTR

The Japan Materials Testing Reactor (JMTR) is located in the Oarai Research Establishment, one of the five research establishments of the Japan Atomic Energy Research Institute (JAERI), about 100 km north-east from Tokyo (Fig. 1.1).

In the Oarai Research Establishment, the High Temperature Engineering Test Reactor (HTTR) is under construction.

Fig. 1.1
JAERI Oarai Research
Establishment



Historical background

In late 1950's, Japanese industries requested the government to construct a material testing reactor for irradiation tests of nuclear fuels and structural materials and for radioisotope production. The Japan Atomic Energy Commission (JAEC) approved the construction of materials testing reactor in JAERI as JMTR, and started the design of the reactor in 1962.

In the design concept, the main characteristics of JMTR were

- (1) flexibility of the core configuration for irradiation tests, and
- (2) adoption of the proven technologies which had been experienced in ETR, ORR and other high flux reactors, for safety and economic reason.

The construction of JMTR started in April 1965.

JMTR achieved the first criticality in March 1968 and started the first two operation cycles in December 1969 as test program. It accomplished 50 MW full power in January 1970. The cycle operation at 30 MW begun in August 1970 and the 50 MW operation started in October 1971. The cumulative power reached 100,000 MWd during the 108th operation cycle in March 1994.

Initially JMTR employed high enriched uranium (HEU) fuel elements. Under the international collaboration on the non-proliferation of fissile materials, JAERI started the program to employ reduced enrichment fuels for research reactors in 1979. Core configuration of JMTR was changed by totally employing medium enriched uranium (MEU) fuels in July 1986, 75th operation cycle. The fuel type was further changed to low enriched uranium (LEU) fuels since 108th operation cycle in Jan. 1994.

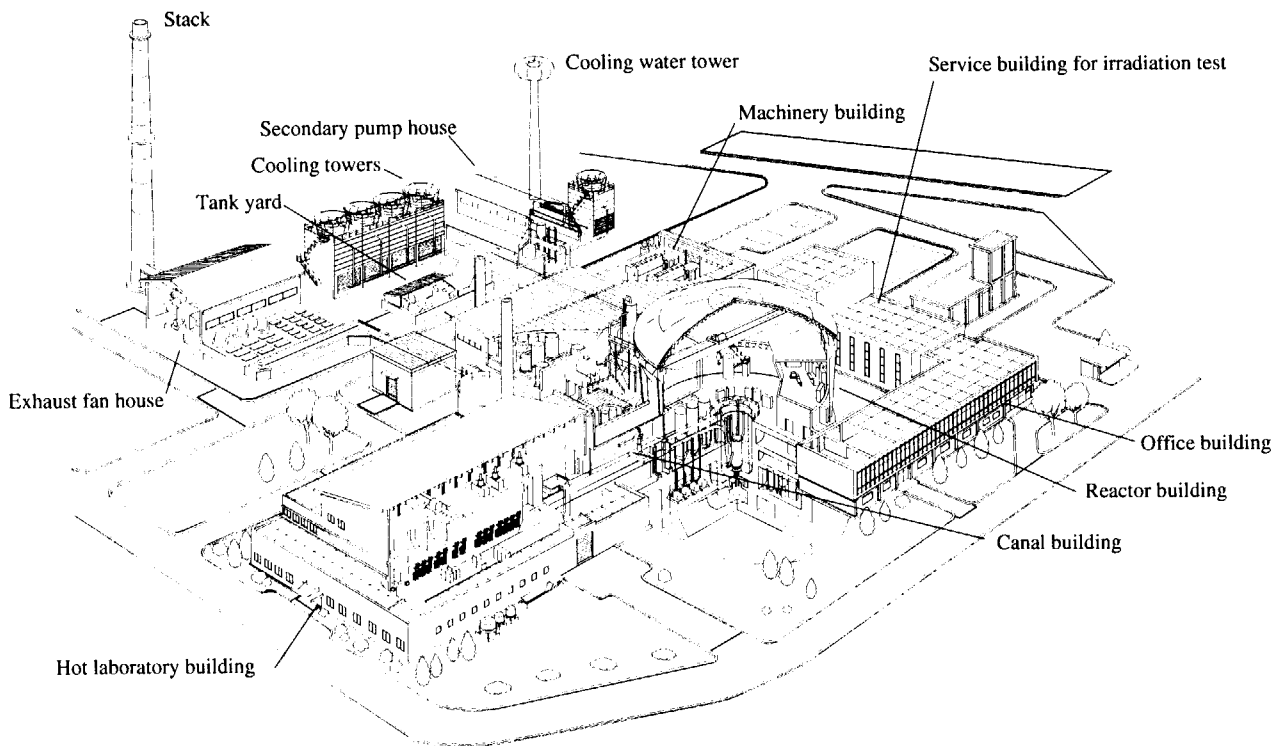
Aug.	1963	Construction of JMTR in Oarai was approved by Japan Atomic Energy Commission (JAEC)
Apr.	1965	Construction of JMTR started
Mar.	1967	Construction of Hot Laboratory started
Apr.	1967	Foundation of Oarai Research Establishment
Mar.	1968	JMTR achieved First criticality
Jan.	1969	Completion of the Hot Laboratory
Apr.	1972	Completion of Oarai Water Loop -2 (OWL-2)
Oct.	1972	Completion of Hydraulic Rabbit Irradiation Facility (HR-2)
Jan.	1977	Completion of Oarai Gas Loop (OGL-1)
	1979	International Collaboration on Non-proliferation of Fissile Material
Jan.	1983	Cumulative power reached 50,000 MWd
Jan.	1984	Completion of Oarai Shroud Irradiation Facility (OSF-1)
Jul.	1986	45% enriched (MEU) fuels were employed
Jan.	1989	Replacement of OSF-1 in-pile stainless steel tube with zircaloy tube
Mar.	1992	JMTR achieved 100 operation cycles
Jan.	1994	20% enriched (LEU) fuels were employed
Mar.	1994	Cumulative power reached 100,000 MWd
Dec.	1995	Removal of JMTRC was began
Jul.	1997	Replacement of pressure surge tank
Dec.	1997	Renewal of Hydraulic Rabbit irradiation facilities (HR-2)

Table 1.1
History of JMTR

2. Overview

JMTR facility consists of the reactor building, the machinery building, secondary pump house, cooling towers, exhaust fan house, tank yard, cooling water tower, main stack, service building for irradiation tests, canal building, hot laboratory building and office building. The arrangement of the buildings is shown in Fig. 2.1.

Fig. 2.1
Arrangement of
the JMTR buildings

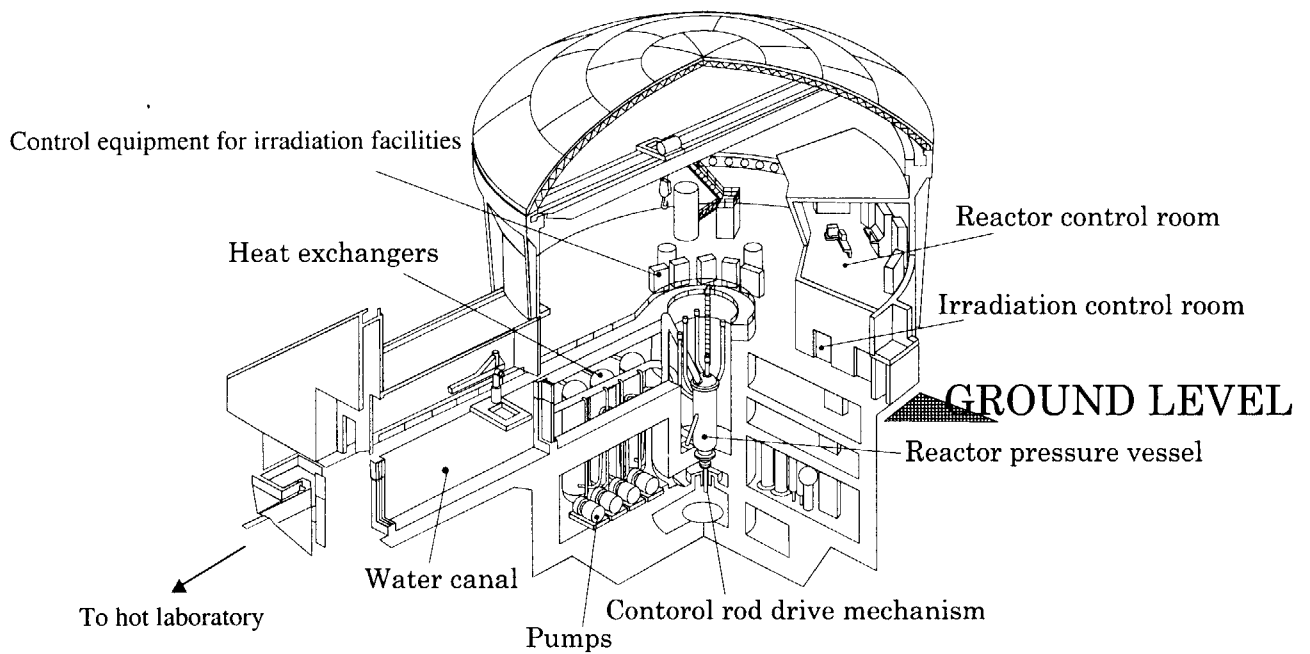


The reactor building has reinforced concrete structure. Its dimensions are 41 m in diameter, 20.4 m high above and 23.5 m deep below the ground level in height. The reactor pressure vessel is placed in the reactor pool near the center of the reactor building (Fig. 2.2).

The reactor control room and the control room for the irradiation facilities are located in the reactor building.

The hot laboratory is connected to the reactor building through a water canal. The irradiated specimens can be transferred to the hot laboratory underwater through the canal without any shielding devices for the post irradiation examination.

Fig. 2.2
Reactor building

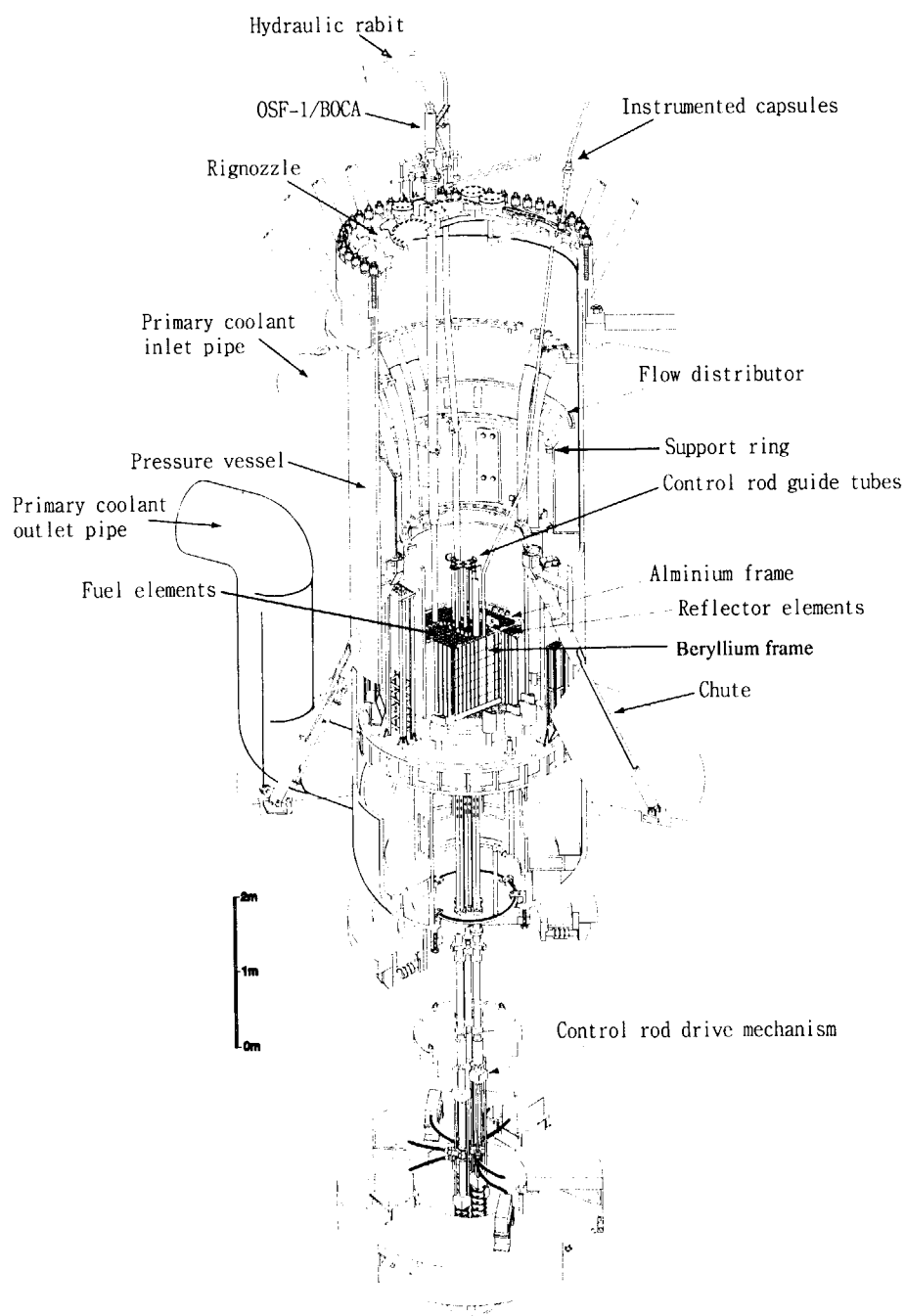


2.1. JMTR

Reactor

JMTR is a tank-in-pool type reactor cooled and moderated by light water with thermal power of 50 MW. JMTR is normally operated as five cycles a year, 26 days per cycle. Fig 2.1.1 shows the cross-section of the reactor. The engineering specifications of JMTR are described in Table 2.1.1. Schematic view of the reactor is shown in Fig. 2.1.2.

Fig. 2.1.1
Cross-section of JMTR



Pressure vessel

The pressure vessel, 9.5 m in height, 3 m in diameter and 34 mm thick, is made of stainless steel and its design pressure is 1.8 MPa. The pressure vessel is installed in the reactor pool which is 13 m in deep. The pressure vessel contains the reactor core, irradiation facilities and etc.. The top closure head of the pressure vessel provides many nozzles for in-pile loops, instrumented capsule irradiation facilities, and hydraulic rabbit irradiation facilities. Two chutes are attached on the side wall of the pressure vessel to

Fig. 2.1.2
Cross-section of JMTR
pressure vessel

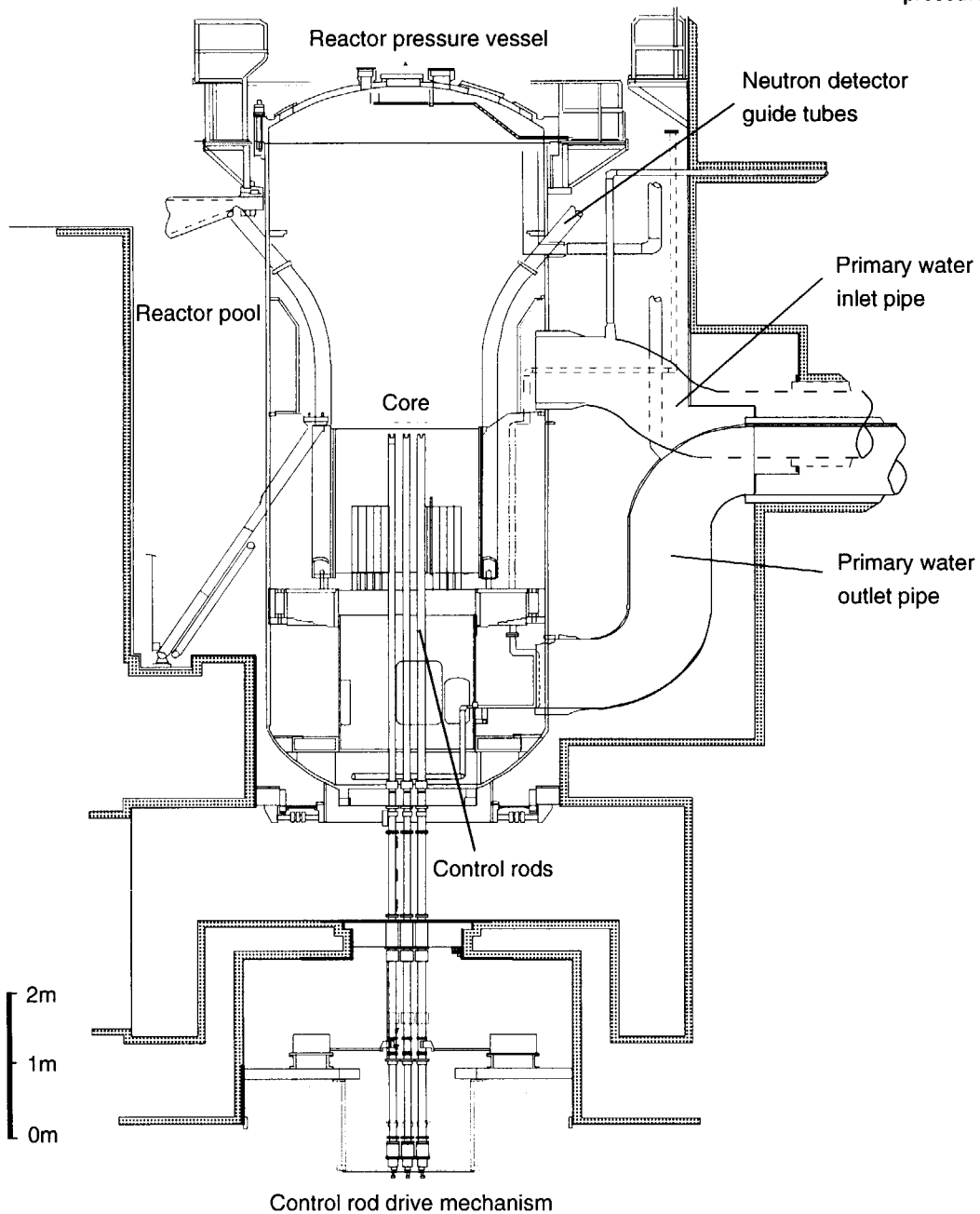


Table 2.1.1
Engineering specifications
of JMTR

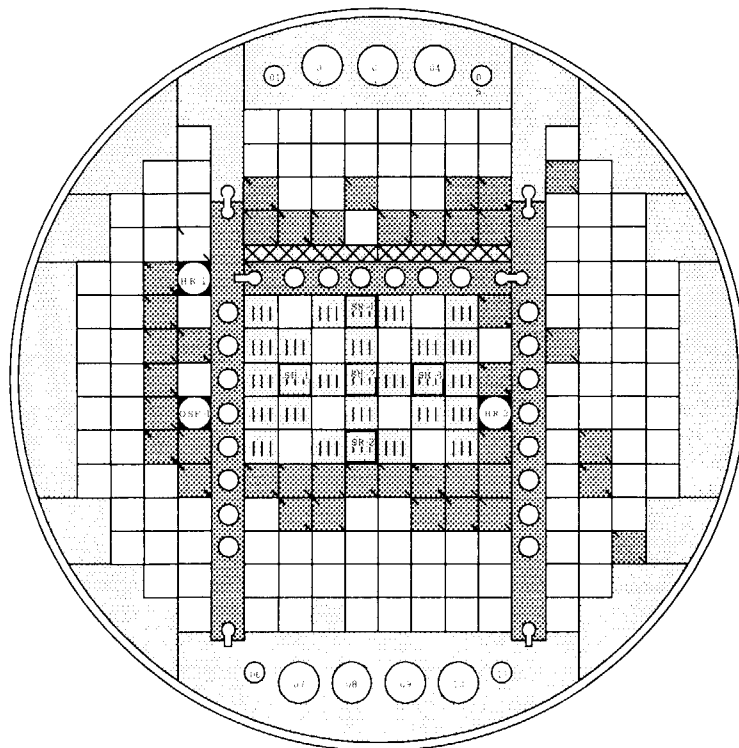
Thermal power			50 [MW]		
Neutron flux	Fuel region	ϕ_n (<0.68 eV)	Max. 4×10^{14} [n/cm ² · s]		
		ϕ_f (>1MeV)	Max. 4×10^{14} [n/cm ² · s]		
	Reflector region	ϕ_n (<0.68 eV)	Max. 4×10^{14} [n/cm ² · s]		
		ϕ_f (>1MeV)	Max. 1×10^{14} [n/cm ² · s]		
Power density	Core average		Approx. 492 [kW/l]		
	Average heat flux		120 [W/cm ²]		
Pressure vessel	Material		Stainless steel		
	Height		9.5 [m]		
	Diameter		3 [m]		
	Thickness		34 [mm]		
Core	Material of structure		Stainless steel		
	Effective height		750 [mm]		
	Equivalent diameter		416 [mm]		
	Core loading(²³⁵ U)		Max. 11 [kg]		
Core components Fuel	Number of fuel elements		Standard fuel element	Fuel follower	
			22	5	
	Type		Plate	Plate	
			76.2 [□] × 1.200 [mm]	63.6 [□] × 890 [mm]	
	Dimension				
	Fuel plate	Number		19 per element	16 per element
		Thickness		1.27 [mm]	1.27 [mm]
		Total length		780 [mm]	769 [mm]
		Thickness of cladding		0.38 [mm]	0.38 [mm]
		Cladding material		Aluminum alloy	Aluminum alloy
		Thickness of meat		0.51 [mm]	0.51 [mm]
		Effective length		750 [mm]	750 [mm]
Meat	Width		61.6 [mm]	49.7 [mm]	
	²³⁵ U content		Approx. 410 [g]	Approx. 275 [g]	
Enrichment	Per element		Approx. 20 [%]	Approx. 20 [%]	
Burnable absorber	Number of Cadmium wires		18 (φ 0.3)	16 (φ 0.3)	
Control rod	Type		Top entry bottom mounted with follower		
	Number		5		
	Absorber	Material	Hafnium		
		Dimension	63.0 [□] × 800 [mm]		
Reflector	Material	Reflector element	Beryllium		
			Aluminum		
		H-shaped frame	Beryllium		
Grid plate	Material		Stainless steel		
Reactivity restriction	Material				
	Max. excess reactivity		15 [% Δk/k]		
	Shutdown margin		<0.9 [Keff]		
Primary cooling system	RPV inlet temperature		Max. 49 [°C]		
	RPV outlet temperature		Approx. 56 [°C]		
	Fuel surface temp		Max. 186 [°C]		
	Fuel channel velocity		10 [m/s]		
	Fuel channel flow rate		125 [m ³ /h]		
	Total flow rate		6.000 [m ³ /h]		
	Core inlet pressure		1.4 [MPa]		
Pressure difference between RPV inlet / outlet		0.32 [MPa]			

transfer the spent fuel and reflectors from the core to the reactor pool. The primary coolant, entering through the primary coolant inlet pipe, flows downwards through the reactor core for heat removal, passes the lower plenum and exits through the primary coolant outlet pipe.

Reactor core

The reactor core, 1,560 mm in diameter and 750 mm in effective height, consists of fuel elements, control rods, reflectors and the H-shaped beryllium frame as shown in Fig. 2.1.3. The H-shaped beryllium frame separates the core into four regions. The reactor core consists of 204 lattice positions, 77.2 mm square each, arranged in a square matrix. The 22 standard fuel elements and 5 control rods are loaded in the lattice positions of center region.

The H-shaped beryllium frame and beryllium and aluminum reflector elements are equipped with irradiation holes. These irradiation holes are filled with solid plugs of the same material when they are not loaded with the capsules.









- | | |
|--|---|
|  Control rod with fuel follower |  Beryllium reflector |
|  Fuel element |  Aluminium reflector |
|  Beryllium frame |  γ-ray shield plate |

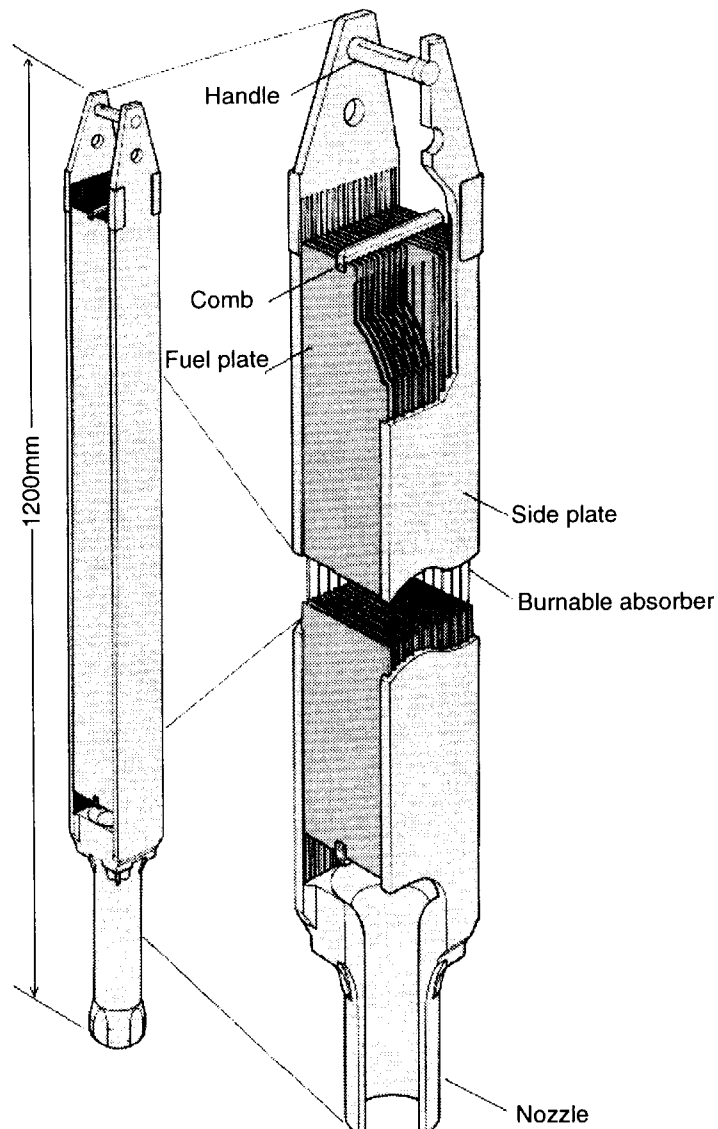
Fig. 2.1.3
Core configuration

Fuel element

The fuel elements are modified ETR type, flat-plate assemblies. They are classified into standard fuel elements and fuel followers.

Each standard fuel element consists of 19 fuel plates which are 1.27 mm thick, 70.5 mm wide, and 780 mm long (Fig. 2.1.4). The fuel plates are attached to the aluminum alloy side plates by a "roll-swagging" technique. As burnable neutron absorbers, cadmium wires with aluminum cladding are inserted into grooves where fuel plates are attached. A fuel plate consists of a 0.5 mm thickness layer of uranium-silicon-aluminum fuel (U_3Si_2-Al) and aluminum cladding.

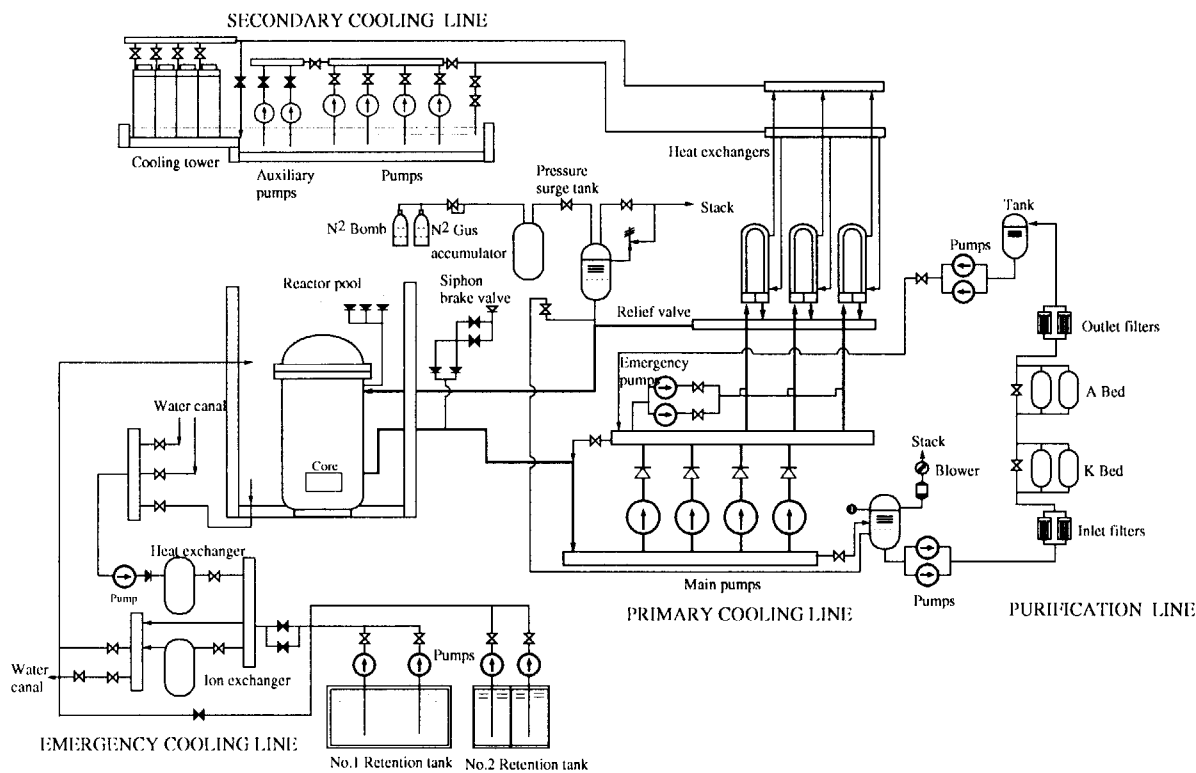
Fig. 2.1.4
Fuel element
(standard element)



Cooling systems

Flow diagram of the reactor cooling system is shown in Fig. 2.1.5. The primary cooling system consists of four main pumps, two emergency pumps, an emergency cooling system and three heat exchangers. Three main pumps and an emergency pump operate during the normal operation. In case of abnormal reactor conditions such as LOCA or loss of primary coolant flow, one main pump and an emergency pump are powered by a diesel engine generator for decay heat removal. The primary coolant flows downward through the reactor core at the flow rate of 6,000 m³/h. Nominal coolant inlet temperature is 49 °C and the corresponding outlet temperature is 56 °C. The heat removed from the core is transferred to the secondary coolant in the heat exchangers and is dissipated into the atmosphere in the cooling tower (Table 2.1.1) .

**Fig. 2.1.5
Flow diagram of the
reactor cooling
systems**



Instrumentation and control system

The nuclear instrumentation of JMTR is composed of start-up channel, log-power channel and linear-power channel. Each channel is composed of identical and independent three channels. Mean value of the three channels is used to measure nuclear power level and period. The trip signals are taken through the 2-out-of-3 circuits.

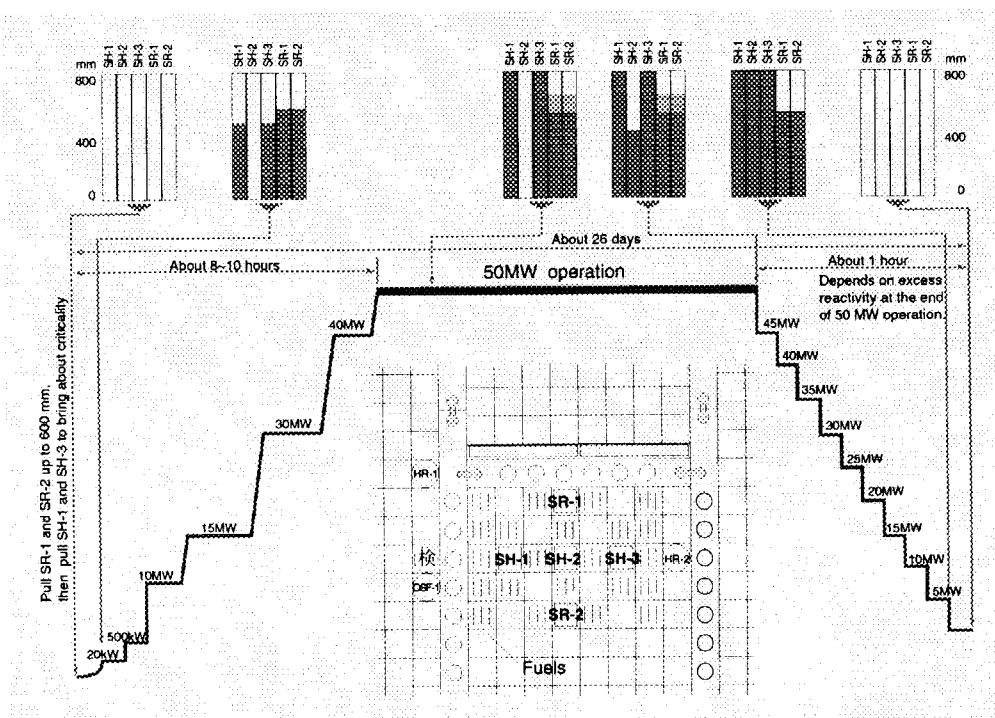
There are five control rods among which three rods are used for shim control and the other two rods are used for regulating. One of the regulating control rods is used for automatic control of the reactor power.

Each rod consists of a box-type hafnium absorber and a fuel follower attached to the bottom of the absorber. The drive mechanism is installed beneath the bottom of the pressure vessel. The control rods move vertically along the guide tubes. When a control rod is withdrawn upwards, the fuel follower displaces the hafnium absorber of the control rod in the core.

Operation procedure

Typical operation procedure of the reactor is shown in Fig. 2.1.6. It takes about 8 hours from the start-up to the full power of 50 MW. The reactor power is increased stepwise up to 50 MW with safety checks of reactor and irradiation experiment facilities.

Fig. 2.1.6
Operation pattern and
position of control
rods during operation



Operation support system: ARGUS

Two computer systems are installed, one for the control of reactor operation and the other for the control of the irradiation facilities. ARGUS is the computer system for the reactor operation and has the following functions:

- (1) monitoring the state of the feed back control circuits,
- (2) logging the major process data and indicating trend,
- (3) checking the data over/under limited value,
- (4) displaying the result of monitoring sequence control under abnormal conditions,
- (5) diagnosing unusual status and indicating the result of diagnosis,
- (6) indicating operation guidance.

ARGUS is also used for the following calculations.

- (1) neutron fluence and irradiation deformation of core components,
- (2) estimation of the primary coolant leakage,
- (3) possible restart time after the scram

The schematic diagram of ARGUS is shown in Fig. 2.1.7.

The support system for the control of irradiation facilities (LOOCAS, IDASS) is described in Chapter 2.2.

Radiation monitoring system

Radiation monitoring in JMTR is carried out continuously by the central radiation monitoring system as shown in Fig. 2.1.8. The central radiation monitoring system and radiation monitoring panel are located in the reactor control room and central radiation monitoring system is located at the radiation management room in the JMTR.

**Fig. 2.1.7
Operation support
system: ARGUS**

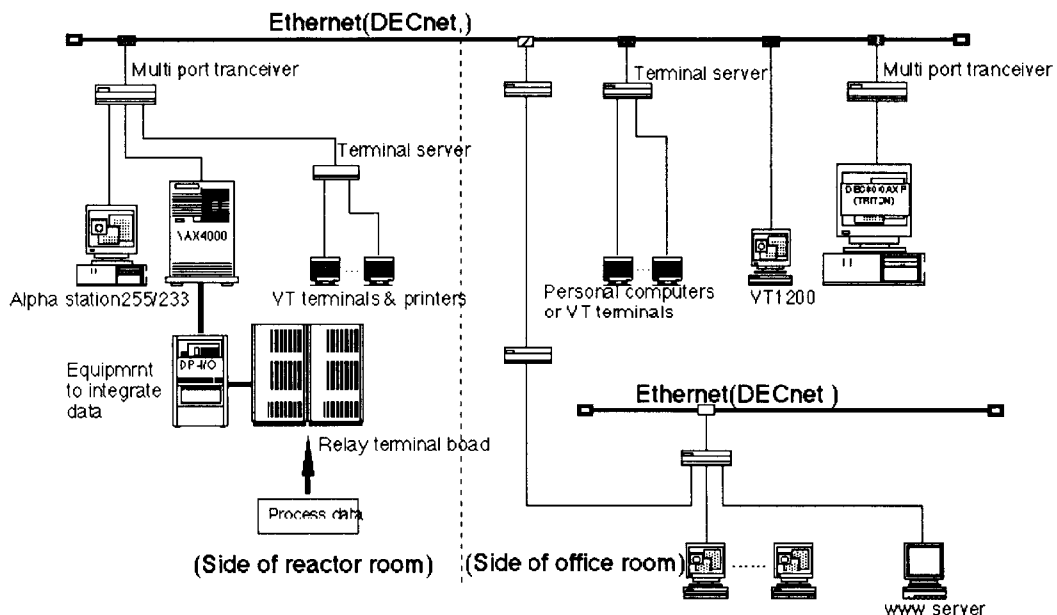
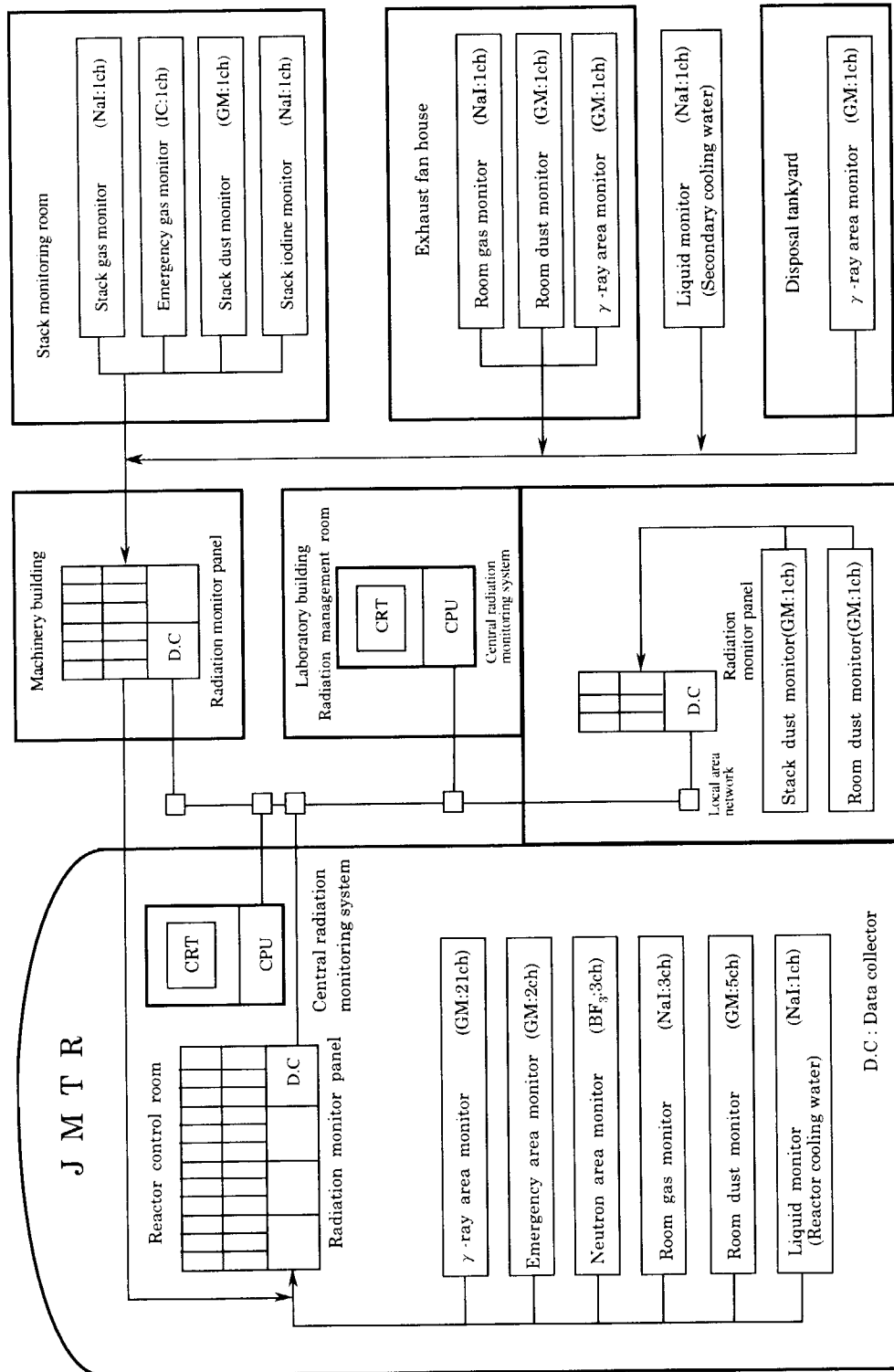


Fig. 2.1.8
Central radiation
monitoring system in
the JMTR



2.2. Irradiation Facilities

JMTR is providing a variety of irradiation facilities in order to meet the requirements of irradiation tests for research and development of nuclear fuels and materials, and radioisotope production.

The capsules are inserted into suitable irradiation holes in the reactor core according to required irradiation conditions. The two Hydraulic Rabbit irradiation facilities (HR-1 and HR-2) and the power ramping test facilities are installed in fixed positions in the reactor core.

Capsule irradiation facilities

The capsule irradiation facilities are used mainly for the irradiation tests of nuclear fuels and materials as well as for radioisotope production. The capsules are classified into three types;

- 1) *non-instrumented capsule*
- 2) *instrumented capsule*
- 3) *advanced type capsule*

The capsules are cooled by the reactor primary coolant. As a standard configuration of the core, up to 60 capsules can be loaded a cycle, of which 20 capsules are the instrumented capsules. The characteristics of irradiation field for the capsules are shown in Table 2.2.1. The types of the capsules are listed in Table 2.2.2 and schematically shown in Fig. 2.2.1.

Fig. 2.2.1
Capsule structure

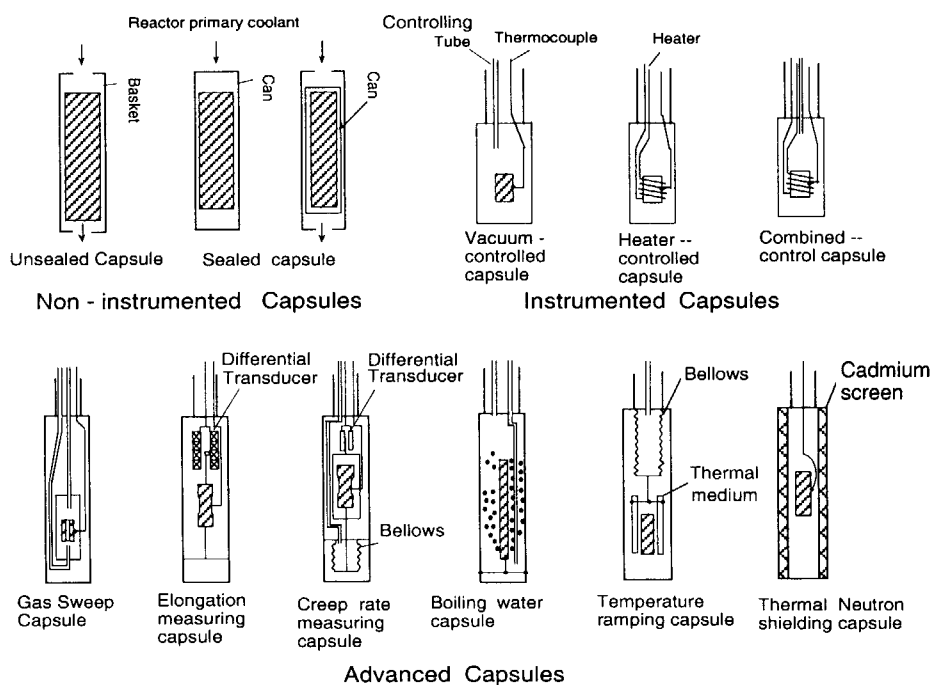


Table 2.2.1
Characteristics of
irradiation field for
capsules

Thermal neutron flux	$1.0 \times 10^{13} \sim 3.0 \times 10^{14} \text{ n}/(\text{cm}^2 \cdot \text{s})$
Fast neutron flux (>1MeV)	$1.0 \times 10^{13} \sim 2.0 \times 10^{14} \text{ n}/(\text{cm}^2 \cdot \text{s})$
γ heating rate	0.5 ~ 10 W/g
Heat generation of heater	Max. 100 kW

Table 2.2.2
Types of capsules

Type of capsule	Structure and function
Non-instrumented Capsule	
Unsealed capsule	Test specimens are held in an open-type basket, and are directly cooled by the reactor primary coolant.
Sealed capsule	Test specimens are contained in a sealed vessel which is cooled by the reactor primary coolant.
Instrumented Capsule	
Non-control capsule	Temperature of test specimen is not controlled. The temperature and/or neutron fluence around the specimens are measured by thermocouples and self-powered neutron detectors (SPND) or fluence monitors (FM).
Vacuum-control capsule	Temperature of test specimen is controlled by changing thermal conductivity of depends on helium gas layer between inner and outer vessels by regulating gas pressure.
Heater-control capsule	Temperature of test specimens is controlled by electric heaters wound around the specimens.
Combined-control capsule	Temperature of test specimens is controlled by combination of the vacuum-control and the heater-control.
Advanced type capsule	
Fission gas sweep capsule	This capsule is designed for measuring activity of FP gas released from coated particle fuels for HTTR fuel. FP gas is swept out to the sweep gas measuring equipment by carrier gas.
Elongation measuring capsule	Elongation of the specimen is measured by a differential transducer or a helium gas micrometer.
Creep rate measuring capsule	Test specimens are stressed by a pressurized bellows and its creep rate is measured by a differential transducer.
Boiling water capsule	Surface temperature of specimens is controlled by the pressure of boiling water which surrounds the test specimens.
Temperature ramping capsule	The temperature of test specimens is rapidly increased by removing a solid thermal medium which has high thermal conductivity and surrounds the test specimens.
Thermal neutron shielding capsule.	Test specimens are surrounded by thermal neutron absorber such as cadmium or hafnium for cutting thermal neutrons.

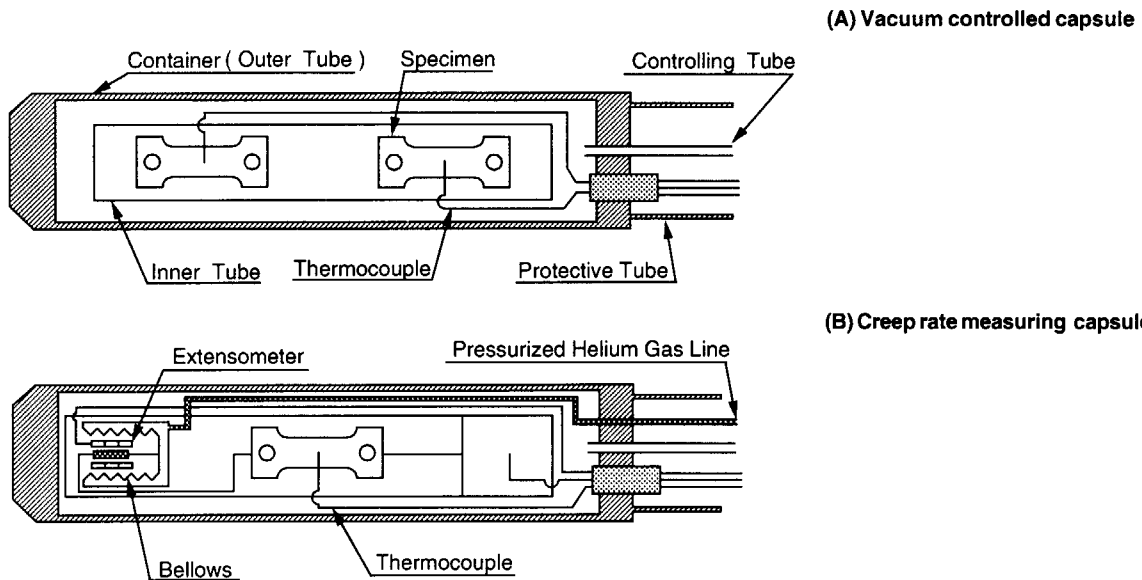
1) *Non-instrumented capsules*

In an unsealed capsule, the reactor primary coolant flows between specimens and the outer tube, and directly cools the specimens. In a sealed capsule, specimens are held in an aluminum or stainless steel can, and cooled indirectly.

2) *Instrumented capsules*

Using instrumented capsule, temperature of specimens and pressure can be controlled and measured on line. The instrumented capsule irradiation facilities consists of a capsule, a protective tube, a guide tube, a connection box and a control panel. The structure of a typical instrumented capsule is shown in Fig. 2.2.2, and a typical configuration of the control system is shown in Fig. 2.2.3. The capsule consists of a container (outer tube) which is made of stainless steel, an inner tube for holding specimens, a protective tube and a guide tube including the vacuum control tubes and the instrument cables. The guide tube is joined to the connection box around the reactor pool. The vacuum control tubes and the instrument cables are joined to the control panel through the connection box.

Fig. 2.2.2
Vacuum-controlled capsule and creep rate capsule



Currently, three methods are available to control temperature of specimen during irradiation.

① Vacuum-control method

Thermal conductivity of the helium gas in the annular space between inner and outer tubes is altered by changing pressure in order to control temperature. Range of the helium gas pressure is normally between 1.33×10^2 Pa and 1.37×10^5 Pa.

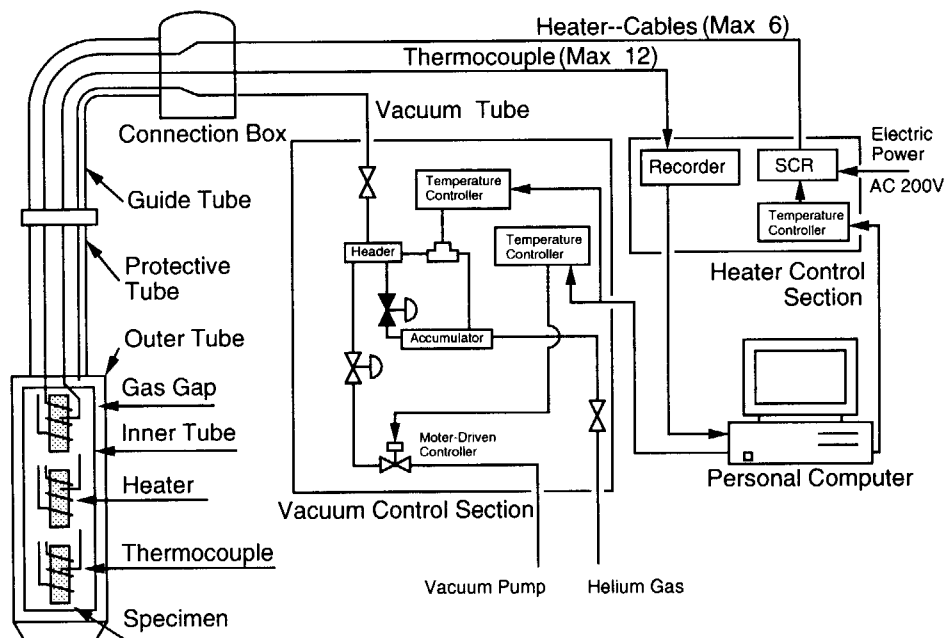
② Heater-control method

The temperature of specimens is controlled by electric heaters around specimens.

③ Combined-control method

The temperature of the specimen is controlled using combination of the two methods, vacuum control and temperate control, mentioned above. This method provides a fine control of the temperature of the specimen.

Fig. 2.2.3
Capsule control system



3) *Advanced type capsules*

Various advanced type capsules have been developed to accomplish required irradiation conditions (see Fig. 2.2.1 and Table 2.2.2).

As a typical example of advanced type capsule, the specification and the system configuration of the Fission Gas Sweep (FGS) capsule are shown in Table 2.2.3 and Fig. 2.1.4.

Table 2.2.3
Characteristics of
fission gas sweep
capsule

Type of fuel	Coated particle fuel
Diameter of coated particle fuel	$920 \times 10^{-6} \text{ m}$
Total amount of ^{235}U	Max. 6 g
Heat generation of the heater	Max. 41.2 kW
Temperature of the specimen	Max. 1600 °C
Flow rate of helium gas	1 g/min
Pressure of helium gas	0.3 MPa

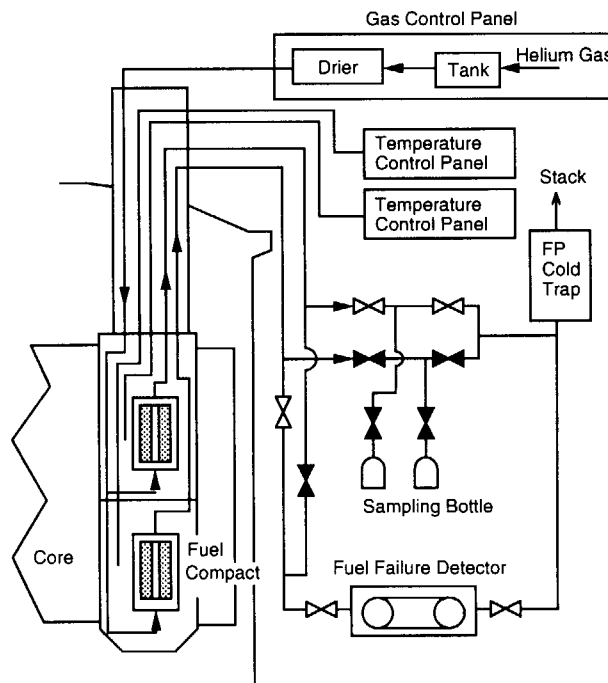


Fig. 2.2.4
Configuration of
fission gas sweep
capsule

Hydraulic rabbit irradiation facilities

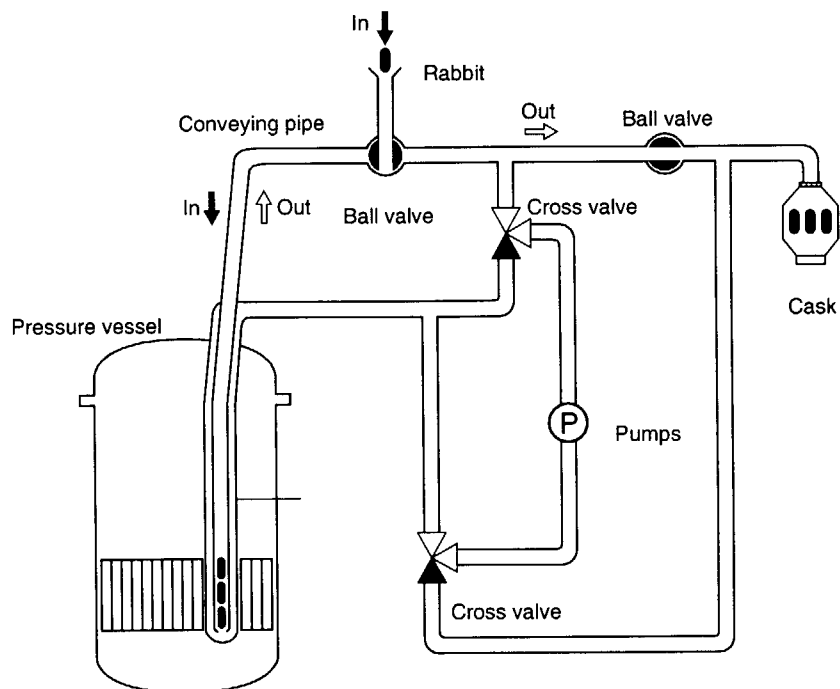
Two hydraulic rabbit irradiation facilities (HR-1 and HR-2) are installed for short term irradiations. The major specifications are shown in Table 2.2.4. The conceptual diagram of hydraulic rabbit is shown in Fig. 2.2.5.

Each facility consists of an in-pile tube, two pumps, a loading station and an unloading station. The specimen is put in a metallic holder called rabbit. The rabbit is transferred into the reactor core and withdrawn from the core by water flow, during the reactor operation by changing the direction of the cooling flow in the facilities.

Table 2.2.4
Major specifications of two hydraulic rabbit irradiation facilities

	HR-1	HR-2
Location in the core	D - 5	M - 11
Thermal neutron flux	$1.1 \times 10^{14}n/(cm^2 \cdot s)$	$1.3 \times 10^{14}n/(cm^2 \cdot s)$
Fast neutron flux (>1MeV)	$8.8 \times 10^{12}n/(cm^2 \cdot s)$	$2.1 \times 10^{13}n/(cm^2 \cdot s)$
γ heat rate	1.1 W/g	2.2 W/g
Coolant	Light Water	Light Water
Temperature of the coolant	Max. 50 °C	Max. 50 °C
Pressure of the coolant	2.0 MPa	2.0 MPa
Flow rate of the coolant	Max. 11.0 m ³ /h	Max. 8.4 m ³ /h
Dimension of the holder	$\phi 32 \times 150$ mm	$\phi 32 \times 150$ mm
Specimen dimension	Max. $\phi 26 \times 120$ mm	Max. $\phi 26 \times 120$ mm
Number of charged rabbit	Max. 3	Max. 3
Time of irradiation	Min. 1 min	Min. 1 min

Fig. 2.2.5
Conceptual diagram of hydraulic rabbit irradiation facility



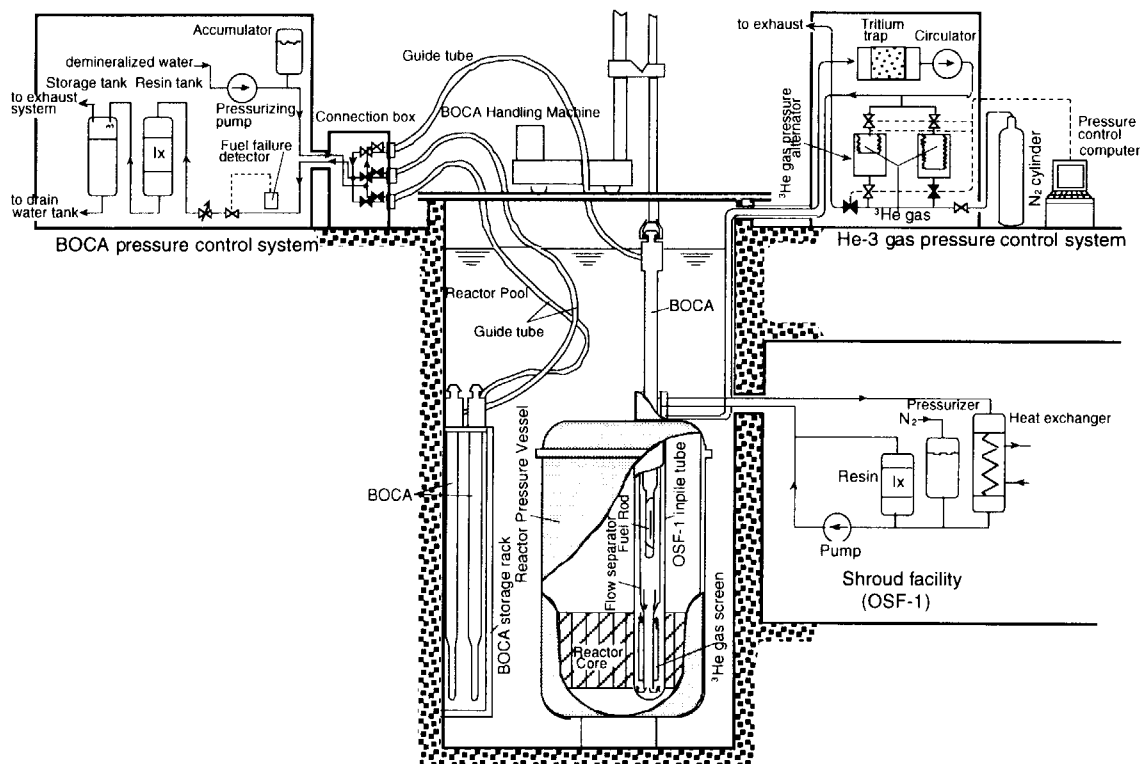
Power ramping test facility

The power ramping test facility consists of the Boiling Water Capsule (BOCA), the Oarai Shroud Facility-1 (OSF-1), BOCA pressure control system, a He-3 gas screen pressure control system and a BOCA handling machine. Arrangement of these components are shown in Fig. 2.2.6. Major specifications are shown in Table 2.2.5.

BOCA	Coolant	Light water
	Press. of the coolant	7.3 MPa
	Flow rate of the coolant	1.0 cm ³ /s
	Linear heat rate	Max. 60 kW/m
	Thermal neutron flux	Max. 2.6×10^{14} n/(cm ² ·s)
	Fast neutron flux (>1MeV)	Max. 2.2×10^{13} n/(cm ² ·s)
OSF-1	Location in the core	D-9
	Coolant	Light water
	Pressure of the coolant	0.4 MPa
	Flow rate of the coolant	1.9 m ³ /h
	Temp. of the coolant	Max. 90 °C
	γ heating rate	Max. 2.5 W/g

Table 2.2.5
Major specifications of the power ramping test facility

Fig. 2.2.6
Power ramping test facility



BOCA is used to contain a fuel rod test element in a coolant condition simulating core channel of the boiling water reactor (BWR). Main structure of BOCA is cylindrical tube of stainless steel with 800 cm long and 6.9 cm in maximum outer diameter. Its inside configuration is explained in Fig. 2.2.7.

Each BOCA is connected to the pressure control system through connection box. Cooling water pressurized at 7.3 MPa is injected from the control system. It flows around the fuel rod test element in the lowest part of the capsule and is boiled due to heat generated in the fuel during irradiation. Four BOCA's can be connected to the connection box in maximum, and one capsule of these is inserted at a time into the in-pile tube of OSF-1 to perform power ramping test.

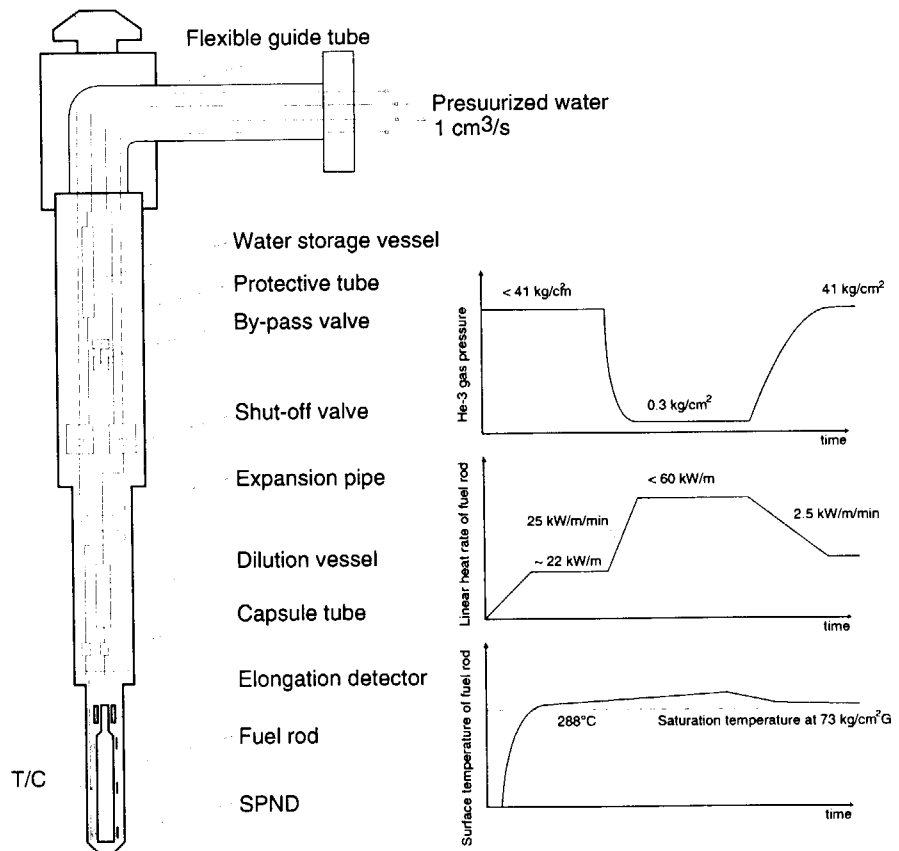
The in-pile tube of OSF-1 is penetrating into the JMTR core through the top head of the reactor. OSF-1 has a penetration at the elevation near reactor top head, through which a BOCA is inserted into the in-pile tube of OSF-1. Inserted BOCA can be exchanged even in the reactor operation using BOCA handling machine.

OSF-1 has an independent cooling circuit to remove heat generated in BOCA. In pile tube has He-3 gas screen, an aluminum annular cylinder containing He-3 gas. Its pressure can be changed in order to control screening effect on thermal neutron, therefore to control fission rate in the fuel rod installed in BOCA.

Typical transients of the He-3 gas pressure, linear heat rate and surface temperature of fuel rod test element during power ramping test are shown in Fig. 2.2.8. Heat generation rate is estimated by calorimetric method based on measured inlet/outlet temperature difference and flow rate of the in-core tube of OSF-1.

Fig. 2.2.7 (left)
Boiling water capsule
(BOCA)

Fig. 2.2.8(Lower right)
Change of linear heat rate and surface temperature for fuel rod by He-3 gas pressure change



Data acquisition system : IOSS

Irradiation Facility Operation Support System (IOSS) is a computer system for monitoring operating condition and collection of the irradiation test data of all irradiation facilities. The configuration of this system is shown in Fig. 2.2.9.

IOSS is capable to collect and record the data from 1024 measurement points in the capsules and other facilities every 2 seconds. Collected data are used to prepare irradiation reports for the users.

Removed irradiation facilities

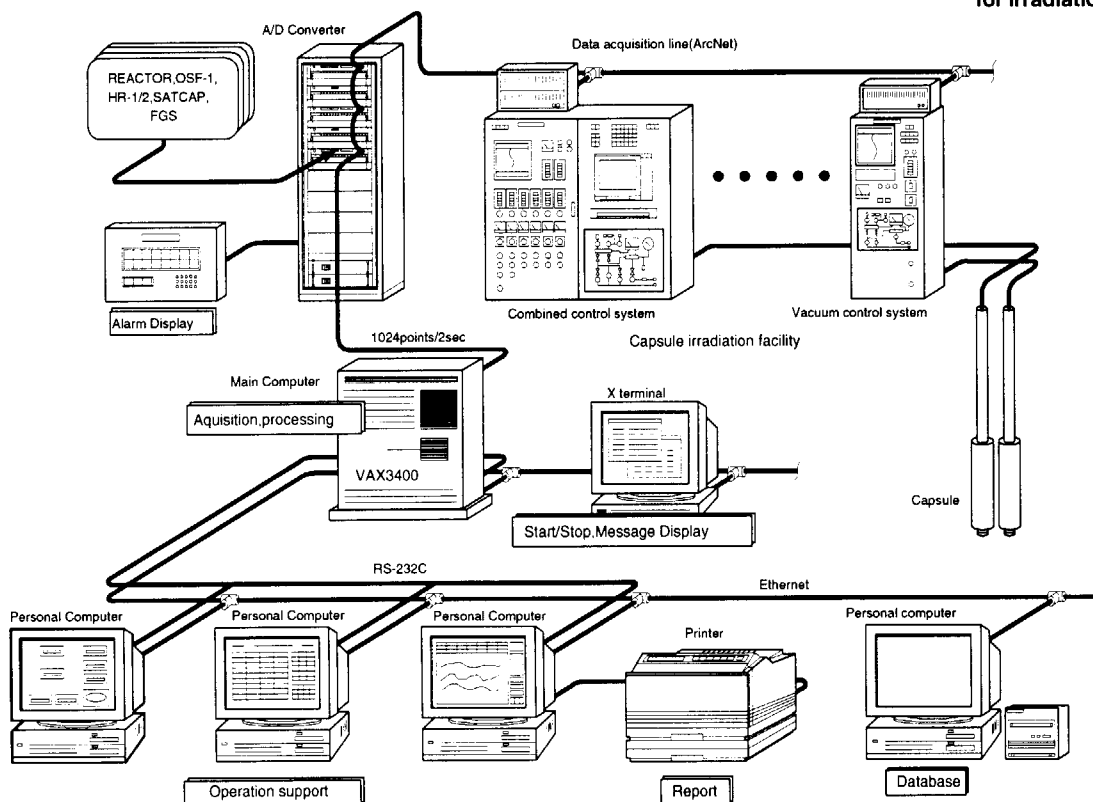
There were several irradiation facilities in JMTR other than the facilities mentioned above. OWL-1 was an in-pile water loop for testing fuels and structural materials of BWR and of PWR. The OWL-2 was other in-pile water loop for the irradiation tests of fuels and materials for PWR, BWR and advanced thermal reactor (ATR). These irradiation facilities simulate PWR, BWR or ATR condition.

NCF was constructed for controlling the total neutron flux or the temperature of the specimen by moving the capsule vertically.

OGL-1 was in-pile gas loop, and built for the irradiation tests to develop the HTTR fuels and materials.

These irradiation facilities were already removed after completion of their original purposes.

Fig. 2.2.9
Data acquisition system
for irradiation facilities

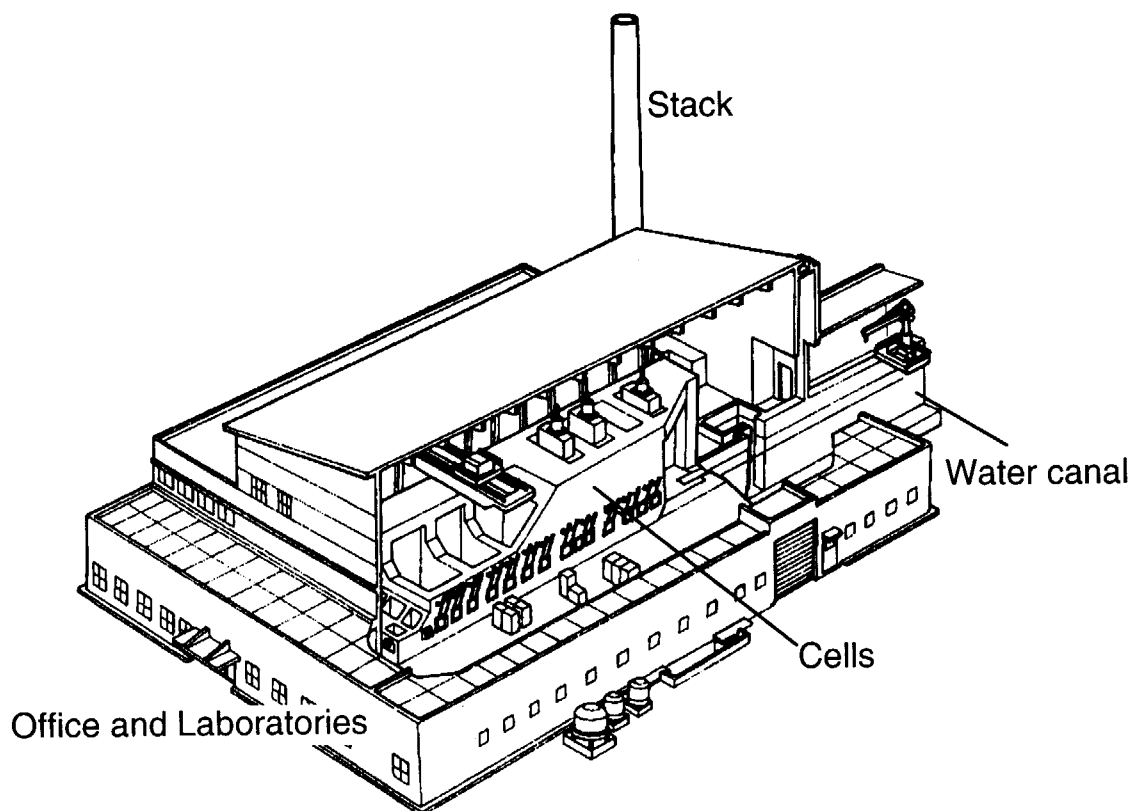


2.3. Hot Laboratory

Specimens irradiated in JMTR are usually transferred to the Hot Laboratory (see Fig. 2.3.1) for post irradiation examination (PIE). The Hot Laboratory is connected to the reactor through a water canal.

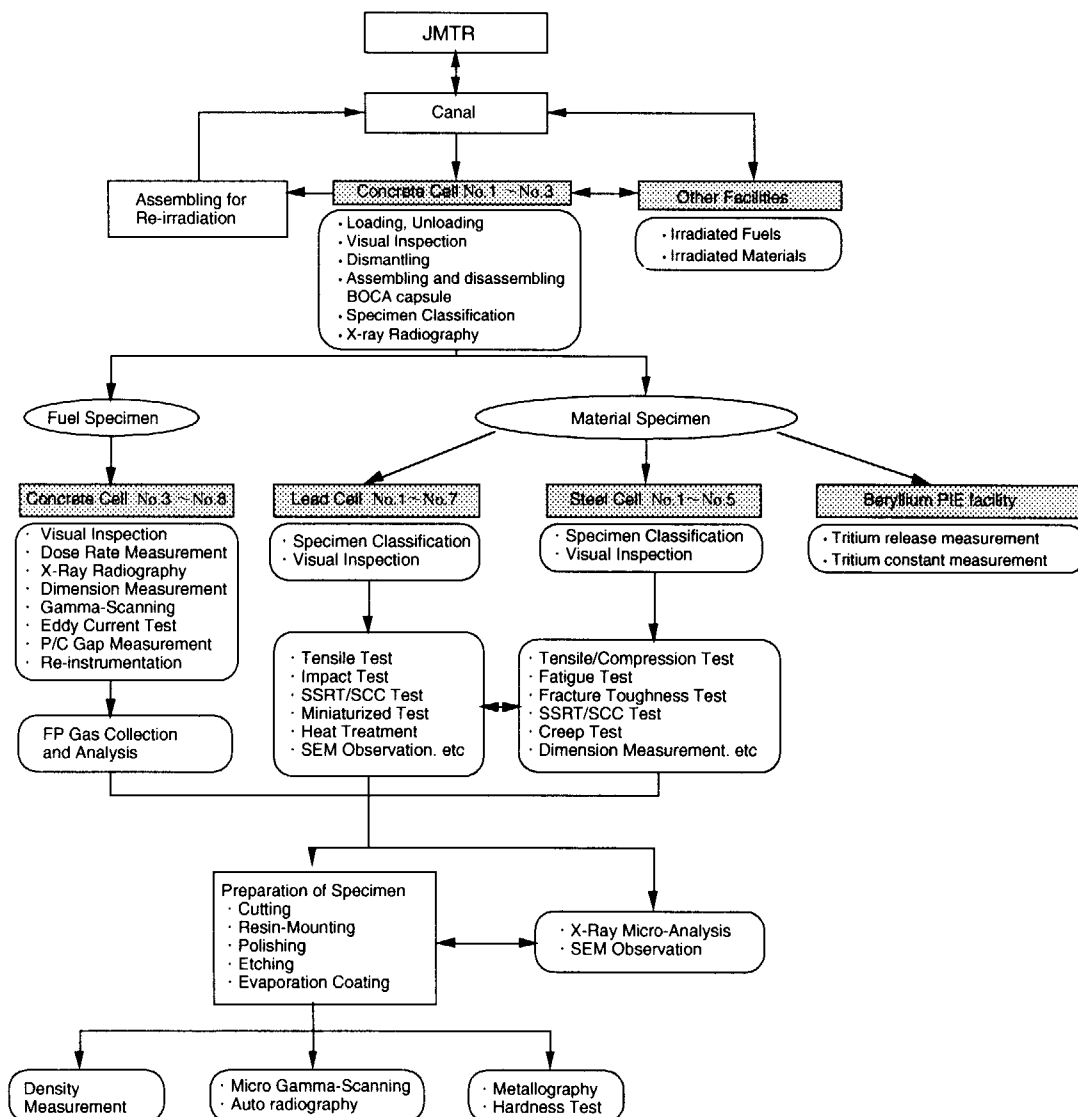
Construction of the hot laboratory started in 1967 and its service started in 1971. Additional steel cells were equipped in the hot laboratory in 1982.

Fig. 2.3.1
Hot laboratory
building



The hot laboratory provides the data of post irradiation examinations (PIE) on the fuels and materials irradiated in the JMTR and/or other reactors. The concrete cells, the lead cells and the steel cells are located in the hot laboratory. After preparatory works for the post irradiation examination in the C-1 through C-3 concrete cells, nondestructive examinations and destructive examinations on irradiated fuel specimens are carried out in other concrete cells. Mechanical property test on irradiated material specimens are carried out in the lead cells and/or the steel cells. The flow diagram of the post irradiation examinations in the hot laboratory is shown in Fig. 2.3.2.

Fig. 2.3.2
Flow diagram of post irradiation examination



Arrangement of hot laboratory

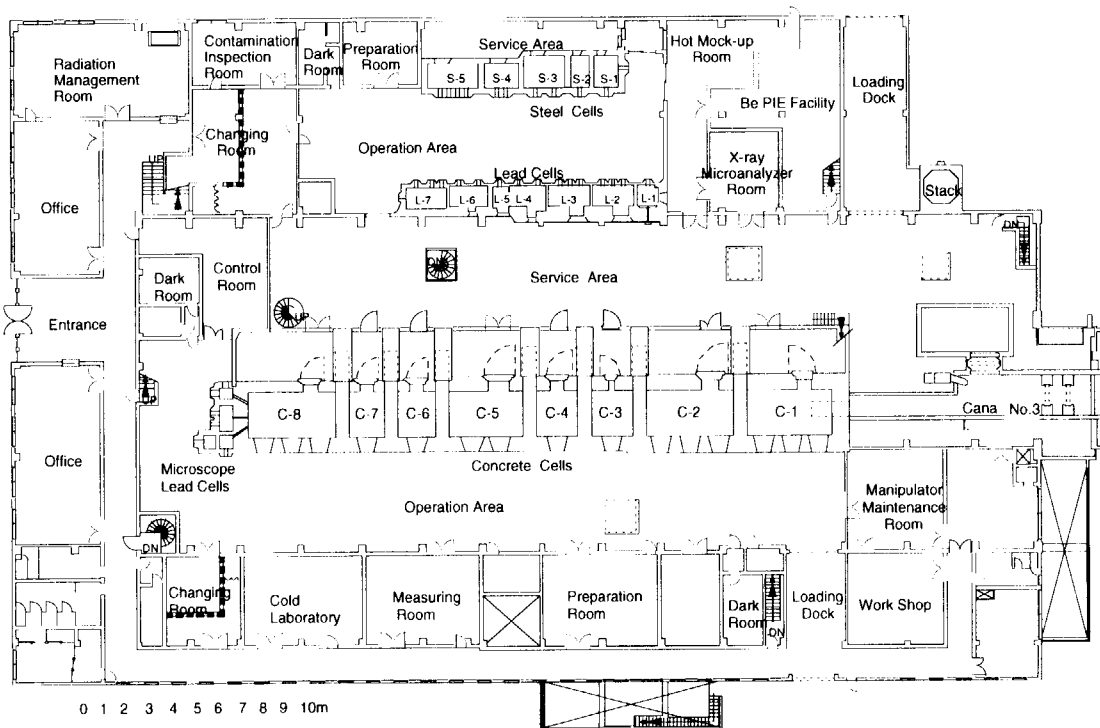
The hot laboratory is connected to JMTR through the water canal which is used to transfer irradiated capsules from JMTR and to JMTR for re-irradiation. The building houses the concrete cells with the microscope lead cells, the lead cells and the steel cells. Each cell is designed as so called β - γ cell. Fig. 2.3.3 shows the arrangement in the ground floor of the hot laboratory. Auxiliary facilities such as the ventilation system, the power supply system and the liquid waste disposal system are located on the basement.

Concrete cells and microscope lead cell

Using 8 concrete cells and 4 microscope lead cells, following works can be carried out:

- ① loading and unloading capsules
- ② disassembling irradiated capsules
- ③ re-capsuling
- ④ re-instrumentations of specimens
- ⑤ nondestructive examinations of fuel specimens
- ⑥ destructive examinations of fuel specimens

Fig. 2.3.3
Hot Laboratory



The maximum length of the fuel specimens to be handled in the hot laboratory is about 1 m. The irradiated capsules in JMTR are transferred into the C-1 cell from the canal after cooled. The capsules irradiated in the other reactors are transported by the transport casks and loaded into the C-1 cell through the posting port installed on the ceiling. The re-instrumentations on the fuel specimens are carried out in the C-7 cell, then re-instrumented fuel specimens are installed into the Boiling Water Capsule (BOCA) in the C-1 cell.

Among the PIEs performed in the concrete cells, Nondestructive Examinations (NDEs) are visual inspection, X-ray radiography, dimensional measurement, gamma scanning, eddy current test and pellet/ cladding (P/C) gap measurement. As Destructive Examinations (DEs), fission gas collection and analysis, density measurement of fuel specimens and sample preparation for metallography, are performed.

Metallography, hardness measurements, autoradiography and micro-gamma scanning for fuels and materials are carried out in the microscope lead cells attached to the concrete cells. Preparatory works for composition analysis and fractography with the X-ray Micro-Analyzer (XMA) installed in another room are carried out in the concrete cells.

The wall of the concrete cells is constructed with the high density magnetite concrete and its thickness is 1 m or 1.1 m. The shielding windows (dry type) with equivalent shielding thickness to the wall are installed in the wall. In the microscope lead cells, lead bricks with thickness of 17.8 cm and shielding windows were built into the wall. Table 2.3.1 shows the specifications of the concrete cells and the microscope lead cells. Fig. 2.3.4 shows the major apparatus and functions of the concrete cells and the microscope lead cells.

Table 2.3.1
Specification of concrete
cells and microscope
lead cells

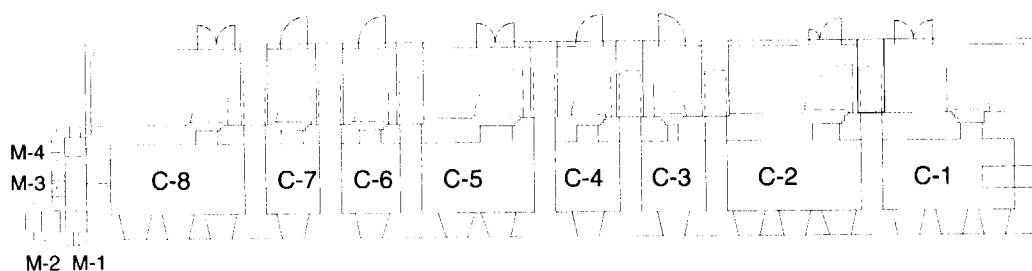
Cell No.	Inside dimension	Shielding wall		Number of windows	Maximum activity (1MeV)
	W x D x H	thickness	density		
C-1	6 x 3 x 5.5 m	1.1 m	>3.8	3	33 pBq
C-2	6 x 3 x 5.5 m	1.1 m	>3.8	3	33 pBq
C-3	3 x 3 x 5.5 m	1.0 m	>3.8	1	3.7 pBq
C-4	3 x 3 x 4.5 m	1.0 m	>3.8	1	1.1 pBq
C-5	5 x 3 x 4.5 m	1.0 m	>3.8	2	1.1 pBq
C-6	2.5 x 3 x 4.5 m	1.0 m	>3.1	1	85 TBq
C-7	2.5 x 3 x 4.5 m	1.0 m	>3.1	1	85 TBq
C-8	6 x 3 x 5.5 m	1.0 m	>3.1	3	85 TBq

(A) Concrete cells

Cell No.	Inside dimension	Shielding wall	Number of windows	Maximum activity (1MeV)
	W x D x H	thickness		
M-1	1 x 1 x 1.1 m	17.8 cm	1	3.7 TBq
M-2	1 x 0.85 x 1.1 m	17.8 cm	1	3.7 TBq
M-3	1.59 x 1 x 1.1 m	17.8 cm	2	3.7 TBq
M-4	1.5 x 1 x 0.95 m	17.8 cm	2	3.7 TBq

(B) Microscope lead cells

Fig. 2.3.4
Functions and major apparatus
in concrete cells



Cell no.	Functions	Main Apparatus & specifications	Cell no.	Functions	Main Apparatus & specifications
C-1	Lifting up irradiated capsules from water canal Irradiated specimens loading and unloading BOCA capsule assembling and dismantling Visual inspection Dose measurement	Loading lift Capacity:500kg Loading cask Shielding wall Pb 150mm End-plug tightener Torque:7kg · m Periscope Mag. ×10 Dose measuring device 3mR ~ 10,000R, 0.1mR/min, 35keV ~ 1.2MeV 0mR ~ 1000R, 0.1mR/min, 40keV ~ 3MeV	(C-5)	Leak test of fuel rod Welding for re-fabrication Machining of end plug	Leak locator Size: φ 50 ~ φ 20, 100 ~ 800mm Medium:White spirit ρ=0.794 Size: φ 9 ~ φ 40 Remote welding machine Size: φ 9 ~ φ 40 Welding method:Tig welding End plug machining device Size: φ 8 ~ φ 20±0.05mm, 100 ~ 800mm
C-2	Dismantling of capsule Cutting of capsule Processing after reweld for irradiated test piece	Diamond cutter Size:Max. φ 60, Blade width 1.0mm Guillotin cutter Size: φ 120 ×5t Power:Max.200ton Milling machine		Weight measurement Density measurement Electromotive force measurement	Mettler balance Cap:Max. 160g ±0.0001g Max.1200g ±0.01g Densimeter Cap:Max. 150g ±0.01g/cc Medium:Metaxylene Electromotive force measuring apparatus Furnace size: φ 40, 150mm Temp range:100 ~ 1000°C in Inert gas
C-3	X-ray radiography Gamma scanning	X-ray radiography system Cap:150kVp, 300kVp, Film size 140×990 Gamma scanning system Scanning speed:5,10,20,40mm/s, Collimator:0.2 ×20,1×15, φ 0.75, φ 1.5	C-6	Electron beam heating facility	Beam power Max.50kW Beam current Max.1.7A
C-4	Eddy current test Pellet/Clad gap measurement Dismantling of NaK capsule	Eddy current testing machine Size: φ 4 ~ φ 17, 100 ~ 1000mm Feed speed: 5 ~ 30mm/s Gap measuring apparatus Size: φ 6 ~ φ 18, 50 ~ 1000mm Gap range:1mm ±5 μm NaK capsule dismantling machine Size: φ 15 ~ φ 50, 150 ~ 800mm Medium:Kerosen (Max. Nak 200cc)	C-7	Making center hole of UO ₂ pellets to insert thermocouple	Drilling machin Size: φ 2.0, 54mm Frozen CO ₂ (-78°C) machining:-160°C
C-5	Dimensional measurement FP gas volume and pressure measurement FP gas analysis Preparation for XMA sample	Dimension measuring apparatus Diameter: φ 5 ~ φ 30 ±0.005mm Bowling : ±3.0mm ±0.02mm Length : 0 ~ 1000mm ±0.02mm Puncturing device and gas collector Size: φ 6.0 ~ φ 17, 30 ~ 1000mm Mass spectrometer Detection limit:Kr, Xe, H ₂ , He, Ar, CH ₄ , O ₂ , O ₂ , N ₂ + CO, CO ₂ 0.01v% Vacuum evaporator Size: φ 30×30H Vacuum (3×10 ⁻⁴ Pa)	C-8	Preparation for metallography	Micro cutter(Diamond cutter) Test piece: Max. φ 30, Cutting width 1mm Grinding polisher: Abrasive paper #180 ~ #100 Ultrasonic cleaner: 100W, 28kHz Resin impregnating machine: Vacuum(10 ⁻² P) Periscope: Magnification ×4.5 ~ ×45
			M-1	Metallography	Magnification: x 50 ~ 900
			M-2	Metallography	Magnification: x 50 ~ 900
			M-3	Metallography Hardness test	Magnification: x 5 ~ 10(zoom) Load: 50, 100, 200, 500, 1,000 g Measuring mag. : x 400
			M-4	Micro-gamma scanning	Step scanning: 0.1 mm Collimater : φ 0.2 ~ 0.5 Detector: Ge-Nal anticoincidence Ge 50cc, 2.5 keV

Master-slave manipulators, power manipulators and in-cell hoists are installed in the concrete cells. Ball socket manipulators are installed in the microscope lead cells.

An isolation room is attached to the each concrete cell to prevent splashing of radioactive materials from the concrete cell to the service area. The isolation room are lined with steel plates on the floor and the lower part of wall for easier decontamination. Each cell has a shielding access door. The access door is a hinge type and manually opened with mild steel shielding wall in the rear side. It is used as entrance for the personnel for decontamination and maintenance works.

Lead cells

The lead cells consist of 7 cells for post irradiation examinations on material specimens. The irradiated specimens to be examined are brought in/out through a wall type posting port installed in the rear wall of the L-1 cell. The L-1 cell is used for interim storage of specimens which require relatively long cooling interval after irradiation.

The post irradiation examinations carried out in the lead cells are tensile test, Stress Corrosion Cracking (SCC) test, instrumented impact test, visual inspection, dimensional measurement, and others.

The post irradiation examinations on miniaturized specimen used in the study of fusion reactor materials are carried out in the lead cells, including the development of testing techniques.

The front wall of the each cell is built up with the lead bricks with a thickness of 15 cm or 20 cm. It has shielding windows (dry type) which have an equivalent shielding thickness to the wall. Table 2.3.2 shows the specifications of the lead cells. Fig. 2.3.5

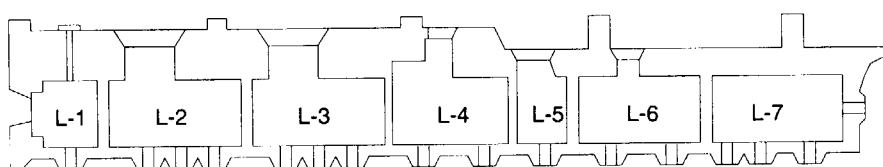
Table 2.3.2
Specification of lead
cells

Cell No.	Inside dimension W x D x H	Shielding wall thickness	Number of windows	Maximum activity (1MeV)
L-1	1.5 x 1.3 x 1.95 m	20 cm	1	1.2 TBq
L-2	2.9 x 1.75 x 2.25 m	15 cm	3	37 GBq
L-3	2.9 x 1.75 x 2.25 m	15 cm	3	37 GBq
L-4	1.2 x 1.75 x 1.8 m	15 cm	2	37 GBq
	1.2 x 1.25 x 1.8 m			
L-5	1.2 x 1.25 x 1.8 m	15 cm	1	37 GBq
L-6	2.8 x 1.25 x 1.8 m	15 cm	2	37 GBq
L-7	2.75 x 1.25 x 1 m	15 cm	4	37 GBq

shows the major apparatus and functions of the lead cells. Each lead cell is provided with a pair of master-slave (M/S) manipulators and some of them are provided with ball socket manipulators.

The rear wall of the each cell is constructed with the ordinary concrete with necessary shielding thickness. Each cell is provided with a shielding access door and a transfer port

Fig. 2.3.5
Functions and major
apparatus of lead cells



Cell no.	Functions	Main Apparatus	Specifications
L-1	Specimen identification	Periscope	Mag.:x10
	Specimen storage	Storage pits	60 pits
L-2	SSRT/SCC test	SSRT/SCC testing machine	Capacity: 30kN Test temp.: ~320 Atmospher: Purified water, Inert gas
	Visual inspection	Periscope	Mag.: x10
L-3	Tensile test	Tensile testing machine (Instron-type)	Capacity: 10kN Test temp.: Max.1500 Atmospher: Vacuum
	Charpy impact test	Instrumented Charpy impact testing machine	Capacity: 300J Test temp.: -120~200°C
	Visual inspection	Periscope	Mag.: x10
L-4	Miniaturized specimen test	Small punch testing machine	Capacity: 5kN Test temp.: -160 ~750 °C Atmospher: Vacuum
	Heat treatment	Heat treatment furnace	Test piece volume:Max. φ30x100l Atmospher: Vacuum or Ar gas Test temp.: Max.1000°C
	Visual inspection	Periscope	Mag.: x10
L-5	Miniaturized specimen machining	Electrical discharge machining device	Atmospher: Oil
L-6	Miniaturized specimen test	High speed punch testing machine	Capacity: 1kN Test temp.: -150°C Atmospher: Vacuum
	Miniaturized specimen handling	Micro-manipulator	
L-7	Fractography	Scanning electron microscope	Mag.: x15~200,000 Resolving power:0.5~3kV 5~30kV 40nm

for the transportation of specimens to the next hot cells. The access door is hinge type and manually opened with mild steel shielding wall in the rear side. The doors are used for entrance and exit of personnel for decontamination and maintenance works of the cells.

Steel cells

The steel cells consist of 5 cells which are mainly used for testing the property of material specimens. Major items of the post irradiation examinations carried out in the cells are high temperature tensile/compression test, fracture toughness test, creep test, fatigue test, SCC test, visual inspection and dimensional measurement.

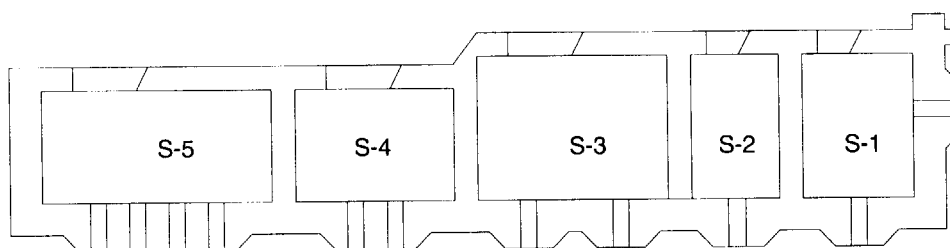
Cell walls of operation side are built with the mild steel with a thickness of 35 cm or 40 cm and the shielding windows (dry type) which have the equivalent shielding thickness to the wall. Table 2.3.3 shows the specifications of the steel cells. Fig. 2.3.6 shows the apparatus and functions of the steel cells.

A pair of master-slave (M/S) manipulators are installed in each cells. Each cell has a shielding access door made of mild steel. The access doors are hinge type built in the rear side of the shielding wall and used for entrance and exit of personnel for decontamination and maintenance works in the cell. Transfer ports installed on the partition walls of the cells are used for transfer of specimens to the adjacent hot cells.

Table 2.3.3
Specification of steel
cells

Cell No.	Inside dimension W x D x H	Shielding wall thickness	Number of windows	Maximum activity (1MeV)
S-1	2 x 1.7 x 2.4 m	35 cm	2	66 GBq
S-2	1.3 x 1.6 x 2.35 m	40 cm	1	5.9 TBq
S-3	3.2 x 1.7 x 2.4 m	35 cm	2	66 GBq
S-4	2.2 x 1.25 x 2.4 m	35 cm	2	66 GBq
S-5	4 x 1.25 x 2.4 m	35 cm	4	66 GBq

Fig. 2.3.6
Functions and major
apparatus of steel cells



Cell no.	Functions	Main apparatus	Specifications
S-1	Low cycle fatigue test	Fatigue testing machine	Capacity: 100kN Atmospher: Vacuum Test temp.: ~900°C Cyclic speed: Max 100Hz
	Dimensional measurement	Dimensional measuring device	Max. Length: 100mm Precision: ±10μ m
S-2	Specimen storage	Storage pits	42 pits
	Visual inspection	TV Monitor	
S-3	Tensile/compression test	Tensile/compression testing machine	Capacity : 50kN (Instron type) Atmospher : Air or Ar gas Test temp.: -150~900°C
	Fracture toughness test	Fracture toughness testing machine	Capacity : 63kN Atmospher : Air Test temp.: -150~500°C
	Visual inspection	Periscope	Mag.: X 10
S-4	SSRT/SCC test	SSRT/SCC testing machine	Capacity : 20kN Atmospher : Purified water or Ar gas Test temp.: ~320°C
	SCC test	UCL/SCC testing machine	Capacity : 5kN Atmospher : Purified water or Ar gas Test temp.: ~320°C
S-5	Creep rupture test	Creep rupture testing machines(3)	Capacity : 10kN Atmospher : Vacuum or Ar gas Test temp.: Max:1000°C
	Creep deformation test	Creep testing machine	Capacity : 5kN Atmospher : Vacuum or Ar gas Test temp.: Max:1000°C

SSRT: Slow Strain Rate Tensile
 SCC: Stress Corrosion Cracking
 UCL: Uni-axial Constant Load

X-ray Micro-Analyzer

The X-ray micro-analyzer (XMA) consists of a sample chamber, an electron gun, an EDS cooling system, a gate valve and a transportation cask (Fig. 2.3.7). The sample chamber is surrounded with a tungsten shielding wall for radiation protection.

The XMA is used for an element analysis of micro sphere on specimens and observation of dispersion status of specified element and observation of surface status by secondary electron, backscattered electron and absorbed electron.

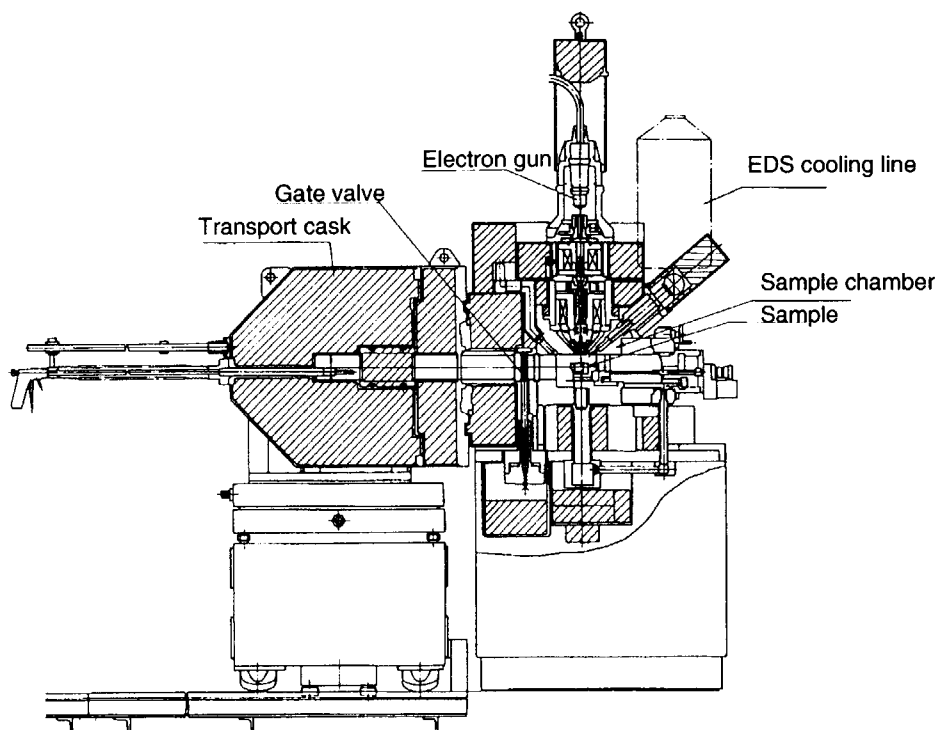
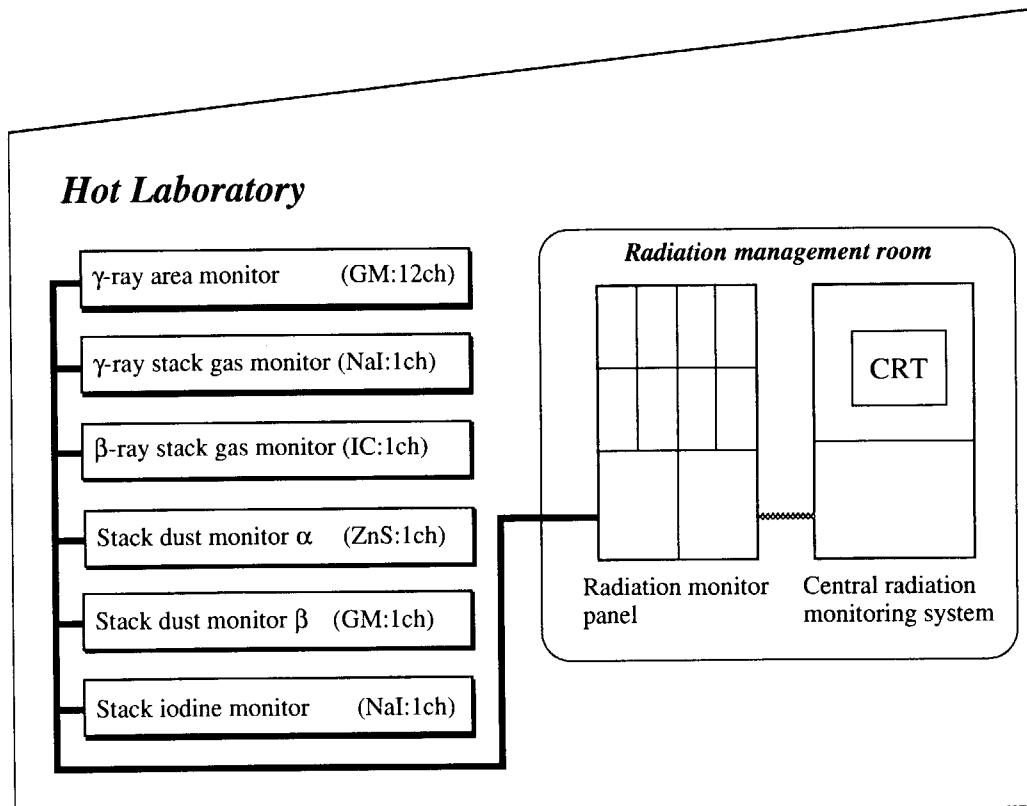


Fig. 2.3.7
X-ray micro-analyzer
(XMA)

Radiation monitoring system

Radiation monitoring in the hot laboratory is carried out continuously by the central radiation monitoring system as shown in Fig. 2.3.8. The central radiation monitoring system and radiation monitoring panel is located at the radiation management room in the hot laboratory.

Fig. 2.3.8
Central radiation
monitoring system in
the hot laboratory



3. Activities in FY1997

3.1. Reactor Operation

JMTR has been operated with a Low Enriched Uranium (LEU) fuel core since its 108th operation cycle in 1994. A renewal work of the pressure surge tank of the reactor primary cooling system has been continued since the previous year. Exchange of vent drain valves of the cooling system was carried out as a countermeasure against small leakage detected by the annual inspection from some valves. The operation of 123rd cycle was postponed till November and operation cycles in FY1997 were changed from expected 4 cycles to 3 cycles resulting in the valve exchanging work. Operation summary of FY1997 is shown in Table 3.1.1. The integrated reactor power of 120th, 121st and 122nd operation cycles attained 116,505.2 MWD. The nuclear characteristic values of each operation cycle were measured at a low-power level of 20 kW prior to the high-power operation for irradiation. Values of excess reactivity, shutdown margin and the worth of the two regulating control rods (SR-1, SR-2) are listed in Table 3.1.2.

During reactor operation, chemical analysis of the reactor cooling water is regularly performed, which detects ^{24}Na , ^{27}Mg , some radioactive isotopes of iodine, etc.. The concentration of the radioactive isotopes are shown in Fig. 3.1.1 and Fig. 3.1.2 for the interval from 116th to 122nd operation cycles. No significant change took place during these operation term. Detected radioactive iodines are considered to be produced by the fission of impure uranium included in the beryllium reflector elements. 1,828.2 m³ of high-purity demineralized water was supplied to the primary cooling channel, the pool-canal and the cooling system of the irradiation facility during FY1997. 294,770 m³ of filtered water was supplied to the secondary cooling channel and to some other utility systems.

Table 3.1.1
Operation summary
of FY1997

Operation cycle No.	Period* ¹	Integral power (MWd)	Operation time* ² (hours:minutes)	Operation efficiency (%)* ³	Cumulative integral power (MWd)
120	97.11.25 ~ 97.12.20	1231.9	613:46	99.3	11,4136.2
121	98. 1.19 ~ 98. 2.13	1227.8	605:05	98.9	11,5364.0
122	98. 3. 2 ~ 98. 3.14				
	98. 3.16 ~ 98. 3.29	1141.2	570:14	94.7	11,6505.2

Note *1 Period indicates the startup and shutdown dates for 50MW operation.

122nd cycle scammed due to the less of commercial power.

*2 Operation time excludes the time to get the nuclear properties of the reactor.

*3 Operation efficiency = Actual integral power / Scheduled integral power (1241 MWd)

Operation cycle No.	Excess reactivity (% Δ k/k)	Shutdown margin (% Δ k/k)	Rod worth of automatic control rods		
			keff	SR-1 (% Δ k/k)	SR-2 (% Δ k/k)
120	11.40	30.7	0.77	0.24	0.20
121	11.45	41.3	0.71	0.23	0.26
122	11.23	42.0	0.70	0.24	0.24

Table 3.1.2
Nuclear characteristics
of each operation cycle

Fig. 3.1.1
Radioactive nuclide
concentration in
primary coolant.
(From 116th to
122nd operation
cycles of JMTR)

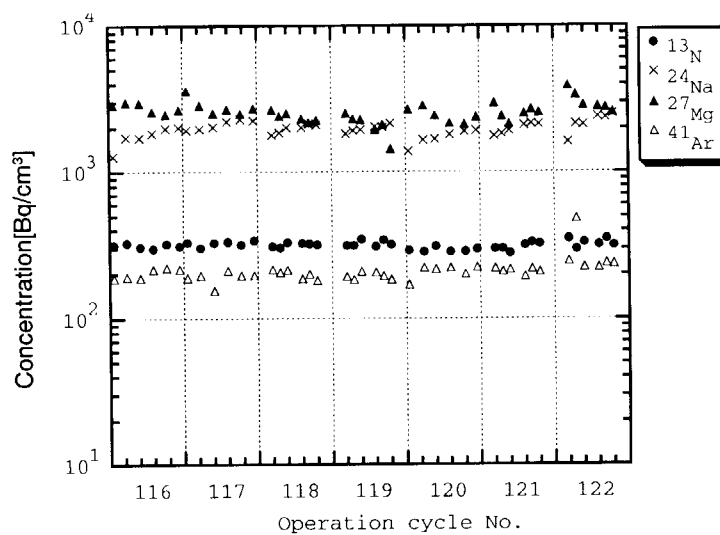
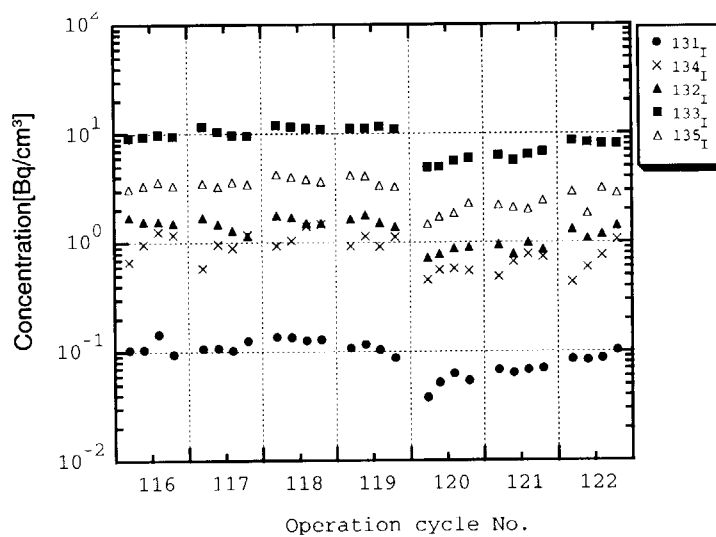


Fig. 3.1.2
Radioactive iodines
concentration in
primary coolant.
(From 116th to
122nd operation
cycles of JMTR)



Personnel exposure and release of radioactive waste

1) Personnel exposure

Records in JMTR during FY1997 are in Table 3.1.3. There has been no occupational exposure exceeding the prescribed effective dose equivalent limit.

2) Release of radioactive gaseous nor liquid waste

Records in JMTR during FY1997 are in Table 3.1.4. Neither radioactive gaseous nor liquid waste released exceeding the release limit specified in the relevant regulations.

Table 3.1.3
Annual effective dose equivalent of personnel at JMTR

Contents	No. of personnel	No. of personnel with accumulated dose (mSv) of each range			collective dose equivalent (person · mSv) ^{*1)}
		Undetectable	$0.2 \leq D \leq 1$	$1 < D \leq 5$	
JAERI personnel	123	123	0	0	0
Visiting researchers	13	13	0	0	0
Consigned employee	209	208	1	0	0.3

*1) Not detect according to internal exposure

Table 3.1.4
Gaseous and liquid waste released from JMTR

Gaseous, dust wastes		
Gaseous	(Bq)	2.9×10^{13} (⁴¹ Ar)
Gross α -emitter		Undetectable
Gross β -emitter		Undetectable
Iodine-131		Undetectable
Liquid wastes ^{*2)}		
Volume	(m ³)	1.8×10^3
Main nuclide		³ H, ⁵¹ Cr, ⁶⁰ Co

*2) Those liquid wastes were transported to Radioactive Waste Management Facilities and there treated.

3.2 Fuel and Reflector Management

Acceptance

The JMTR standard fuel elements and followers are manufactured by CERCA (France) and BWXT (USA). Thirty-nine standard fuel elements and 25 fuel followers were supplied for JMTR in FY1997. In order to reduce transportation times of them, fuel elements for two operation cycles were manufactured at one fabrication contract.

Delivery of spent fuel

JMTR spent fuel had been transported to reprocessing plants in Europe, and then to plants in USA in order to extract the uranium still remaining in the fuel. The JMTR spent fuel transportation had been continued until the end of 1988. However USA had ceased spent nuclear fuel reprocessing, while USDOE committed to prepare an environmental review of the impacts of accepting spent nuclear fuel from foreign research reactors. After USDOE decided to implement a new acceptance policy in 1996, JMTR commenced transport of the spent fuel elements (60 elements) to Savannah River Site in June 1997. It was the first transportation not only in Japan but in Asian also. Prior loading of spent fuel elements into the casks, staff of USDOE inspected their integrity. They confirmed that all fuel elements to be shipped showed good integrity.

Inspection

Twelve times of the safeguard inspection measures were carried out on the basis of the inspection agreement between Japanese Government and IAEA.

Renewal of pressure surge tank

In the period of annual inspection in 1996, very small cracks penetrating a plate of a manhole-nozzle stub of the pressure surge tank were detected. Resulting in investigation of the cause of initiation and propagation of the cracks, it was decided that the tank should be replaced.

After obtaining an approval for design and construction method issued by the Science and Technology Agency (STA), the renewal work had commenced. A configuration of the tank is shown in Fig. 3.2.1.

The new surge tank was manufactured and installed in JMTR in this fiscal year. A water level gauge of the surge tank was also replaced to a new system. After installing the tank was inspected by STA as well as during manufacturing, the renewal work was completed with acceptance of the certification of the relevant inspections conducted by STA. The time schedule of the renewal work is shown in Table 3.2.1.

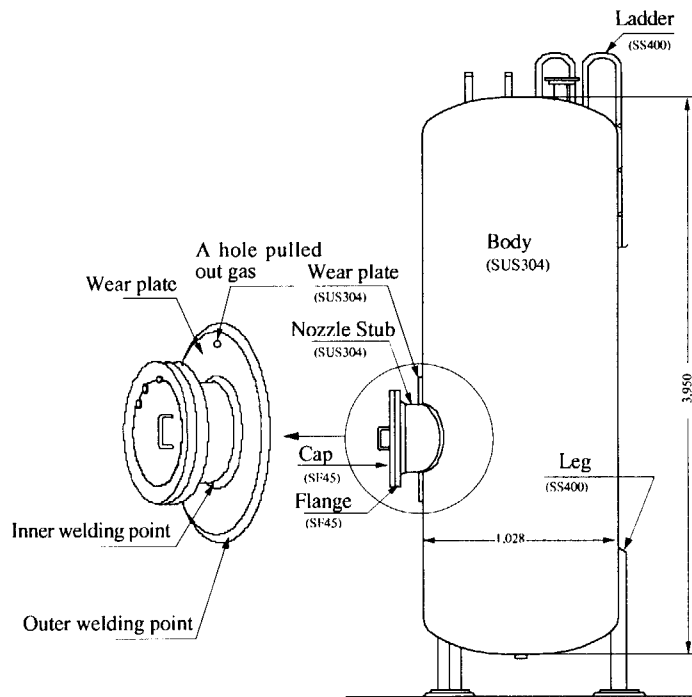


Fig. 3.2.1
The outline drawing of pressure surge tank

FY1997								
January	February	March	April	May	June	July	August	September
		△	△	△	△	△		
		Obtaining of material		Manufacture, assembling and weld				
					△	△		
					Remove and set			
					△	△		
					Inspection by STA			

Table 3.2.1
Schedule to exchange pressure surge tank

3.3. Utilization of Irradiation Facilities

JMTR has several kinds of irradiation facilities. These are the equipment for capsule irradiation tests, OFS-1 shroud facility and hydraulic rabbit driving devices. Using these facilities, various irradiation tests, the radioisotope productions and irradiation technique development have been performed. Irradiation tests are conducted by the requests of research staffs of JAERI, of universities and of other research organizations. Irradiated materials are mostly fuels and structural materials, which are being used in nuclear facilities or under development to be used.

Capsules and hydraulic rabbits irradiated during FY1997 are summarized in Table 3.3.1, Table 3.3.2 and Table 3.3.3, as breakdowns by the type of irradiation device, related research field and user category, respectively. Total irradiation cycle (sum of the irradiation cycle for each capsule) for capsules and total irradiation time (sum of the irradiation time) for the hydraulic rabbits are also shown in Table 3.3.2 and Table 3.3.3. Radioisotope productions in FY1997 are shown in Table 3.3.4. Breakdowns according to the related research field and user category are shown in Fig. 3.3.1 and Fig. 3.3.2.

Table 3.3.1
JMTR irradiation results
in FY1997

Irradiation Device		Reactor Operation			Total
		120cy	121cy	122cy	
Capsules		32	29	23	84
(type)	Instrumented	18	16	15	49
	Non-Instrumented	13	12	7	32
	FGS	1	1	1	3
(material)	Fuel	5	3	3	11
	Material	27	26	20	73
BOCA		2	4	5	11
Rabbits		22	15	8	45

Related Research Field	Capsule & BOCA		Hydraulic Rabbit	
	item	cycle·item	item	hour·item
Fusion R&D	16	31		
LWR R&D	13	19		
Researches at Universities	7	9	43	2819
Irradiation Technique	5	14	2	36
RI Production	4	4		
FBR Fuel Development	3	7		
ATR Fuel Development	1	3		
HTTR Fuel Development	1	6		
Fundamental Researches	1	2		
Total	51	95	45	2855

Table 3.3.2
Purpose of JMTR
utilization in FY1997
(Capsule, BOCA and
Hydraulic Rabbit)

User Category	Capsule & BOCA		Hydraulic Rabbit	
	item	cycle·item	item	hour·item
JAERI (Laboratories)	14	30		
JAERI (JMTR)	17	41	2	36
JAERI (Isotope)	4	4		
Universities	7	9	43	2819
PNC	1	3		
Others	8	8		
Total	51	95	45	2855

Table 3.3.3
Users of JMTR
Utilization in FY1997
(Capsule, BOCA and
Hydraulic Rabbit)

Radioisotope	Target	Application	Production
^{192}Ir	Ir pellet($\phi 1.1 \times 1.2\text{mm}$)	Radiation source of non-destructive inspection	24 TBq
$^{191}\text{Ir}(n,\gamma)$	Ir pellet($\phi 0.6 \times 3.5\text{mm}$)	Radiation source for treatment of cancer	
^{33}P	S powder	Tracer in agricultural and industrial field	7.4 GBq
$^{31}\text{S}(n,p)$			
^{89}Sr	SrCO_3 powder	Radiation source for treatment of cancer	3.7 MBq
$^{88}\text{Sr}(n,\gamma)$			
^{188}Re	$^{186}\text{WO}_3$ powder	Radiation source for treatment of cancer	100 MBq
$^{186}\text{W}(2n,\gamma) \rightarrow ^{188}\text{W}$, $^{188}\text{W}(\beta^-) \rightarrow ^{188}\text{Re}$			

Table 3.3.4
List of capsules and
Rabbits irradiated for
radioisotope production
in FY1997

Fig. 3.3.1
Capsules irradiated in JMTR during FY1997

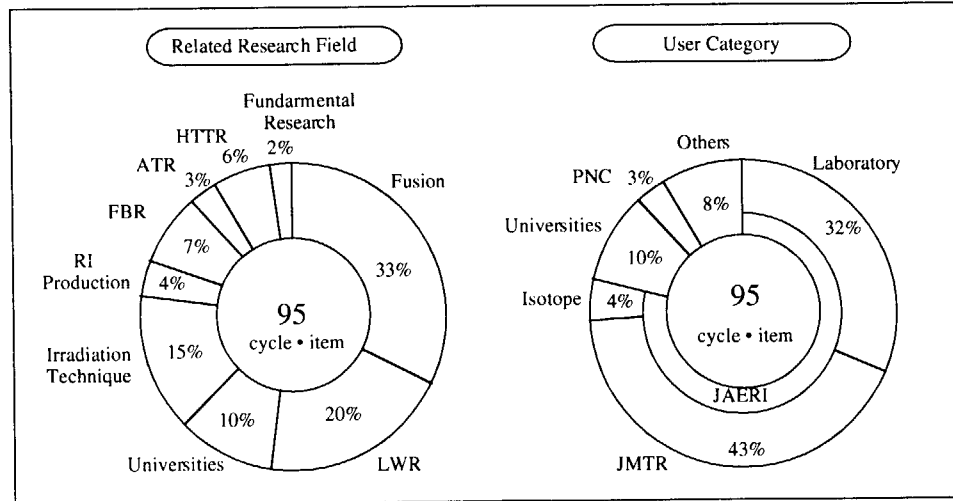
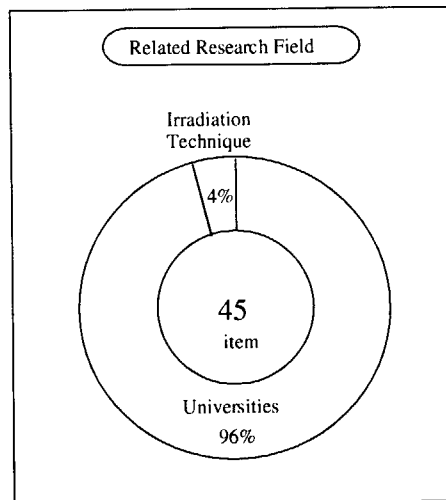


Fig. 3.3.2
Hydraulic Rabbits irradiated in JMTR during FY1997



3.4. Maintenance Engineering

Improvement of evaluation on maintenance records

The computer software has been developed to acquire daily patrol data of reactor facilities into a handy computer such as HANDY TERMINAL. Lists of 738 facilities and devices have been registered using the ID number for each device. From the ID number, it is possible to sort and classify the patrol data for every week or month, for each device.

3.5. Post Irradiation Examinations

Post irradiation examinations (PIEs) performed in the hot laboratory during FY1996 were on LWR fuels subjected to power ramping test, NSRR test fuels, structural materials of LWR, HTTR and fusion reactor, shape memory alloys, and others. Remote recapsuling of BOCAs for the power ramping tests in JMTR and their remote dismantling after the tests were also performed.

Nuclear fuels

1) Fuel rods for power ramping test

A fuel rod segment irradiated in power reactors was installed into and take out from the BOCA in the C-1 concrete cell. After assembling of the BOCA, the fuel rod was shipped to the Nuclear Fuel Development Co. (NFD) hot laboratory for PIEs. Concerning the fuel rods irradiated for the tests by JAERI researchers, their PIEs were carried out in the concrete cells.

2) Nuclear Safety Research Reactor (NSRR) test fuel rods

Destructive tests on the test fuel rods of NSRR were carried out such as FP gas collections and analyses, and metallography after the nondestructive tests. These fuels were also examined by micro-gammascanning, autoradiography and density measurements.

Structural materials

1) Structural materials of LWR

Test pieces of stainless steel for core internal were irradiated to develop the life estimation of LWR. The PIEs on these test pieces were performed as tensile test, slow-strain-rate tensile test, metallography and scanning electron microscopy.

2) Structural materials of HTTR

Test pieces of materials of pressure vessel and control rod cladding were irradiated to study their characteristics. The PIEs on test pieces of pressure vessel materials were carried out by small punch test. PIEs on the specimens of control rod cladding material were performed as metallography and scanning electron microscopy.

3) Structural materials of fusion reactor

Test piece of stainless steel (SUS316 (JIS)) and Inconel 625 for vacuum vessel of fusion reactor were irradiated to study the re-welding characteristics. The PIEs such as weldment test, milling machining, dimension measurement, visual inspection, tensile test, metallography and scanning electron microscopy were carried out.

4) Structural materials of capsules

Test pieces of shape memory alloys were irradiated to study the effect of neutron irradiation. The PIEs such as Charpy impact test, high temperature tensile test, constant-load deformation test, fracture toughness test, fractography and metallography were carried out. Test pieces of friction welding materials (Nb-1Zr/SUS304 (JIS)) for capsule were also irradiated to study irradiation effect on the material. The PIEs such as tensile test, hardness test, metallography and X-ray microanalysis were carried out.

5) Treatment of radioisotope production capsules

During FY1996, 11 radioisotope production capsules were treated in the hot laboratory and dismantled in the C-2 concrete cell. Produced radioisotopes were 3.12×10^{14} Bq of ^{192}Ir , 2.5×10^{12} Bq of ^{33}P , 9.9×10^{11} Bq of ^{51}Cr , 6.6×10^{11} Bq of ^{35}S and 6.1×10^{12} Bq of ^{169}Yb , 3.7×10^6 Bq of ^{89}Sr and 1.0×10^9 Bq of ^{188}Re . There were transported to the Department of Radioisotope Production in the Tokai Establishment of JAERI.

Personnel exposure and release of radioactive waste

1) Personnel exposure

In the hot laboratory, there was no occupational exposure exceeding the prescribed effective dose equivalent limit as shown in Table 3.5.1.

2) Release of radioactive gaseous and liquid waste

There was no release of gaseous and liquid wastes from the hot laboratory exceeding the release limit specified by relevant regulation. Amount of gaseous and liquid wastes released from the hot laboratory are shown in Table 3.5.2.

Table 3.5.1
Annual effective dose equivalent of personnel in the hot laboratory

Contents	No. of personnel	No. of personnel with accumulated dose (mSv) of each range			collective dose equivalent (person · mSv) ^{*1)}
		Undetectable	$0.2 \leq D \leq 1$	$1 < D \leq 5$	
JAERI personnel	26	23	3	0	1.1
Visiting researchers	4	4	0	0	0
Consigned employee	172	167	5	0	1.2

*1) Not detect according to internal exposure

Table 3.5.2
Gaseous and liquid wastes released from the hot laboratory

Gaseous, dust wastes		
Gaseous (Bq)	8.6×10^9 (^{85}Kr), 3.3×10^8 (^{41}Ar)	
Gross α -emitter	Undetectable	
Gross β -emitter	Undetectable	
^{131}I	Undertectable	
Liquid wastes ^{*2)}		
Volume (m ³)	6.5×10^1	
Main nuclide	^{60}Co , ^{134}Cs , ^{137}Cs	

*2) Those liquid wastes were transported to Radioactive Waste Management Facilities and there treated.

4. Topics in FY1997

4.1. Evaluation of Neutron Field for Irradiation

With progress of nuclear material developments, the needs on irradiation test shifts to the one with high quality and high precision. Since effect of neutron energy spectrum on the irradiation damage is regarded to be important from the viewpoint of irradiation correlation, detailed spectrum information and neutron spectrum adjustment are needed in irradiation tests for R&D of light water reactor or fusion reactor materials. The technology development has been conducted since 1992 to positively respond to these requirements.

Neutron energy spectra which have been provided for JMTR users are the data evaluated for each layer of the core (fuel region, reflector layer No.1, 2, etc.) based on the multi-foil measurement using JMTRC (JMTR Critical Facility). It is difficult to evaluate neutron spectrum accurately at local position in irradiation capsule using these layer-wise spectra because of strong dependence on capsule structure materials. The development of evaluation procedure of neutron energy spectrum at local position in irradiation capsule is therefore proceeded. Analysis of neutron spectrum at local position using multi-foil method and 3-D Monte Carlo code MCNP with cross-section data library of JENDL3.2 was started from FY1996. The MCNP calculation model was described to 3-dimensional geometry in whole core of JMTR. Evaluation of calculated neutron flux at local position was conducted in FY1997. Fig. 4.1.1 shows JMTR core configuration and hydraulic rabbit. The result of evaluation of fast neutron flux at local position in hydraulic rabbit was shown in Table 4.1.1. The calculated neutron flux in this case was overestimated by 2 %. As a result of verification of calculated neutron flux using measured data of neutron fluence monitor using various types of irradiation capsules, it was confirmed that calculation could estimate fast neutron flux within about 10 % error at local position.

The evaluation of neutron flux or spectrum at local position need long-time calculation (about few month) for getting of reasonable calculation data. Therefore, examination of shortening for calculation time using variance reduction technique in Monte Carlo calculation was started from 1997. As an examination of the calculation time shortening, calculation model of fuel element was simplified (Fig. 4.1.2). As the result, the calculation time was shorten to about 1/3.

In order to respond to the requirement of JMTR users, the calculated neutron spectrum at irradiated sample position was offered from February 1997. An example of calculated neutron spectrum is shown in Fig. 4.1.3. Calculated neutron spectrum at an optional neutron energy group within 137 Groups (MGCL group structure) can be provided for JMTR users.

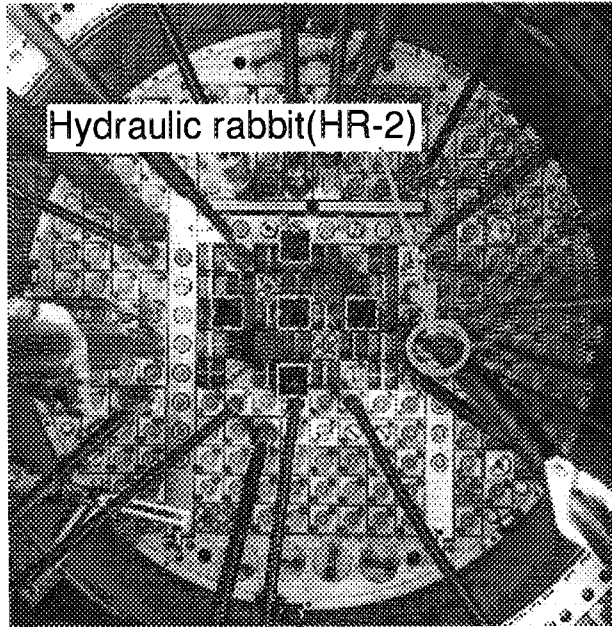
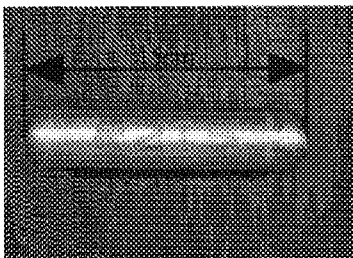
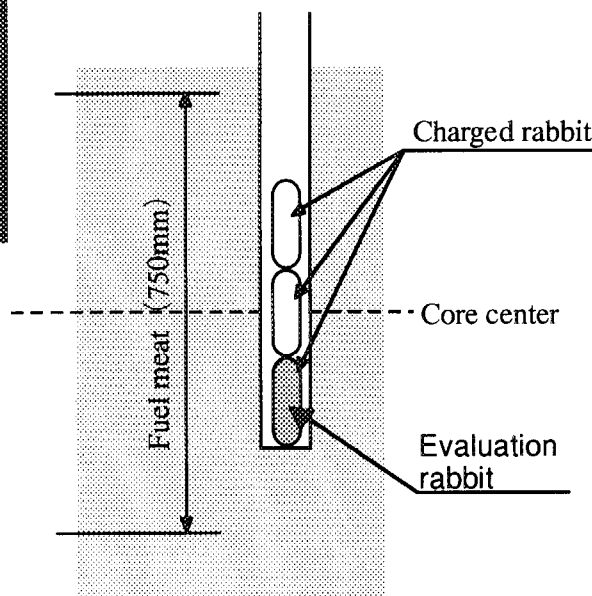


Fig. 4.1.1
JMTR core and hydraulic rabbit

(a) JMTR core



(b) Rabbit (Al)



(c) Concept of irradiation position of hydraulic rabbit

MCNP cal.	Measurement	Ratio
$6.581 \times 10^{17} \text{ n/m}^2\text{s}$	$6.435 \times 10^{17} \text{ n/m}^2\text{s}$	1.02

Table 4.1.1
Evaluation of fast neutron flux in hydraulic rabbit

Fig. 4.1.2
Fuel element model

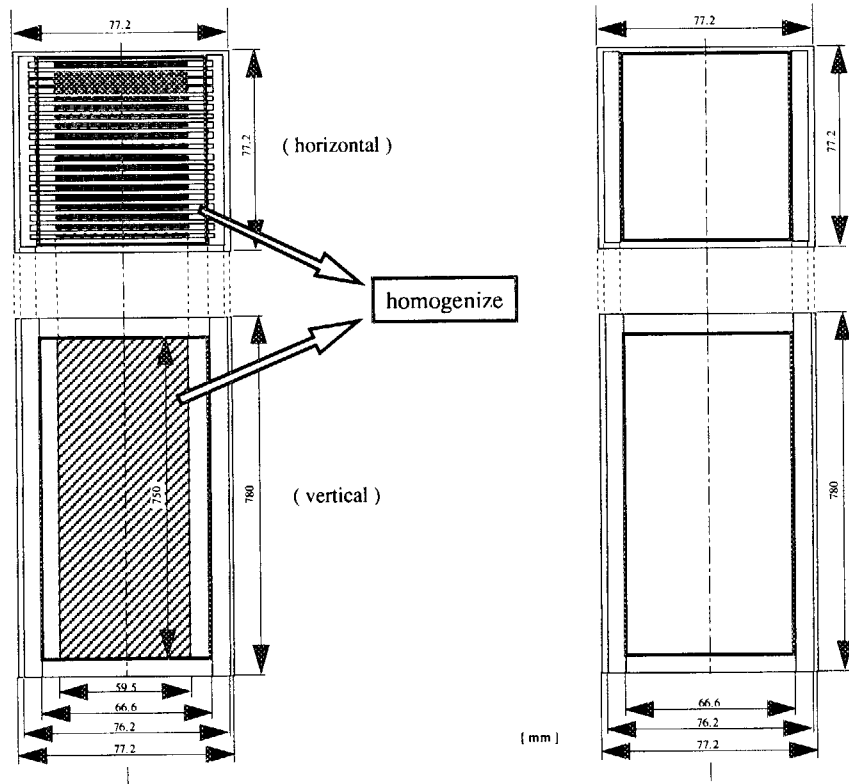
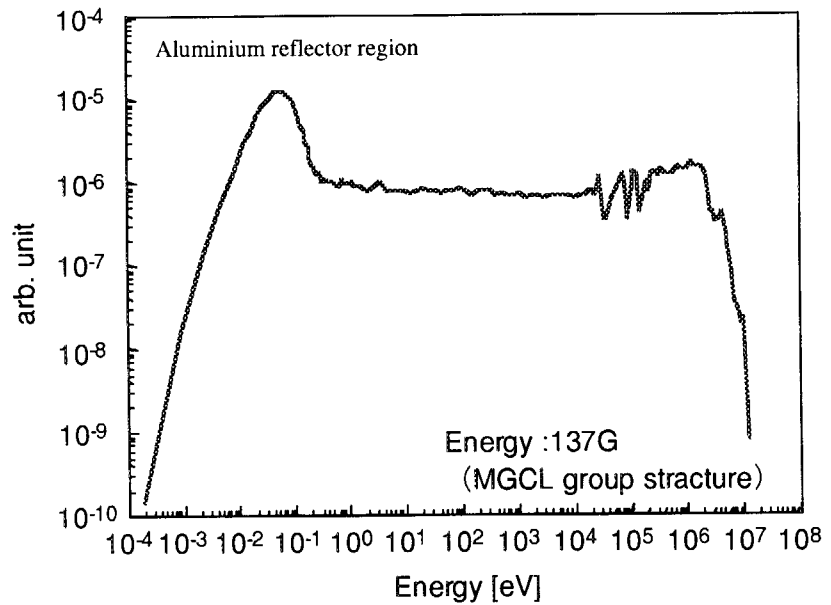


Fig. 4.1.3
Neutron spectrum in
sample position by
MCNP



4.2. Design of Capsules and Irradiation Facilities

Development of the oxygen potential sensor

To examine mechanism of the chemical behavior of nuclear fuel under irradiation, an oxygen potential sensor is being developed. The oxygen potential sensor uses the zirconia as a solid electrolyte. In FY1997, a gas supply type of oxygen potential sensor in which the gas is used as a standard pole and a measurement pole was newly made. The conceptual scheme is shown in Fig. 4.2.1. The out pile test result with the gas supply type is shown in Fig. 4.2.2. This result shows that the electromotive force was stable beyond 770 K.

The gas type sensor was irradiated up to $4.0 \times 10^{23} \text{ m}^{-2}$ of fast neutron fluence for the 2 cycles (about 50 days) from 120th to 121st operation cycle. This is shown in Fig. 4.2.3. This result shows that the electromotive force is stable byword 870 K under irradiation. It was found that the oxygen ion conduction function of the solid electrolyte was hardly affected by neutron irradiation if the temperature beyond 870 K.

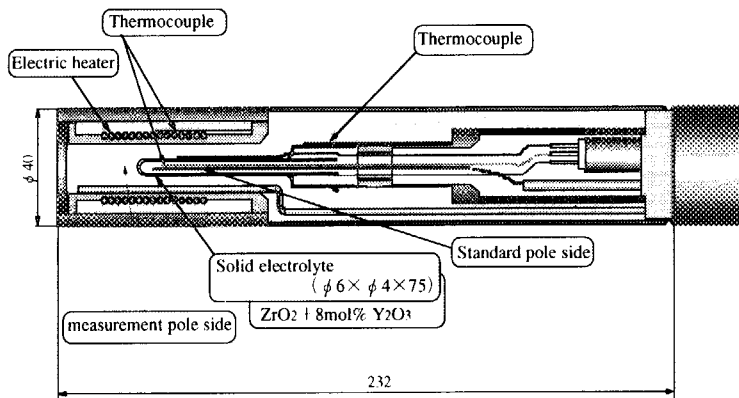


Fig. 4.2.1
Gas supply type oxygen sensor

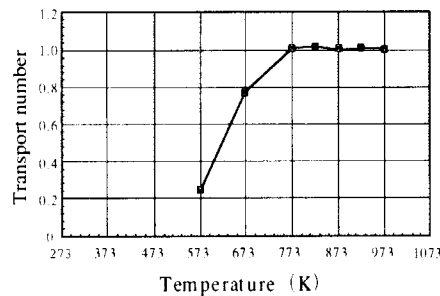
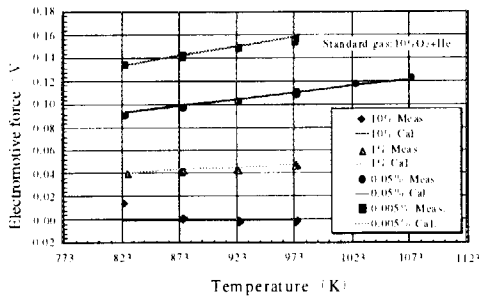


Fig. 4.2.2
Transport number of the oxygen sensor (right)

Fig. 4.2.3
Electromotive force under irradiation (left)

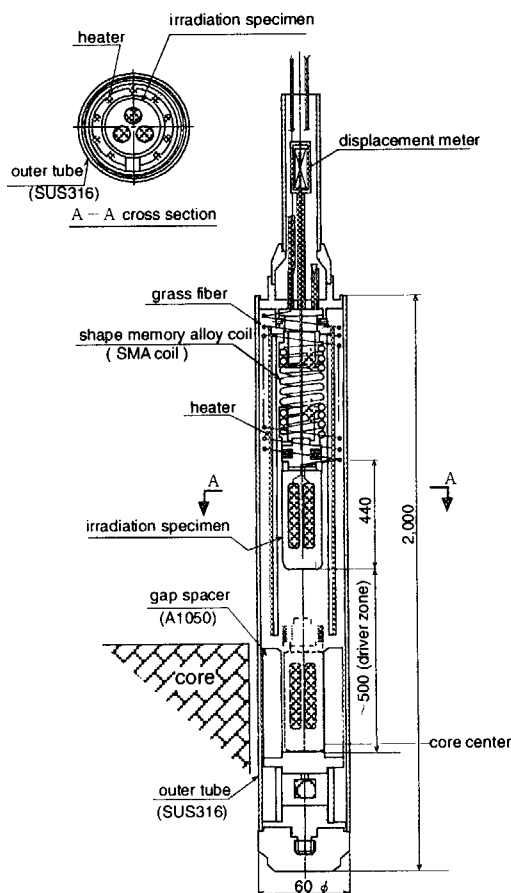
Applied technique of shape memory alloy

-Vertical migration type capsule of irradiation sample-

The coil of Shape Memory Alloy (SMA) is capable of moving a sample unit in long span. And it is confirmed that the SMA capability hardly changed under irradiation.

The irradiation sample in a vertical migration type capsule was moved perpendicularly by elastic force using the temperature change of the SMA coil. The schematic drawings of the capsule is shown in Fig. 4.2.4. The SMA coil was made to be Ti50-Ni50 (at %), coil wire diameter was 2 mm, mean diameter of coil was 26 mm, free length was 172 mm and migration length was 430 mm in design. The irradiation test of the capsule was carried out for the 2 cycles (about 50 days) from 120th to 121st cycles in FY1997. In the 120th cycle, vertical migration test were 2 times under irradiation, and the migration length was about 320 mm. And in the 121st cycle, the migration length was about 290 mm. But after the reactor shutdown, it was possible to insert to the designed point (core center) where the migration length was about 430 mm. The reason why the migration length during irradiation was shorter than the designed one was assumed that the irradiation temperature of the coil became over 368 K which is the reversible transformation start temperature.

Fig. 4.2.4
Schematic drawings of
capsule



Coupling irradiation techniques

The coupling irradiation techniques are the combined irradiation between the JMTR and the other irradiation facilities (a fast reactor, an accelerator, a light water reactor, etc.). This irradiation is the techniques which enable the new irradiation research. At the first step, in FY1995, non-instrumented capsule was irradiated. At the second step, in FY1996 irradiated sample (RI : radioisotope) were assembled in the instrumented capsule main body in the hot cell. In FY1997, in the water canal this capsule main body was jointed with a vacuum tube and 12 thermocouple lines, and covered by the protection tube. The capsule was loaded in the JMTR, and irradiated up to $1.0 \times 10^{25} \text{ m}^{-2}$ of fast neutron fluency for the 4 cycles (about 100 days) from 120th to 123rd cycles. Assembly flow chart of the capsule is shown in Fig. 4.2.5. And the irradiation temperature results are shown in Fig. 4.2.6. The target of irradiation temperature was 773 K, but there were the dispersion of irradiation temperatures from 700 K to 790 K. Next plan is to develop a re-irradiation capsule and a returnable capsule which can control irradiation temperature with an electrical heater by FY1999.

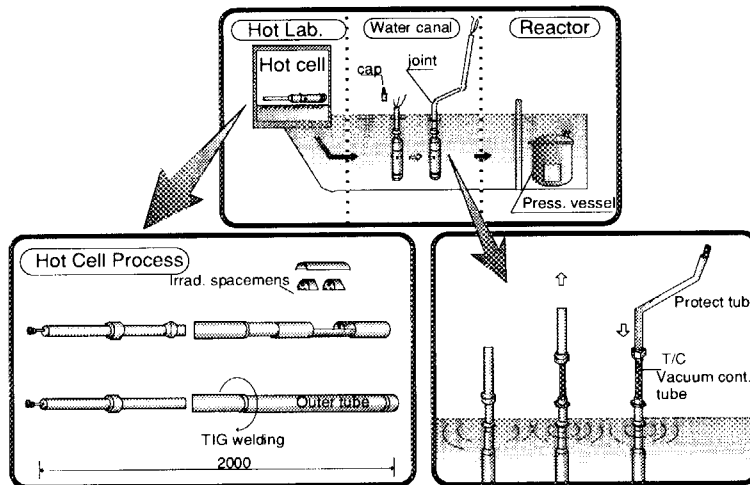


Fig. 4.2.5
Assembly flow chart of the capsule

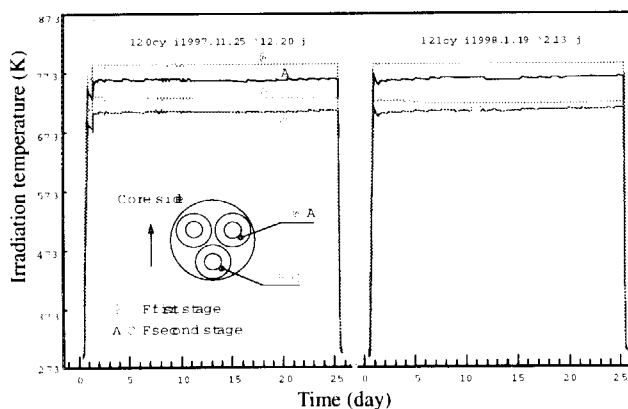


Fig. 4.2.6
Irradiation temperature results

Loading test under irradiation

In order to grasp the irradiation effect of the reactor structure material, the thermal neutron trap type creep capsule was newly developed and fabricated. In FY1997, the thermal neutron trap type creep capsule was irradiated in the JMTR. This structure is shown in Fig. 4.2.7. The thermal neutron trap used the graphite as a thermal neutron multiplication material. There were 2 specimens in a capsule, the size of specimen GL (gauge length) was $\phi 2 \text{ mm} \times 10 \text{ mm}$, and the 2 kinds of stresses were between 196 MPa and 294 MPa. The irradiation temperatures of the specimens were controlled within 820 K to 826 K. The Creep curve is shown in Fig. 4.2.8. In this creep curve, the first, secondary and third creep strains could be measured. And, the photograph of the broken specimens is shown in Fig. 4.2.9. It was verified that this creep capsule was able to measure the material creep strain precisely by Fig. 4.2.8 and 4.2.9.

Fig. 4.2.7
Thermal neutron trap type creep capsules

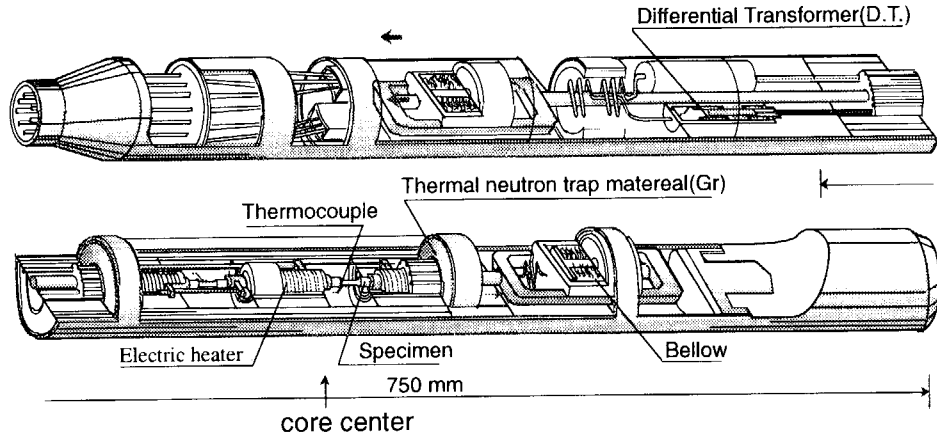


Fig. 4.2.8
Creep curve result (left)

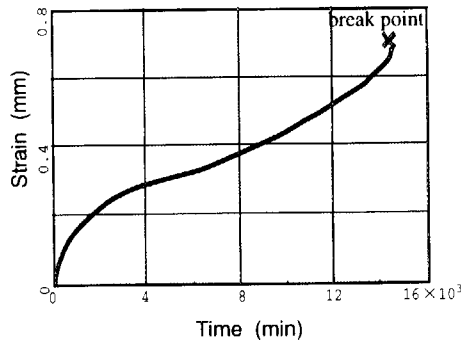
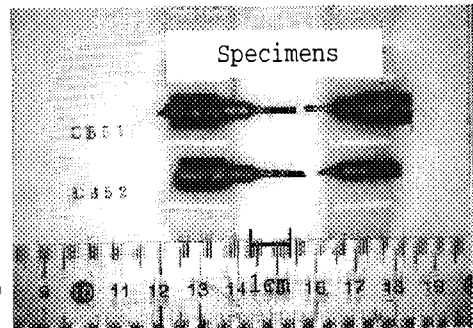


Fig. 4.2.9
Broken specimens (right)



4.3. Safety Analysis of JMTR with New Core Configuration

Outlines

The JMTR is currently operated by employing "mixed core configuration" in which 20 LEU (low enrichment uranium) standard fuel elements, 2 MEU (medium enrichment uranium) standard fuel elements and 5 LEU fuel followers (connected to control rods) are used in each operating cycle. For enhancement of fuel economy and early utilization of MEU fuel stocks, it was decided to increase the number of MEU fuels loaded into the core from 2 to 6, without significant change of neutronic characteristics. Safety analysis has been performed to confirm the safety of the reactor with this new core configuration (hereafter called as "MEU 6" core).

Results of the Safety Analysis

In the MEU 6 core configuration, 6 MEU fuel elements and 21 LEU fuel elements (16 standard elements and 5 control rod followers) will be loaded for each operation cycle (see Fig. 4.3.1). Safety analysis of the JMTR with new core configuration has been performed by same methods adopted in the analysis for current license application. The results are summarized as follows:

- ① Core neutronics analysis reveals maximum peaking factor in the MEU 6 core is 3.12, lower than current license limit 3.14. Excess reactivity, shutdown margin, reactivity variation rate at control rod withdrawal and reactivity coefficients (void, temperature and Doppler) are equivalent to the values evaluated in the analysis for current license application, and satisfying the safety design policy on the core neutronics. Average burn-up of MEU fuel elements increases to about 20 % from 15 % of current core configuration, but still satisfies safety design policy in which the average burn-up of fuel elements is required to be less than 40 %.
- ② Steady state thermal analysis with rated power shows the maximum fuel temperature and the minimum DNB ratio are equivalent to the values in the analysis for current license application, and satisfying the safety design policy on the thermal characteristics of the core (see Fig. 4.3.2).
- ③ Automatic power control system has the capability to stabilize the core power against reactivity disturbance assumed to be imposed during operation.
- ④ The results of thermohydraulic analyses for design bases event (eight kinds of anticipated transients and five kinds of the accidents, which are common with the safety analysis for current license application) are satisfying safety criteria on integrity of the fuel and the core as well as on integrity of primary cooling system pressure boundary.

According to these results, it is confirmed that reactor operation with MEU 6 core will satisfy the limit of neutronic power distribution, safety design policy and the criteria for safety analysis. Relevant application about the change of reactor operation condition will be submitted to the regulatory authority in the next fiscal year (1998) and reactor operation with MEU 6 core will start.

Fig. 4.3.1
Core configuration

Mixed core configuration (with 2 MEUs) employed in current operation. Mixed core configuration (with 6 MEUs) newly introduced operation.

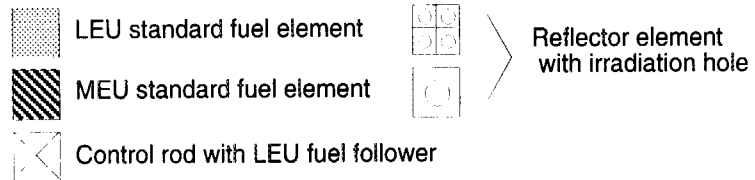
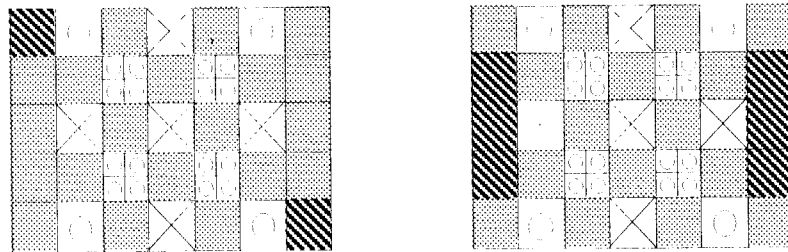
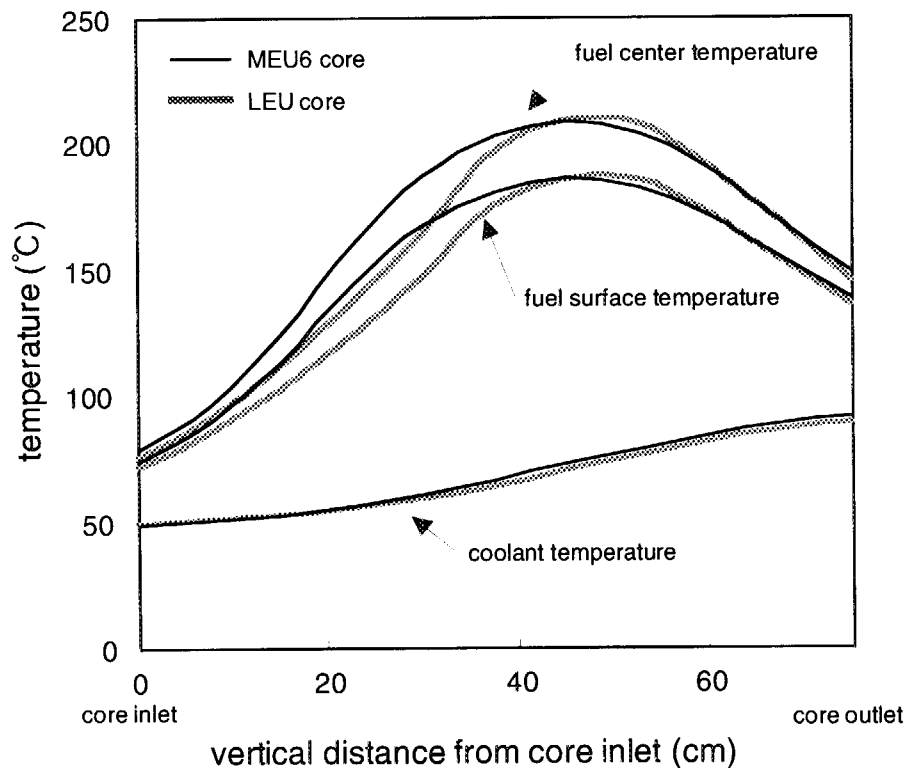


Fig. 4.3.2
Temperature distributions in coolant in the hot channel, of surface and center of adjacent fuel plate, at rated power operation



4.4. Neutron Irradiation Studies for Fusion Blanket Development

Pebble development

1) Tritium breeder

As the fabrication method of Li_2TiO_3 pebbles, the wet process is the most advantageous from a view point of mass production, etc.. The vibratory dropping system for mass fabrication was developed, and characteristics of Li_2TiO_3 pebbles fabricated by this system were evaluated.

Vibratory dropping system is shown in Fig. 4.4.1. The relationship between the viscosity of the PVA/4HF solution and contents of 4HF and PVA is shown in Fig. 4.4.2. From this figure, the viscosity of the PVA/4HF solution was larger than 300 cP. The diameter and sphericity of Li_2TiO_3 pebbles were controlled by a diameter and frequency of the vibration nozzle. The frequency of the vibration nozzle was selected the values of 80 Hz. The density of Li_2TiO_3 pebbles increased with increasing the sintering temperature and sintering time. The extent of grain coarsening and achievable final density depend on the rate-controlling mechanism in the coarsening and densification kinetics.

The characteristics of Li_2TiO_3 pebbles were described as follows. The density and diameter of Li_2TiO_3 pebbles became about 82.9 %T.D. and 1 mm at 1200 °C for 4 hours, respectively. The sphericity of Li_2TiO_3 pebbles, which is the rate of long diameter and short diameter, was 1.08. Grain size of Li_2TiO_3 pebbles was 10~20 μm .

From the results of these tests, excellent prospects were obtained concerning mass fabrication of Li_2TiO_3 pebbles with a target density (80-85 %T.D.) by this system.

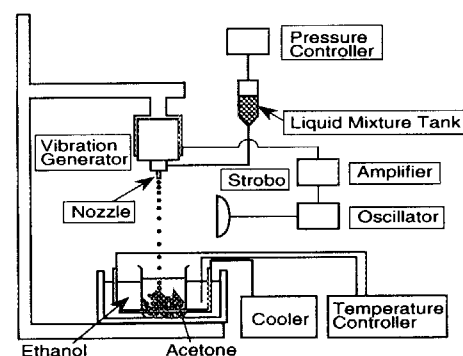


Fig. 4.4.1
Schematic drawing of vibratory dropping system for mass production.

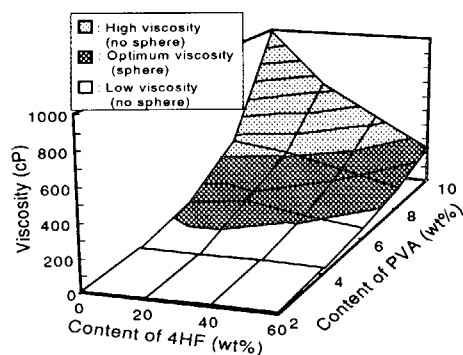


Fig. 4.4.2
Relationship between the viscosity of the solution and contents of 4HF and PVA.

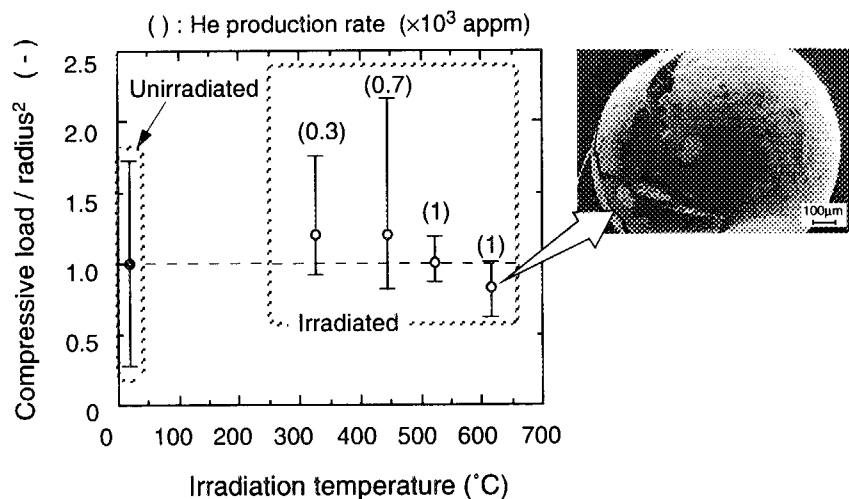
2) Neutron multiplier

Mechanical properties of the neutron irradiated beryllium pebbles were studied. Specimens were produced by the rotating electrode method, and were irradiated by the four helium sealed inner capsule during 10 cycle of the JMTR. Irradiation temperature and helium production rate were 327, 445, 524, 616 °C and $0.3, 0.7, 1.0, 1.0 \times 10^3$ appmHe for each temperature. Compression tests were carried out in the "Beryllium PIE Facility" of JMTR hot-laboratory as the PIE. The result at the room temperature is shown in Fig .4.4.3 The vertical axis is normalized by the average of the for the unirradiated sample. Mechanical properties of the beryllium pebble specimen show the feature of larger-grained specimens, and rapid decreasing was not observed.

To enhance the beryllium pebbles study, the world wide collaboration was proposed at the International Workshop on Beryllium Technology for Fusion (IEA).

On the other hand, beryllium pebbles will also contribute to a beryllium neutron reflector of JMTR because the beryllium pebble packed neutron reflector has long life time and different characterization by different packed density.

Fig. 4.4.3
Results of compression
test of beryllium



3) Tritium release properties from Li_2TiO_3 pebbles

The in-pile functional test of blanket mockup with Li_2TiO_3 and Be pebbles is started in JMTR. In this test, it is carried out to evaluate the effects of various parameters, i.e. sweep gas flow rate, irradiation temperature and hydrogen content in sweep gas, on tritium release.

The block diagram of irradiation facility and vertical cross section of in-pile mockup is shown in Fig. 4.4.4. Result of tritium release at reactor power-up is shown in Fig. 4.4.5. The amount of HT+HTO and HT were calculated from the measured values of the each tritium concentration, the sweep gas flow rate, the pressure in an ionization chamber and temperature. At this time, the sweep gas flow rate was $200 \text{ cm}^3/\text{min}$ and moisture and oxygen concentrations in the helium sweep gas were less than 10 ppm and 0.05 ppm, respectively. When the T_{CL} and the temperature at outside edge of Li_2TiO_3 pebble bed (T_{EL}) became about $140 \text{ }^\circ\text{C}$ and $118 \text{ }^\circ\text{C}$, respectively, the tritium release from Li_2TiO_3 pebbles started. Then, amount of HT+HTO increased with increasing T_{CL} and T_{EL} . The experiments were conducted in order to evaluate the effect of hydrogen content in the sweep gas on tritium release from Li_2TiO_3 at the sweep gas flow rate of $200 \text{ cm}^3/\text{min}$. According to the effect of hydrogen concentration on tritium release, the change of hydrogen concentration was followed by positive tritium release peaks for increase of hydrogen concentration and by negative release peaks for decrease of hydrogen concentration.

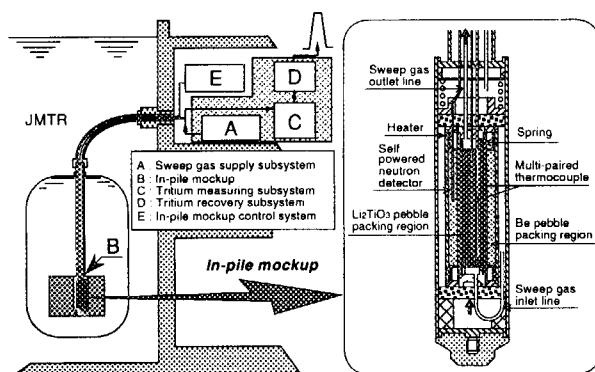


Fig. 4.4.4
Block diagram of irradiation facility and vertical cross-section of in-pile mockup.

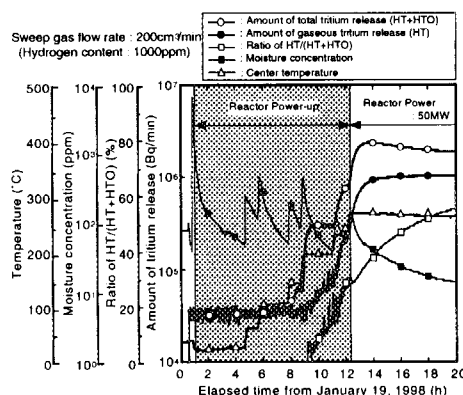


Fig.4.4.5
Result of tritium release at reactor power-up.

Development of mock-up for in-pile functional test

1) Preliminary nuclear design of pulse operation simulating mock-up

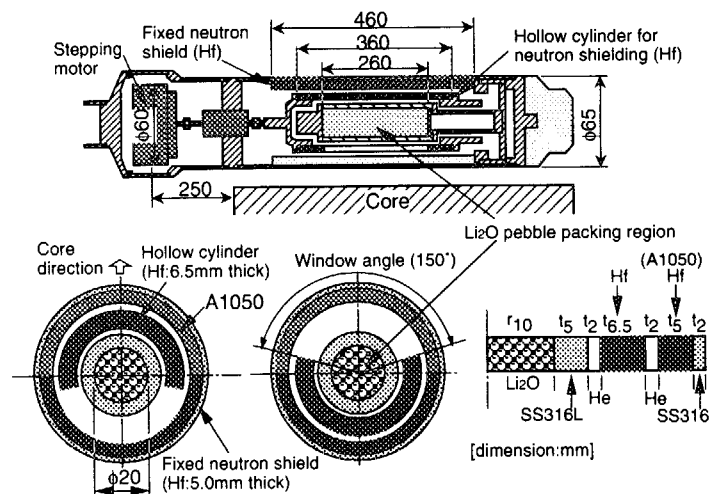
The operating mode of fusion experimental reactor (ex. ITER) is a pulse operation, and the tritium breeding blanket installed in this reactor is irradiated pulsatively by neutron. Therefore, engineering data (temperature control characteristics, etc.) under neutron pulse operation are necessary to design this blanket. In order to get these engineering data, in-pile functional tests of tritium breeding blanket have been planned using the JMTR (Japan Materials Testing Reactor). Nuclear design of pulse operation nuclear mock-up was performed by using the three dimensional Monte Carlo code MCNP4A with FSXLIBJ3R2 (based on JENDL3.2).

Irradiation field quality factor 'R', which is defined by thermal neutron flux ratio of neutron irradiation condition and neutron shut-off condition, is less than 0.1, because R value of 0.1 is necessary to observe tritium release property and thermal property in in-pile functional tests, exactly. The results of nuclear calculation are shown in Table 4.4.1. From the calculation results of case 1, R was 0.33. From the calculation results of case 2, R was the smallest (R=0.14) at 150° window angle. From the results of case 3, the pulse operation simulating mock-up with a hollow cylinder of 6.5 mm thickness, window angle of 150° and fixed neutron shield of 5.0 mm thickness was satisfied with irradiation field quality (R=0.1) and had best characteristic as simulation filed of pulse operation mode for in-pile functional tests in the JMTR. Construction of pulse operation simulating mock-up is shown in Fig. 4.4.6. Consequently, it was obvious that there are bright prospects for in-pile functional tests with pulsed operation simulating mock-up in the JMTR.

Table 4.4.1
Results of nuclear calculation

Items		Case1	Case2	Case3
Hollow cylinder thicknes	(mm)	5.0	5.0	6.5
Window angle of hollow cylinder	(°)	120	150	150
Fixed neutron shield thickness	(mm)	---	6.5	5.0
Irradiation field quality factor R		0.33	0.14	0.10

Fig. 4.4.6
Construction of pulse operation simulating mock-up



Development of tritium permeation barrier

In a fusion blanket design, a ceramic coating on structural materials has been considered as a tritium permeation barrier. Therefore, the fabrication technique of Cr₂O₃-SiO₂ coating had been developed by Chemical Densified Coating (CDC) method. However, Cr₂O₃-SiO₂ coating had open pores in the coating. For filling open pores, the densification treatment by P₂O₅ was considered. In this study, the preliminary characterization of Cr₂O₃-SiO₂ coating and Cr₂O₃-SiO₂-P₂O₅ coating were carried out. Fabrication process and conditions of CDC method are shown in Fig. 4.4.7 and Table 4.4.2.

In the verification test of open pores, the solution with NaCl and CuCl₂ was sprayed on the surface of each coating at 50 °C. Then, if there were open pores in the surface coating, rust appeared. From apparent observation, small rust was observed after 24 hours in Cr₂O₃-SiO₂ coating. On the other hand, in Cr₂O₃-SiO₂-P₂O₅ coating, rust did not observe after 240 hours. Thermal shock test was performed by water quenching from 400 °C or 600 °C. Thickness of Cr₂O₃-SiO₂ coating was 25, 50 and 80 μm. Thickness of Cr₂O₃-SiO₂-P₂O₅ coating was 50, 100 and 200 μm. Peeling and cracking did not occur in Cr₂O₃-SiO₂ coating of 25 and 50 μm thickness and Cr₂O₃-SiO₂-P₂O₅ coating of 50 and 100 μm thickness after the thermal shock test. An adhesion specimen with coating and a substrate without coating were joined by the bonding agent. Next, the joined specimen was placed in the tensile machine. The adhesion strength of Cr₂O₃-SiO₂ coating and Cr₂O₃-SiO₂-P₂O₅ coating were ~39 MPa and ~36 MPa at room temperature, respectively. It was obvious that the adhesion strength of Cr₂O₃-SiO₂ coating and Cr₂O₃-SiO₂-P₂O₅ coating was similar.

It was obvious that the number of open pore in the coating decreased by the densification treatment of P₂O₅. From the results of the adhesion test, there was no significant difference between Cr₂O₃-SiO₂ coating and Cr₂O₃-SiO₂-P₂O₅ coating. However, from the results of the thermal shock test, the thermal shock resistivity of Cr₂O₃-SiO₂-P₂O₅ coating was better than that of Cr₂O₃-SiO₂ coating.

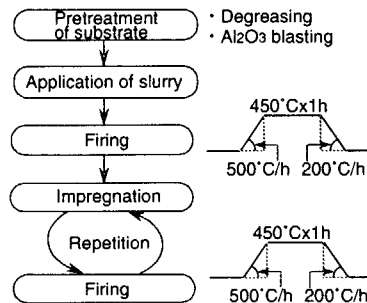


Fig. 4.4.7
Fabrication process of
Chemical Densified
Coating (CDC) method

Coating	Cr ₂ O ₃ -SiO ₂ coating	Cr ₂ O ₃ -SiO ₂ -P ₂ O ₅ coating
Slurry	SiO ₂ granules + CrO ₃ solution	SiO ₂ granules + CrO ₃ solution + H ₃ PO ₄ solution
Impregnation	CrO ₃ solution	CrO ₃ solution + H ₃ PO ₄ solution
Repetition No.	15 times	6 times

Table 4.4.2
Fabrication conditions
of Cr₂O₃-SiO₂ coating
and Cr₂O₃-SiO₂-P₂O₅
coating

Development of instrumentation

In order to investigate the effect of temperature on Self-Powered Neutron Detector (SPND) output current, three types of SPNDs were irradiated in the Japan Materials Testing Reactor (JMTR) up to $\sim 1 \times 10^{24}$ n/m² (>1 MeV), and electrical properties of these SPNDs were compared. The standard typed SPND (type 1) is constructed from Rh as emitter, SS316 as collector and Al₂O₃ (99.5 wt.%) as insulator. The high temperature typed SPND (type 2) is constructed from Rh as emitter, Inconel 600 as collector and Al₂O₃ (99.5 wt.%) as insulator. The hybrid typed SPND (type 3) is constructed from Pt-Rh clad Co as emitter, Inconel 600 as collector and Al₂O₃ (99.5 wt.%) as insulator. Mineral Insulated cable (MI cable) of type 1 is constructed from Ni as core wire, SS316 as sheath material and MgO (99.87 wt.%) as insulator. And MI cable of type 2 and 3 constructed from Inconel 600 as core wire and sheath material, and Al₂O₃ (99.6 wt.%) as insulator. Configuration of SPNDs are shown in Fig. 4.4.8 and Fig. 4.4.9. The relative value of SPND output current with irradiation temperature is shown in Fig. 4.4.10. The SPND output current of type 1 changed up to $\sim 11\%$ with irradiation temperature. The SPND output current of type 2 was stable to temperature changes (below $\sim 4\%$) from 400 °C to 600 °C. On the other hand, the SPND output current of type 3 changed up to $\sim 20\%$ with irradiation temperature. From the results of the out-of-pile test, the reason of the type 3 SPND output current change with irradiation temperature was obvious the Seebeck effect between Ni as emitter terminal and Inconel as core wire of MI cable.

Fig. 4.4.8
Configuration of standard typed SPND and high temperature typed SPND

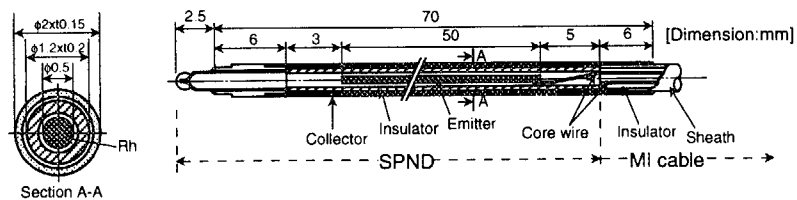


Fig. 4.4.9
Configuration of hybrid SPND

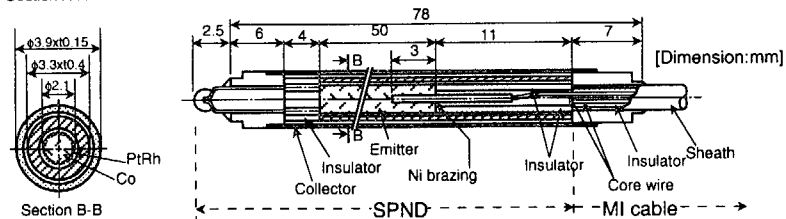
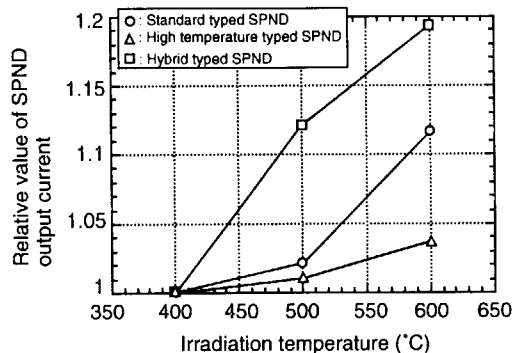


Fig.4.4.10
Relative value of SPND output current with irradiation temperature



Electron beam heating facility

Since plasma facing components such as the first wall and the divertor are exposed to high heat load and high neutron flux generated by the plasma, it is urgent to develop plasma facing components which stand them.

The electron beam heating facility ("OHBIS", Oarai Hot-cell electron Beam Irradiating System) had been established in a hot cell of JMTR hot laboratory in order to estimate thermal shock resistivity of plasma facing materials and heat removal capabilities of divertor element under steady state heat load. In this facility, un-irradiated / irradiated plasma facing materials (beryllium, carbon based materials and so on) and divertor elements can be treated. These samples are irradiated by electron beam with the maximum power of 50 kW, and exposure time of the beam is not less than 0.1 ms.

In this year, an electron beam dumper (heat sink component : Fig. 4.4.11) for conditioning of an electron beam was renewed, and the running performance of an plunger pump and new secondary cooling device which cools the electron beam dumper was estimated. On the performance of the electron beam dumper, the critical heat flux of the dumper is 38 MW/m^2 , and the vacuum in a vessel with the dumper is 7.5×10^{-6} Torr under the cooling water pressure of 40 kg/cm^2 of cooling water pressure. On the secondary cooling device, a new cooling equipment (11 kW) was installed. Thermal shock tests of neutron irradiated samples will be done in next year.

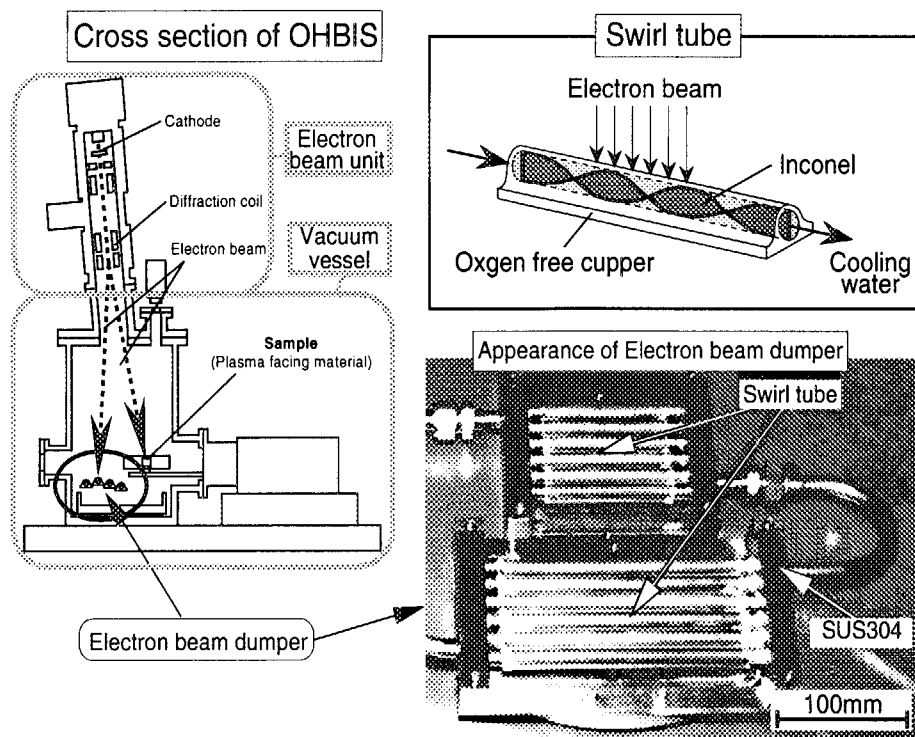
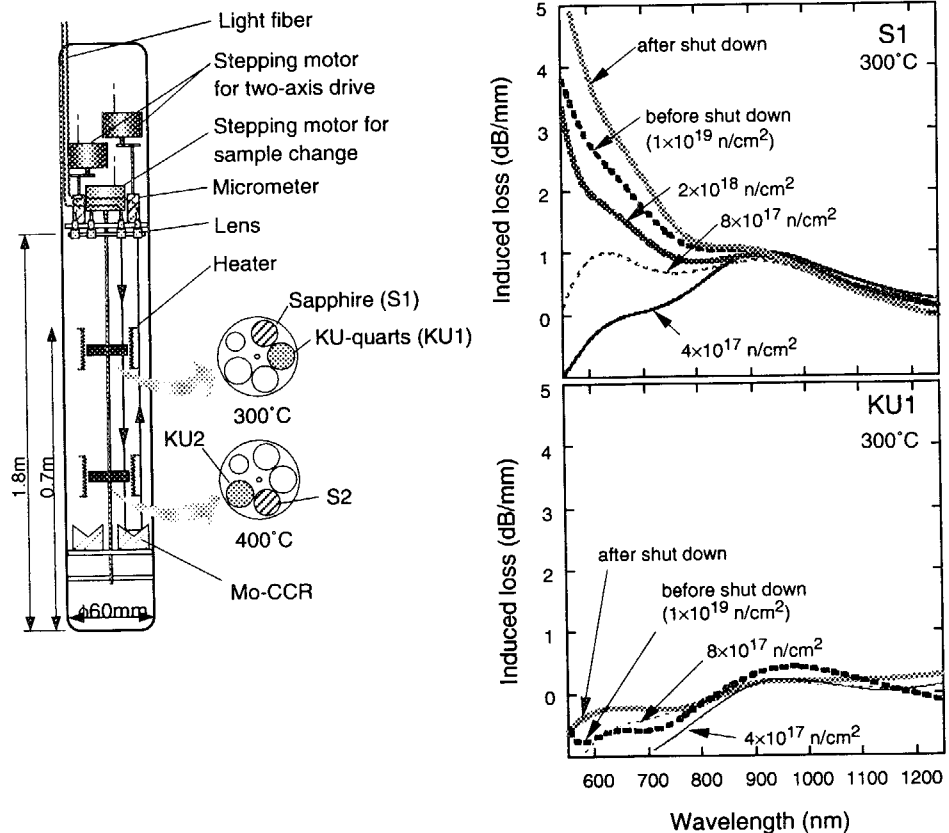


Fig. 4.4.11
Renewed electron beam dumper

Irradiation test of window materials for the plasma diagnostic component

Induced loss of the light transmission spectrum for sapphire and KU-quartzs, that are the candidate materials for the instrumentation windows of plasma diagnostic component in fusion reactors, was investigated by the light measurement capsule in the JMTR. Light measurement capsule and results of irradiation test are shown in Fig. 4.4.12. Induced loss of sapphire and KU-quartzs increased with increasing neutron fluence and decreased with increasing irradiation temperature, and KU-quartzs showed smaller decrease of induced loss than sapphire. It was clear that KU-quartzs in the short wavelength and of sapphire in the infrared range are suitable. However, transmission spectrum in the short wavelength was significantly affected by the low irradiation temperature. Additionally, developed light measurement capsule will expect as new applications for the instrumentation of irradiation test, for example, visible observation, swelling or deformation, temperature control etc.

Fig. 4.4.12
Light measurement capsule and results of irradiation test



Development of joining technology for structure materials

1) Irradiation tests of joints fabricated by friction welding

The effects of neutron irradiation on tensile properties of the Cu alloys to type 316 stainless steel (SS316) joints fabricated by friction welding method were examined. Additionally, irradiation tests of Al₂O₃-dispersed copper alloy (Al-15), oxygen free copper (OF-Cu) and SS316 were conducted. The Al-15/SS316 and OF-Cu/SS316 joints were irradiated in the Japan Materials Testing Reactor (JMTR), and tensile tests and metallographical observation of these joints have been performed as the post irradiation examination (PIE).

Effect of irradiation temperature on the yield strength of Al₂O₃-dispersed copper alloy is shown in Fig. 4.4.13. Yield strength of irradiated Al-15 was inferior to that of un-irradiated Al-15. All irradiated specimens of Al-15/SS316 and OF-Cu/SS316 joints fractured at the copper sides. Tensile strength at 293 K for the Al-15/SS316 joints irradiated at 693 K was equal to that of the base metal (Al-15) irradiated in the same condition. On the other hand, tensile strength of Al-15/SS316 joints was smaller than that of Al-15 in the tensile tests at the same temperature as each irradiation temperature. The SEM micrographs of the fracture surfaces for irradiated Al-15 and Al-15/SS316 joint after tensile tests are shown in Fig. 4.4.14. Fracture surface of Al-15/SS316 joint was more brittle and exhibited dimpled transgranular fracture.

In this study, useful data of the irradiated Al-15/SS316 and OF-Cu/SS316 joints fabricated by friction welding method were obtained to design of fusion reactors.

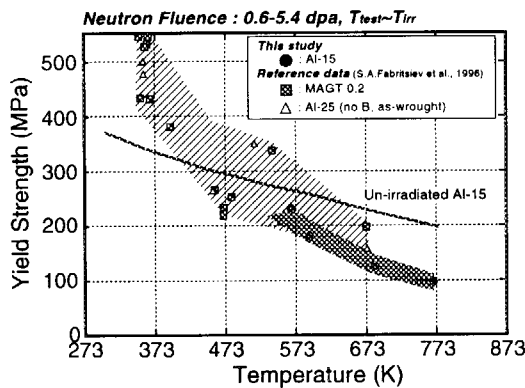


Fig. 4.4.13
Effect of irradiation temperature on the yield strength of Al₂O₃-dispersed copper alloys

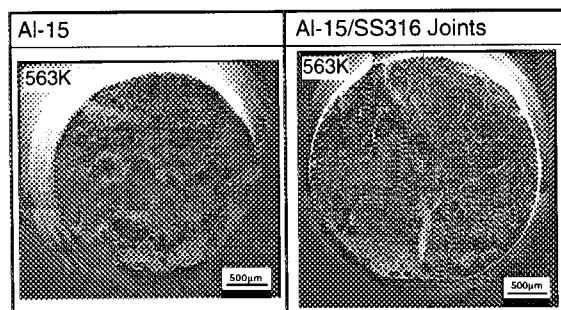


Fig. 4.4.14
SEM micrographs of the fracture surfaces of irradiated Al-15 and Al-15/SS316 joint after tensile tests

2) Reweldability test of irradiated materials by TIG welding Method

Reweldability tests of un-irradiated and/or irradiated Inconel 625 has been performed by the tungsten inert gas (TIG) welding process and the weldments of mechanical properties were evaluated.

The specimens made of Inconel 625 for rewelding tests were irradiated in the JMTR (Japan Materials Testing Reactor) with a fast neutron fluence of $\sim 2.0 \times 10^{20} \text{ n/cm}^2$ ($E > 1 \text{ MeV}$) and a thermal neutron fluence of $\sim 5.0 \times 10^{20} \text{ n/cm}^2$ ($E < 0.682 \text{ eV}$) at temperatures of 150 °C and 200 °C. After neutron irradiation, welding was carried out from both sides of the specimens, and three combinations of reweldments were performed, i.e. irradiated/irradiated, irradiated/un-irradiated and un-irradiated/un-irradiated. The un-irradiated/un-irradiated combination was selected for preliminary testing. The following tests for all kinds of rewelded joints have been performed: tensile (testing temperatures: 20 °C, 150 °C and/or 200 °C), hardness, metallographical observation and SEM/XMA analysis.

The tensile strength of the un-irradiated/un-irradiated and irradiated/un-irradiated welded joint specimens was close to each other within the scattering of 5 %. In particular, the ultimate strengths were 796 MPa and 802 MPa for the unirradiated welded joint and for the irradiated/un-irradiated joint, respectively, at the test temperature of 150 °C (see Fig. 4.4.16). Fracture was found in the unirradiated base metal part for both joints. The irradiated/irradiated weld joints fractured at the welded metal which has a slightly higher strength of 813 MPa at 150 °C than the un-irradiated base metal. The hardness of the weld metal was the same as the un-irradiated base metal. However, small bubbles were revealed by SEM/XMA analysis in the weld metal and in the heat affected zone (see Fig. 4.4.17).

Fig. 4.4.16
Effect of irradiation
on tensile strength of
weldments of Inconel
625 at 150 °C.

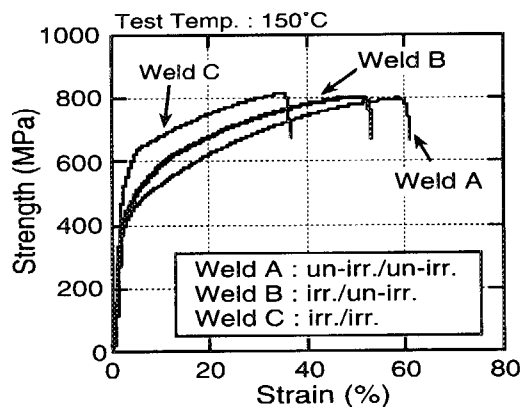
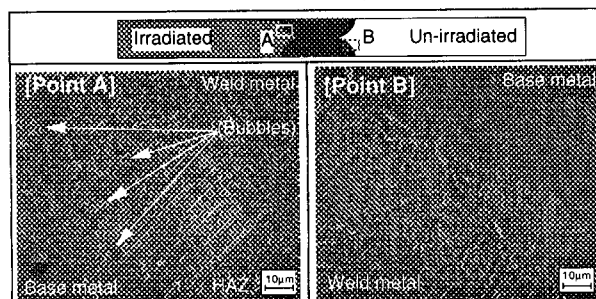


Fig. 4.4.17
SEM micrographs of
cross section for the
irradiated/un-irradiated
weldment .



4.5. Post Irradiation Examination (PIE)

Development of measuring technique for environmentally assisted crack growth test

It is very important for an Environmentally Assisted Crack (EAC) growth test in the high temperature and high-pressurized water to evaluate the life reliability of nuclear structural materials under neutron irradiation. Therefore, a Slow Strain Rate Tensile (SSRT) test and a crack growth characteristic test have been performed on several kinds of stainless steel in the Hot Laboratory. In this study, the application of an Alternating Current Potential Drop (ACPD) method to measure crack growth length was discussed because the method was very efficiency for the EAC growth test in the high temperature and high-pressurized water as the corrosive environment.

Fig. 4.5.1 shows an experimental apparatus developed for the study on the EAC growth. In this apparatus, triangular wave or sine wave load can be applied to a test specimen in the high temperature and high-pressurized water, and the crack length can be measured by using the ACPD method under remote manipulation. The ACPD method has advantages that the potential drop is measured with highly sensitive and this method can be easily applied to the Post Irradiation Examination (PIE) in the hot cell. However, the method has a disadvantage that the potential drop depends on the connecting position of the terminal wire for measuring the output voltage. It is found that the value of the load current, the diameter of the lead wire, the connecting conditions of the terminal wire and the level of the noise signal are very important factors to evaluate the crack growth length by using the ACPD method.

Fig. 4.5.2 shows a block diagram of the ACEP method. A load current of nearly 0.25 A was applied to measure the crack length for Compact Tension (CT) specimen of 0.4 inch in thickness. In order to reduce the contact resistance, the terminal wires were connected with the specimen by the spot welding machine. Lead wires for the measurement of the load current and the output voltage are made of the same material as the specimen, and are 0.5 mm in diameter. Specimens with the machined slit crack of 0.2 mm in width, from 1 mm to 4 mm in length, and fatigue crack of 2 mm in length were prepared to evaluate the relationship between the crack length and the potential drop. An insulation material used between the specimen and its fixture to reduce the noise level in the ACPD was zirconium oxide.

The relationship between the crack length and the potential drop shown in Fig. 4.5.3 is to evaluate the effect of the connecting position of terminal wire for the output voltage. The connecting position of the terminal wire for the voltage affected the value of the potential drop. The tendency that the potential drop increased with increasing the crack length is not influenced by the connecting position of the terminal wire for the voltage.

As a preliminary examination, the ACEP method was applied to EAC growth tests performed in the high temperature and high-pressurized water for the unirradiated material, and results obtained were as follows:

- ① The noise level on the signal of the potential drop was reduced by the ACPD method in comparison with the Direct Current Potential Drop (DCPD) method that is conventional for the crack growth measurement.
- ② In the ACEP method, the connecting position of the terminal wire for the output voltage affected the value of potential drop, but didn't affect the slope of the curve showing the relation between the crack length and the potential drop.
- ③ The reduction of the diameter of the terminal wire caused the drop of the amplifier output.

Fig. 4.5.1
Experimental apparatus for study on environmentally assisted crack growth test

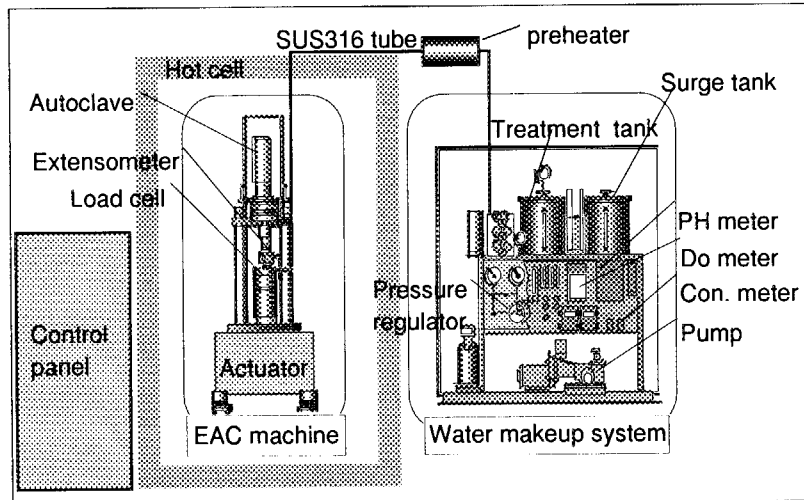
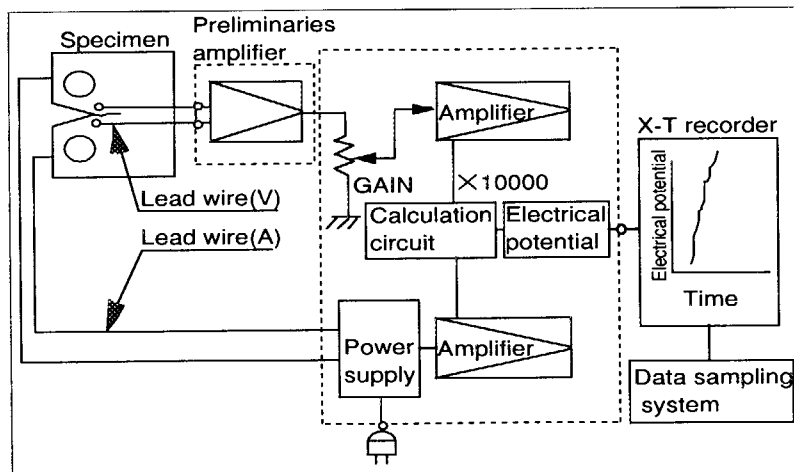


Fig. 4.5.2
Block diagram of alternating current potential drop method



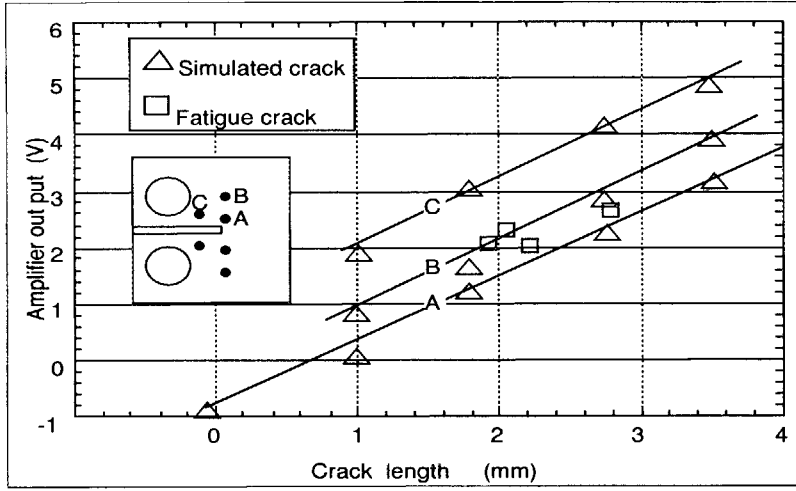


Fig. 4.5.3
Relationship between
crack length and poten-
tial drop

Electric discharge machining of miniaturized specimen from irradiated material

The technique of machining test specimen from the radioactive material and sample in the hot cell is required to reduce the radioactive wastes, and to use the surveillance test specimens of the light water reactor and the specimens finished the post irradiation examinations effectively. In the hot laboratory, the development of the Electric Discharge Machine (EDM) was performed to reprocess the test specimen from the radioactive material and sample in the hot cell. An exterior view of the remote handling equipment of the EDM is shown in Fig. 4.5.4. Before the electric discharge machining, a material or a sample set on the machining stage of 150 mm in length and 200 mm in width is immersed in the working liquid filled in the container of 170 mm in length, 200 mm in width and 180 mm in depth. The electrode for the machining is located by NC system with the minimum control value of 1 mm. A power circuit of this equipment is a pulse type with current capacity of 1 A, and can supply the electrode with the reversed polarity bias to keep the consumption of the electrode to a minimum. The electrode formed into the shape of the specimen was made of copper and tungsten, and was fixed to the tip of the connecting rod made of stainless steel. The feature of this equipment is that the newly locking mechanism of the connecting rod was developed to permit the easy exchange of the rod with the electrode in the hot cell, and to reduce the contact resistance. In general, the connecting rod with the electrode was locked to the body of the EDM by using some screw bolts. This EDM has a tapered supporting plate to catch the connecting rod with the tapered part to be supported on the plate. According to the development of this EDM with the newly locking mechanism, the miniaturized tensile specimen with an accuracy of $\pm 10 \mu\text{m}$ for the designed size can be machined from the TEM disk of 3 mm in diameter. In future works, important points of this development are to improve the accuracy of the machining and to evaluate the effect of the heat affect zone on the result of post irradiation examination using the test specimen. Moreover, the electric discharge machining of the specimens from the radioactive materials and samples will be performed by the remote manipulation in the hot cell.

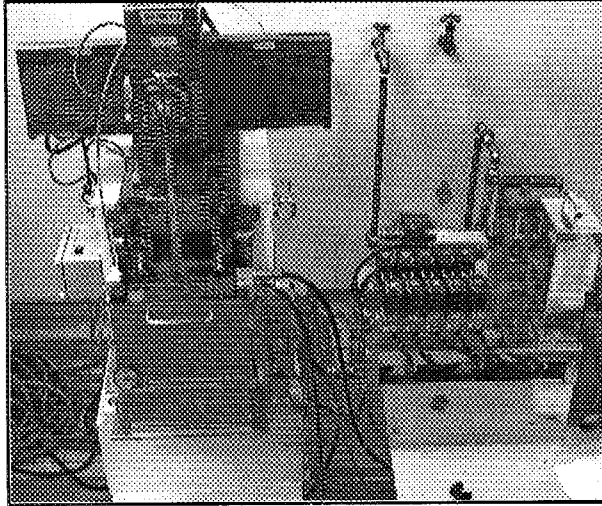


Fig. 4.5.4
Remote handling
equipment of electric
discharge machine

4.6. Application of Infrared Thermography to Nondestructive Diagnostic for Structures and Components in the JMTR

Nondestructive testing and evaluation method using infrared thermography as a remote sensing technique has been applied in many industrial fields to examine the integrity of materials, structures, components and so on. However, few investigations of this method have been performed for the nuclear structures and components. The applicability of the infrared thermography to the nondestructive diagnostic for nuclear power plants was discussed on the basis of the thermal images of the structures and components in the JMTR.

Thermal image on the outside surface of the boundary wall of the JMTR canal building is shown in Fig. 4.6.1. This surface was heated by sun before noon, and cooled by cold wind in the shade in the afternoon. Typical area of the liner temperature distributions, which is higher than its surrounding temperature on the heated surface and lower than its surrounding one on the cooled surface, is observed in these thermal images. It was revealed that these temperature distributions corresponded to the areas where cracks have been repaired previously.

Fig. 4.6.2 shows the thermal image of the coupling and bearing of the circulating pump in the JMTR secondary cooling system. The thermal images of the connecting shaft, coupling and bearing is obviously different between the running and stopping of the circulation.

A lot of thermal images of the structures and components in the JMTR were measured by the infrared thermography. These images will provide useful data to perform the non-destructive diagnostic of the nuclear power plant using the infrared thermography.

Fig. 4.6.1
Thermal image of the boundary wall of the JMTR canal building

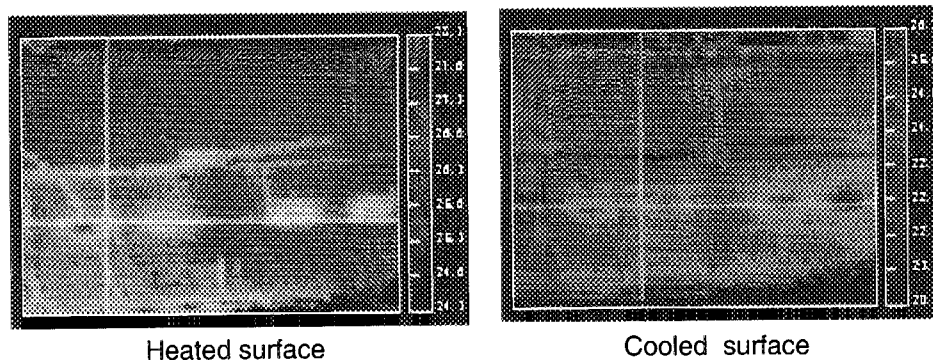
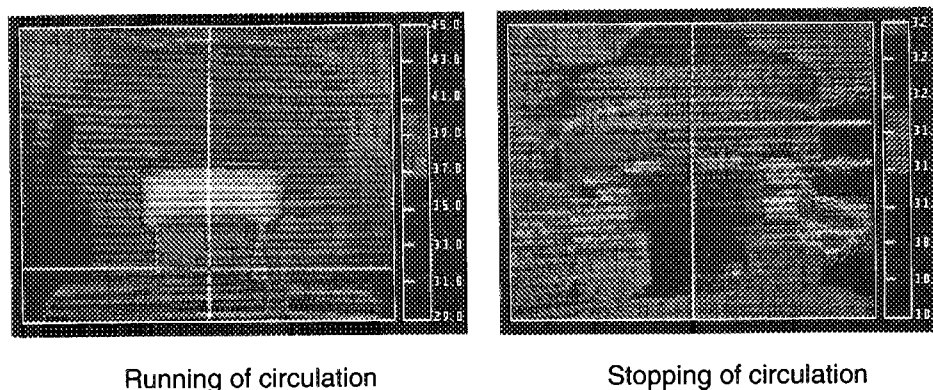


Fig. 4.6.2
Thermal image of the circulating pump in the JMTR secondary cooling system



4.7. Replacement of Vent Valves in Primary Cooling System

Just a little leakage of water, about 1 drop per minute, was detected on the surface of a vent valve in the primary cooling system on July 18th in 1997, during the final periodic inspection of a repaired Pressure Surge Tank before use it. Therefore, 49 same type of ss316 steel valves produced by casting including the damaged vent valve were investigated to perform the safety operation of the JMTR. Several indicators of defects for 15 valves were shown by the liquid penetrant testing, leakage-illumination testing and SUMP (Suzuki Universal Micro Printing) testing. As a result of the investigation for the damaged vent valve, a blowhole of 1 mm in length on the joint surface of the valve body and brown corrosion products in the blowhole were detected. The reason why the intergranular cracks occurred in the valve body was that the corrosion in the blowhole extended along the grain boundary around the HAZ in the valve body. It was confirmed that the intergranular crack propagated starting from the blowhole toward inside and outside of the valve body around the Heat Affect Zone, HAZ, caused by welding. Cr and C at the grain boundary near the joint surfaces of the valve body were observed by the SEM. Moreover, electric conductivity of the water gathered in the narrow space between the joint surface of the valve body and the valve closure was higher than that of the primary cooling water.

Finally, 49 valves of seal-welded type in the primary cooling system were replaced by new valves of gasket seal type.

5. International Cooperation

5.1. International Cooperation

International Cooperation has been performed under the framework of bilateral agreement or international organ's tasks. There are shown in Table 5.1.1

Table 5.1.1
International Coopera-
tive

Program	Theme	Counterpart	Duration	Scope of cooperation	Number of dispatched researcher
KAERI-JAERI cooperative program	Post-irradiation examination and evaluation techniques of irradiated materials	KAERI	Nov.97 (6 day)	Technical Information exchange mutual visits by both sides	2
STA Scientist Exchange Program	Heater-control capsule	KAERI	J1.97 (11day)		1

5.2. STA Scientist Exchange Program

In FY1998 two foreign Scientists were accepted under the STA Scientist Exchange Program List of the accepted Scientists is shown in Table 5.2.1

Research subject	Counterpart	Duration	Number of received researcher
Operation and maintenance management, fuel management, core management for a materials testing reactor	KAERI	Sep. 97 (3 month)	1
Operation and management of irradiation facilities of a materials testing reactor	BATAN	JL.97 (6 month)	1

Table 5.2.1
STA Scientist Exchange Program

5.3. Report of Third International Workshop on Beryllium Technology for Fusion

Third International Workshop on Beryllium Technology for Fusion was held on October 22-24, 1997, at the Sangyou Kaikan in Mito City with 68 participants who attended from the Europe, the Russian Federation, the Kazakstan, the United States and Japan.

The items of topics and number of presentation are shown in the following table. To utilize beryllium in the pebble type blanket, a series of discussions were intensified in multiple view points such as the swelling, He/T release from beryllium pebble irradiated up to high He content, effective thermal conductivity, tritium permeation and coating, and fabrication cost, and so on. As the plasma facing material, life time of beryllium and coated beryllium, dust and particle production, joining, waste treatment, mechanical properties and deformation by swelling were discussed as important issues. Especially, it was recognized throughout the discussions that the comparative study by the different researchers should be carried out to establish the reliability of the data reported in the workshop and in others. To enhance the comparative study, the world wide collaboration for the relative evaluation of the beryllium was proposed by the International Organization Committee and the proposal was approved by all of the participants. The details will be informed by the International Organization Committee in near future. The next workshop will be held in Europe in 1999. There are shown in Table 5.3.1.

Table 5.3.1
Items and number of
presentstion

Items	Contents	Number of resentation
Beryllium application for ITER	Design of plasma facing component and data base for the ITER	2
Production and characterization	Beryllium pebble, S-65C etc.	6
Chemical compatibility and corrosion	Chemical reactivity with steam	3
Forming and joining	Diffusion bonding with Cu alloys	7
Plasma / tritium interaction	Interaction with hydrogen isotopes	6
First wall application	Thermal shock and cycle test	5
Neutron irradiation effects	Swelling, tritium release, mechanical properties	10
Health and safety issues	Protection of beryllium aerosol	3
Hot news	Joining and irradiation test	3

6. Summary

This report describes the activities in the JMTR performed in the fiscal year of 1997. JMTR was operated for 3 cycles and utilized for the research and development program on the technology of LWRs and fusion reactor, as well as for fundamental research of fuels and materials, and for radioisotope productions.

The irradiation service was routinely conducted mainly for satisfying the requirements for the laboratories inside JAERI and for the universities and private companies outside JAERI. Irradiations for RI productions were also performed.

R&D works on irradiation and PIE techniques have been extensively performed.

They are:

- Power ramping tests for LWR fuels
- Evaluation technique in a local neutron spectrum for irradiation utilization
- Oxygen potential sensor for oxide fuel pellet
- Advanced capsules for vertically moving, re-instrumentation, re-loading and coupling irradiation
- Post-irradiation examination techniques for measuring of crack length using an alternation current potential drop method and machining of miniaturized specimen by remote handling
- Research on the blanket materials and components for thermonuclear fusion reactor

7. Publications

Reports

1. 1996, "Mechanical properties of austenitic stainless steels irradiated at 323K in the Japan Materials Testing Reactor", Y. Matsui, et al., J. Nucl. Mater.
2. 1996, "Effects of residual strain on deformation processes of neutron-irradiated Ti-Ni and Ti-Pd Shape memory alloys", T. Hoshiya, et al., J. Nucl. Mater.
3. 1996, "Effects of neutron irradiation on mechanical properties of Nb - 1%Zr/SS304 joints fabricated by friction welding", K. Tsuchiya, et al., Fusion. Technol.
4. 1996, "Preliminary characterization of interlayer for Be/Cu functionally gradient materials thermophysical properties of Be/Cu sintered compacts", S. Saitou, et al., Function Graded Materials.
5. 1996, "Thermal properties of neutron irradiated beryllium", E. Ishizuka, et al., Proc. 5th Int. Workshop on Ceramic Breeder Blanket Interaction.
6. 1996, "Status of fusion blanket irradiation in JAERI", H. kawamura, et al., Proc. of 5th Int. Workshop on Ceramic Breeder Blanket Interaction.
7. 1996, "Fabrication development of ceramic tritium breeders by sol-gel method", K. Tsuchiya, et al., Proc. of 5th Int. Workshop on Ceramic Breeder Blanket Interaction.
8. 1996, "Reactivity test between beryllium and copper alloys", N. Sakamoto, et al., Proc. of 5th Int. Workshop on Ceramic Breeder Blanket Interaction.
9. 1996, "Present status and prospect of Tritium-material interaction studies", H. kawamura, et al., Proc. of Int. Tritium Workshop.
10. 1997, "Characterization of self-powered neutron detector at high temperature under neutron irradiation", M. Nakamichi, et al., Fusion Technol.
11. 1997, "Reactivity test between beryllium and dispersion strengthened copper", N. Sakamoto, et al., Fusion Technol.
12. 1997, "Reprocessing technology development for irradiated beryllium", H. kawamura, et al., Fusion Technol.
13. 1997, "Design study of in-pile blanket mockup simulated neutron pulse operation of fusion reactor", M. Nakamichi, et al., Fusion Technol.
14. Oct.-1997, "Study on the visual detection of defects in divertor structures for the fusion reactor by means of infrared thermography (Influence of heating methods on visual detection)", T. Ishii, et al., J. of the Visualization Soc. of Japan. Vol.17, No.67. P.36-42

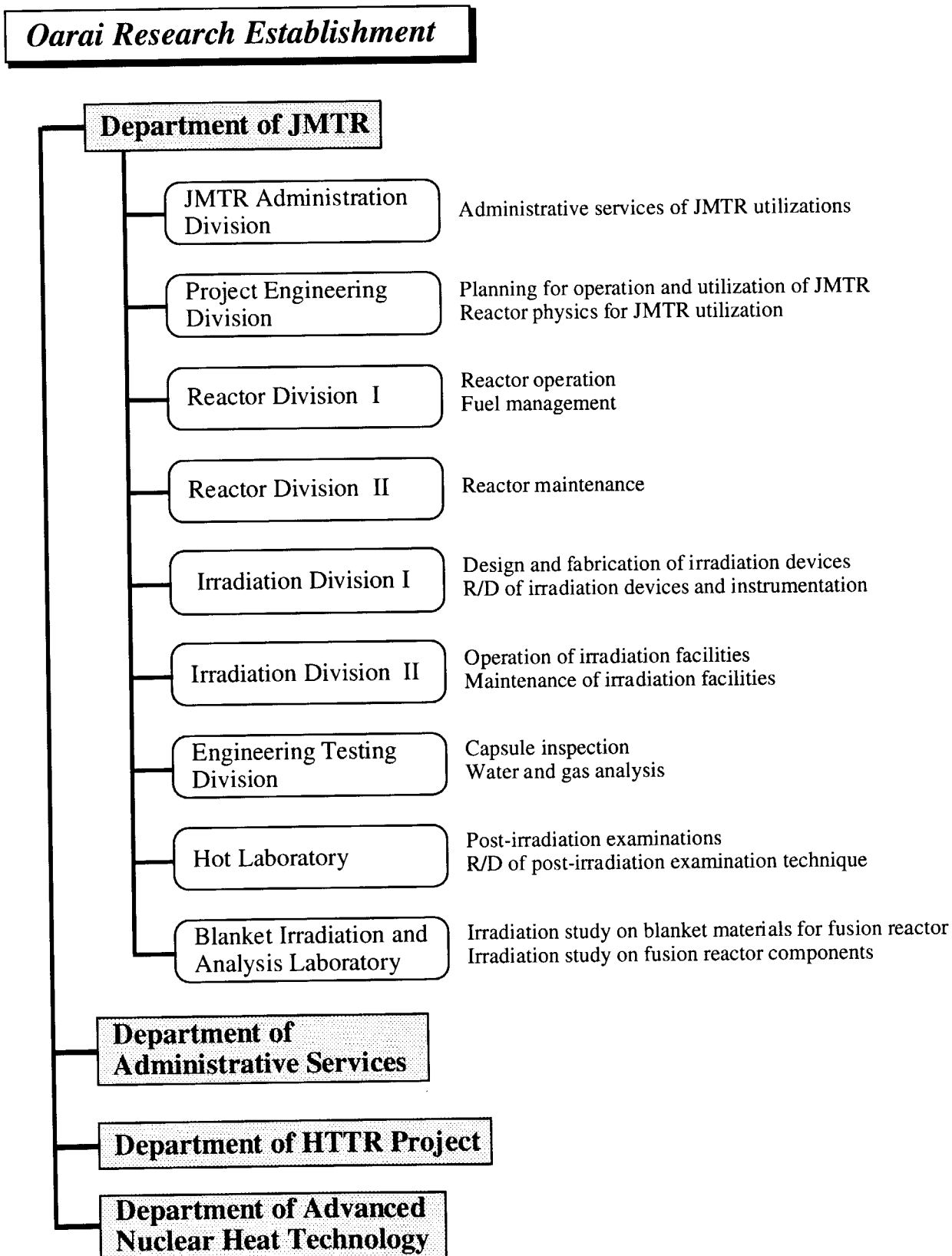
Contributions to conferences

1. May-1997, "Sol-gel fabrication development of ceramic tritium breeders", K. Tsuchiya, et al., 99th Annual Meeting of the American Ceramic Society (u.s.).
2. May-1997, "Density dependence on thermal properties of Li_2TiO_3 pellet", S. Saitou, et al., 99th Annual Meeting of the American Ceramic Society.
3. Sep.-1997, "Nondestructive evaluation for characterizing neutron irradiation embrittlement of nuclear materials by ultrasonic", N. Ooka, et al., JSME Ibaraki district Conference.
4. Sep.-1997, "Nondestructive testing of structures and components in the nuclear facilities using thermography", M. Naka, et al., JSME Ibaraki district Conference.
5. Oct.-1997, "Properties of precipitation hardened steel irradiated at 323K in the Japan Materials Testing Reactor", M. Niimi, et al., 8th Int. Conf. on Fusion Reactor Materials (ICFRM-8)
6. Oct.-1997, "Irradiation techniques in pressurized water using hybrid type of saturated temperature capsule in JMTR", Y. Matsui, et al., 8th Int. Conf. on Fusion Reactor Materials (ICFRM-8)
7. Oct.-1997, "Characterization of Y_2O_3 coating under neutron irradiation", M. Nakamichi, et al., 8th Int. Conf. on Fusion Reactor Materials (ICFRM-8)
8. Oct.-1997, "Fabrication development and preliminary characterization of Li_2TiO_3 pebbles by sol-gel method", K. Tsuchiya, et al., 8th Int. Conf. on Fusion Reactor Materials (ICFRM-8)
9. Oct.-1997, "Improvement of hydriding properties of a Zr_1Ni_1 alloy by adding third transition metals for tritium recovery", T. Kabutomori, et al., 8th Int. Conf. on Fusion Reactor Materials (ICFRM-8)
10. Oct.-1997, "Microstructure and mechanical properties of neutron irradiated beryllium", E. Ishizuka, et al., 8th Int. Conf. on Fusion Reactor Materials (ICFRM-8).
11. Oct.-1997, "Low cycle fatigue properties of 8Cr-2WVTa ferritic steel at elevated temperatures", T. Ishii, et al., 8th Int. Conf. on Fusion Reactor Materials (ICFRM-8).
12. Oct.-1997, "Microstructure and mechanical properties of neutron irradiation beryllium", E. Ishizuka, et al., 3rd IEA Int. Workshop on Beryllium Technology for Fusion.
13. Oct.-1997, "Density improvement of Li_2O_3 pebbles fabricated by wet proces", K. Tsuchiya, et al., 6rd Int. Workshop on Ceramic Breeder Blanket Interactions
14. Oct.1997, "Application of thermography as a technique for nondestructive evaluation on Nuclear facilities", M. Naka, et al., CORENDE Regional Congress of NDT & E (Argentina)
15. Oct.-1997, "Development of a remote controlled small punch testing machine", M. Oumi, et al., AESJ
16. Oct.-1997, "Investigation of the applicability of revised method for determination of excess multiplication factor of the JMTR", Y. Nagao, et al., AESJ

-
17. Mar.-1998, "Electrical properties on ceramic coated wire and polyimide wire under neutron irradiation", H. Sagawa, et al., AESJ.
18. Mar.-1998, "Electrical properties on mineral insulated cables under neutron irradiation", H. Sagawa, et al., AESJ.
19. Mar.-1998, "Replacement of partition tube for power ramp test facility in JMTR", M. Kanno, et al., Yayoi, Tokyo Univ.
20. Mar.-1998, "Development of sweep gas sensor with the protonic conductor", H. Sagawa, et al., AESJ.
21. Mar.-1998 "The first transport of the JMTR spent nuclear fuel to the USA under the new off-site fuels policy", T. Akashi, et al., AESJ.
22. Mar.-1998, "Revised methods for large positive reactivity of nuclear reactor", Y. Kaneko, et al., AESJ.
23. Mar.-1998, "Development of irradiation-coupling techniques-irradiation of the coupling capsule with instrumentation in JMTR", Y. Matsui, et al., AESJ.
24. Mar.-1998, "Neutron irradiation characteristic tests of oxygen sensors for fuel rod", H. Hiura, et al., AESJ.
25. Mar.-1998, "Development of fabrication techniques of test specimen from irradiated materials by using electro-spark machine", M. Oumi, et al., AESJ.
26. Mar.-1998, "JMTR spent fuel transport to the USA", M. Watanabe, et al., Yayoi, Tokyo univ.
27. Mar.-1998, "Evaluation of characterization of power ramping tests for LWR fuels in JMTR", H. Nabeya, et al., UTNL-Report.
28. Mar.-1998, "Development of crack length measuring technique by remote manipulation under high temperature and pressurized water environment", M. Oumi, et al., JSME annual meeting.
29. Jul.-1997, "Investigation of applicability of revised method for determination of large positive reactivity of operating reactor-analyses of excess multiplication factor measurement in the JMTRC using revised method", Y. Nagao, et al., JAERI-Reserch 97-048.
30. Sep.-1997, "Design and fabrication of flow partition tube with He-3 gas screen for OSF-1", M. Kannno, et al., JAERI-Tech 97-042.
31. Feb.-1998, "Annual report of JMTR, FY1996 April 1, 1996 March 31, 1997", JMTR JAERI-Review 98-004.
32. Jan.-1998, "Proceedings of the 3rd IEA international workshop on beryllium technology for fusion", H. kawamura, et al., JAERI-Conf 98-001.
33. Sep.-1997, "Study on neutron irradiation behavior of beryllium as neutron multiplier", E. Ishizuka, First Symposium on Utilization of Research Reactor and JMTR
34. Sep.-1997, "Preliminary fabrication test of lithium oxide pebbles by wet method with vibration Nozzle", K. Tsuchiya, et al., AESJ.

35. Oct.-1997, "High efficiency of ZrNi alloy for its tritium getter properties (3)-deterioration mechanism on cyclic hydrogen absorption - Desorption -", T. Kabutomori, et al., Atomic Energy Society of Japan JAERI-Review 98-004.
36. Mar.-1998, "Reweldability test of irradiated structure materials by TIG welding method (2)", K. Tsuchiya, et al., AESJ.
37. Mar.-1998, "In-pile functional test on fusion blanket with JMTR (1) -Fabrication of irradiation test facility on fusion blanket -", H. Sagawa, et al., AESJ.
38. Mar.-1998, "In-pile functional test on fusion blanket with JMTR (2)-Preliminary verification of irradiation data analysis -", M. Nakamichi, et al., AESJ.
39. Mar.-1998, "Light transmission properties of window materials for ITER diagnostic component under the neutron irradiation", E. Ishizuka, et al., AESJ.

8. Organization



This is a blank page.

国際単位系 (SI) と換算表

表1 SI基本単位および補助単位

量	名称	記号
長さ	メートル	m
質量	キログラム	kg
時間	秒	s
電流	アンペア	A
熱力学温度	ケルビン	K
物質量	モル	mol
光度	カンデラ	cd
平面角	ラジアン	rad
立体角	ステラジアン	sr

表3 固有の名称をもつSI組立単位

量	名称	記号	他のSI単位による表現
周波数	ヘルツ	Hz	s ⁻¹
力	ニュートン	N	m·kg/s ²
圧力, 応力	パスカル	Pa	N/m ²
エネルギー, 仕事, 熱量	ジュール	J	N·m
工率, 放射束	ワット	W	J/s
電気量, 電荷	クーロン	C	A·s
電位, 電圧, 起電力	ボルト	V	W/A
静電容量	ファラド	F	C/V
電気抵抗	オーム	Ω	V/A
コンダクタンス	ジーメンズ	S	A/V
磁束	ウェーバ	Wb	V·s
磁束密度	テスラ	T	Wb/m ²
インダクタンス	ヘンリー	H	Wb/A
セルシウス温度	セルシウス度	°C	
光束度	ルーメン	lm	cd·sr
照射度	ルクス	lx	lm/m ²
放射能	ベクレル	Bq	s ⁻¹
吸収線量	グレイ	Gy	J/kg
線量当量	シーベルト	Sv	J/kg

表2 SIと併用される単位

名称	記号
分, 時, 日	min, h, d
度, 分, 秒	°, ', "
リットル	l, L
トン	t
電子ボルト	eV
原子質量単位	u

1 eV = 1.60218 × 10⁻¹⁹ J

1 u = 1.66054 × 10⁻²⁷ kg

表4 SIと共に暫定的に維持される単位

名称	記号
オングストローム	Å
バ	b
バ	bar
ガ	Gal
キュリー	Ci
レントゲン	R
ラ	rad
レ	rem

1 Å = 0.1 nm = 10⁻¹⁰ m

1 b = 100 fm = 10⁻²⁸ m²

1 bar = 0.1 MPa = 10⁵ Pa

1 Gal = 1 cm/s² = 10⁻² m/s²

1 Ci = 3.7 × 10¹⁰ Bq

1 R = 2.58 × 10⁻⁴ C/kg

1 rad = 1 cGy = 10⁻² Gy

1 rem = 1 cSv = 10⁻² Sv

表5 SI接頭語

倍数	接頭語	記号
10 ¹⁸	エクサ	E
10 ¹⁵	ペタ	P
10 ¹²	テラ	T
10 ⁹	ギガ	G
10 ⁶	メガ	M
10 ³	キロ	k
10 ²	ヘクト	h
10 ¹	デカ	da
10 ⁻¹	デシ	d
10 ⁻²	センチ	c
10 ⁻³	ミリ	m
10 ⁻⁶	マイクロ	μ
10 ⁻⁹	ナノ	n
10 ⁻¹²	ピコ	p
10 ⁻¹⁵	フェムト	f
10 ⁻¹⁸	アト	a

(注)

- 表1-5は「国際単位系」第5版、国際度量衡局1985年刊行による。ただし、1 eVおよび1 uの値はCODATAの1986年推奨値によった。
- 表4には海里、ノット、アール、ヘクタールも含まれているが日常の単位なのでここでは省略した。
- barは、JISでは流体の圧力を表わす場合に限り表2のカテゴリーに分類されている。
- EC閣僚理事会指令ではbar, barnおよび「血圧の単位」mmHgを表2のカテゴリーに入れていない。

換算表

力	N (=10 ⁵ dyn)	kgf	lbf
	1	0.101972	0.224809
	9.80665	1	2.20462
	4.44822	0.453592	1

粘度 1 Pa·s (N·s/m²) = 10 P (ポアズ) (g/(cm·s))

動粘度 1 m²/s = 10⁴ St (ストークス) (cm²/s)

圧	MPa (=10 bar)	kgf/cm ²	atm	mmHg (Torr)	lbf/in ² (psi)
	1	10.1972	9.86923	7.50062 × 10 ³	145.038
力	0.0980665	1	0.967841	735.559	14.2233
	0.101325	1.03323	1	760	14.6959
	1.33322 × 10 ⁻⁴	1.35951 × 10 ⁻³	1.31579 × 10 ⁻³	1	1.93368 × 10 ⁻²
	6.89476 × 10 ⁻³	7.03070 × 10 ⁻²	6.80460 × 10 ⁻²	51.7149	1

エネルギー・仕事・熱量	J (=10 ⁷ erg)	kgf·m	kW·h	cal (計量法)	Btu	ft·lbf	eV
	1	0.101972	2.77778 × 10 ⁻⁷	0.238889	9.47813 × 10 ⁻⁴	0.737562	6.24150 × 10 ¹⁸
	9.80665	1	2.72407 × 10 ⁻⁶	2.34270	9.29487 × 10 ⁻³	7.23301	6.12082 × 10 ¹⁹
	3.6 × 10 ⁶	3.67098 × 10 ⁵	1	8.59999 × 10 ⁵	3412.13	2.65522 × 10 ⁶	2.24694 × 10 ²⁵
	4.18605	0.426858	1.16279 × 10 ⁻⁶	1	3.96759 × 10 ⁻³	3.08747	2.61272 × 10 ¹⁹
	1055.06	107.586	2.93072 × 10 ⁻⁴	252.042	1	778.172	6.58515 × 10 ²¹
	1.35582	0.138255	3.76616 × 10 ⁻⁷	0.323890	1.28506 × 10 ⁻³	1	8.46233 × 10 ¹⁸
	1.60218 × 10 ⁻¹⁹	1.63377 × 10 ⁻²⁰	4.45050 × 10 ⁻²⁶	3.82743 × 10 ⁻²⁰	1.51857 × 10 ⁻²²	1.18171 × 10 ⁻¹⁹	1

1 cal = 4.18605 J (計量法)
 = 4.184 J (熱化学)
 = 4.1855 J (15 °C)
 = 4.1868 J (国際蒸気表)
 仕事率 1 PS (仏馬力)
 = 75 kgf·m/s
 = 735.499 W

放射能	Bq	Ci
	1	2.70270 × 10 ⁻¹¹
	3.7 × 10 ¹⁰	1

吸収線量	Gy	rad
	1	100
	0.01	1

照射線量	C/kg	R
	1	3876
	2.58 × 10 ⁻⁴	1

線量当量	Sv	rem
	1	100
	0.01	1

